

Fundamentals and applications of X-ray diffraction. Applications in catalysts characterization.

Przemysław Rzepka

Outline

1. Crystal lattice. Symmetry
2. X-ray diffraction
3. Braggs' peaks positions. Indexing
4. Relative intensities of Braggs' Peaks. Structure factor. Structure refinement
5. Sample preparation
6. Examples

What is crystal?

A material has a crystal structure if its constituents (such as atoms, molecules, or ions) are arranged in a 3D translationally periodic order forming a crystal lattice.

Crystal = Lattice * Motif

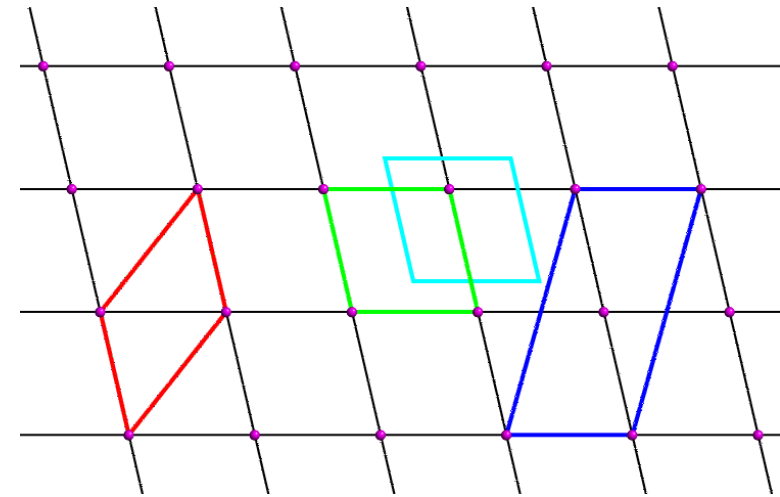
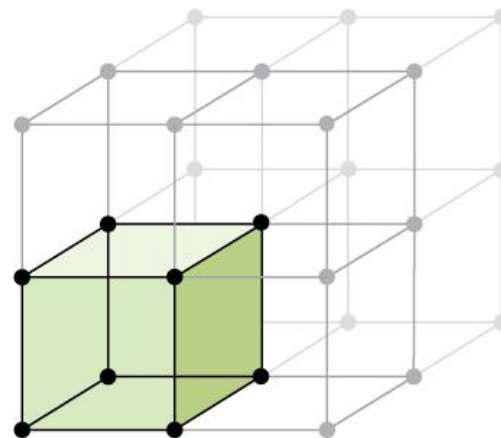
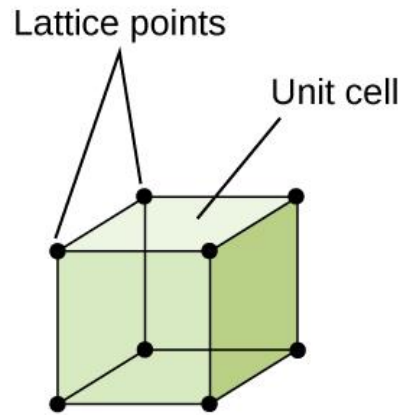
What is crystal?

A material has a crystal structure if its constituents (such as atoms, molecules, or ions) are arranged in a 3D translationally periodic order forming a crystal lattice

$$\text{Crystal} = \text{Lattice} * \text{Motif}$$

A material is a crystal if displays a sharp diffraction pattern with most of intensity concentrated in relatively sharp Bragg peaks.

Unit cell. Translational symmetry



Unit cell: smallest unit that repeats in the lattice (translation)

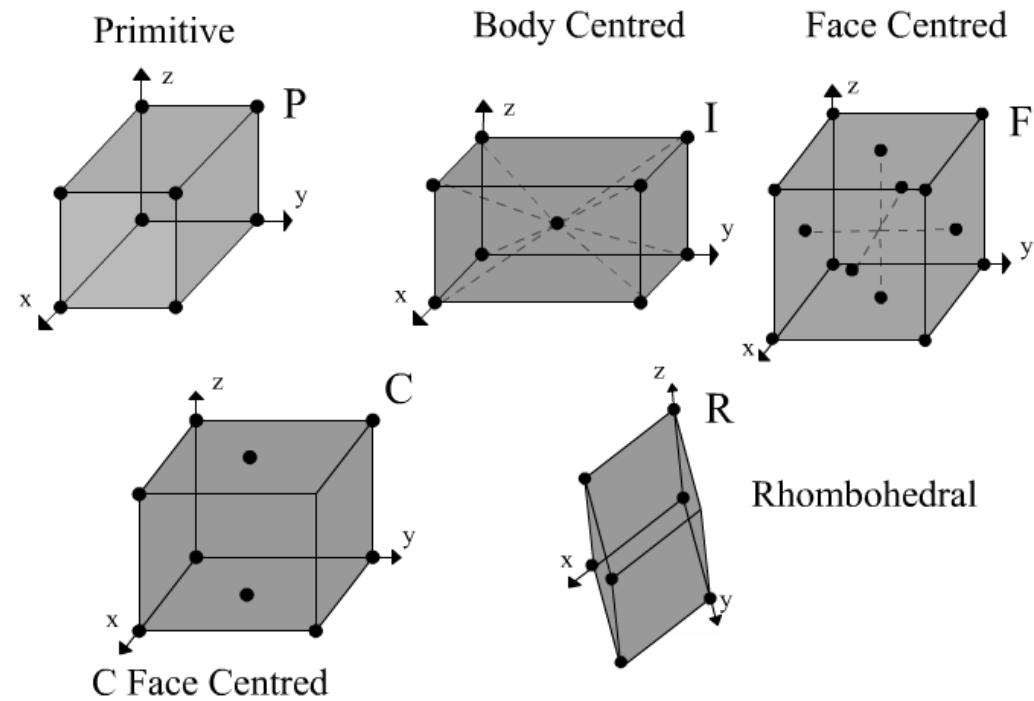
- minimum number of lattice points
- origin on one lattice point
- angles as close to 90° as possible

Unit cell centering

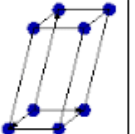
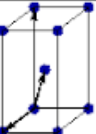
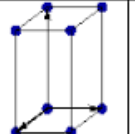
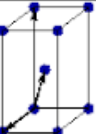
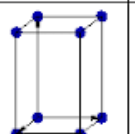
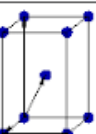
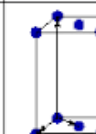
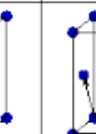
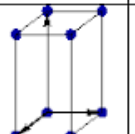
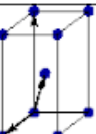
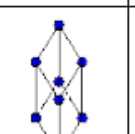
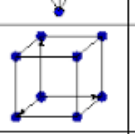
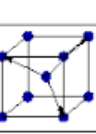
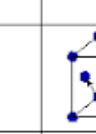
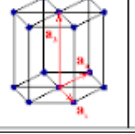
Unit cell: smallest unit that repeats in the lattice (translation)

- Primitive unit cell: lattice point only at corners
- Non-primitive unit cell: lattice points also at other positions

Centring Type	Symbol
Primitive - no centring	P
A-face centred	A
B-face centred	B
C-face centred	C
All-face centred	F
Body centred	I
Rhombohedrally centred	R

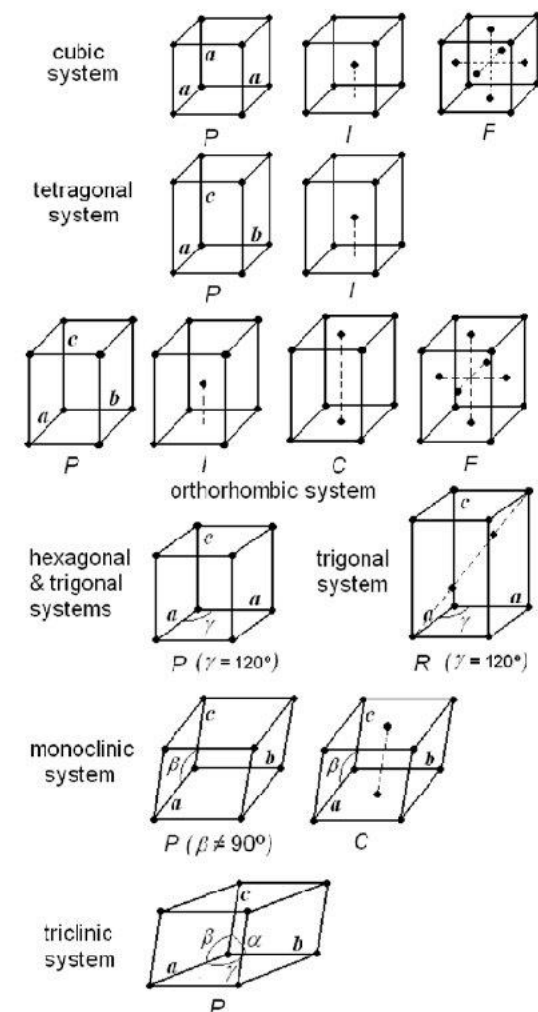


Crystal systems

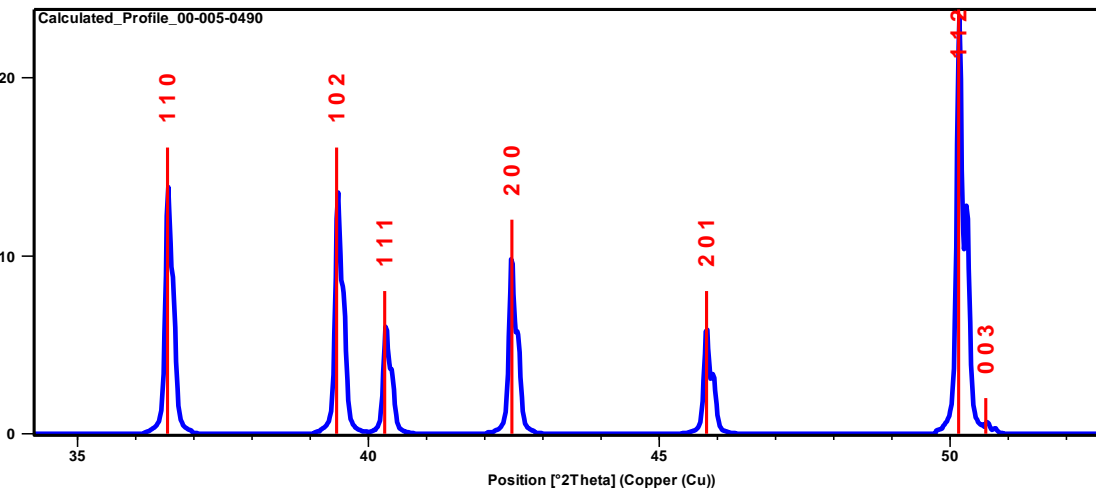
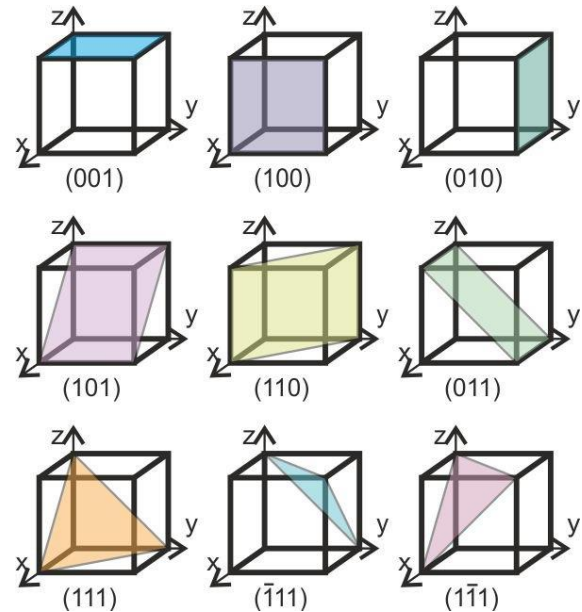
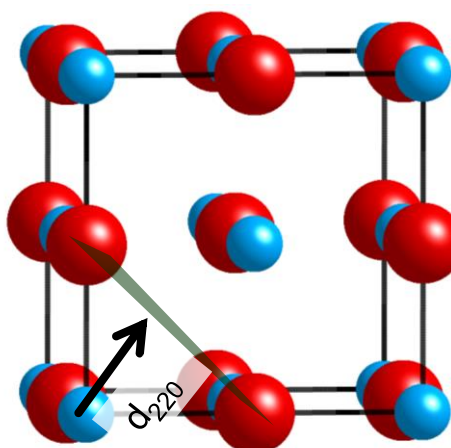
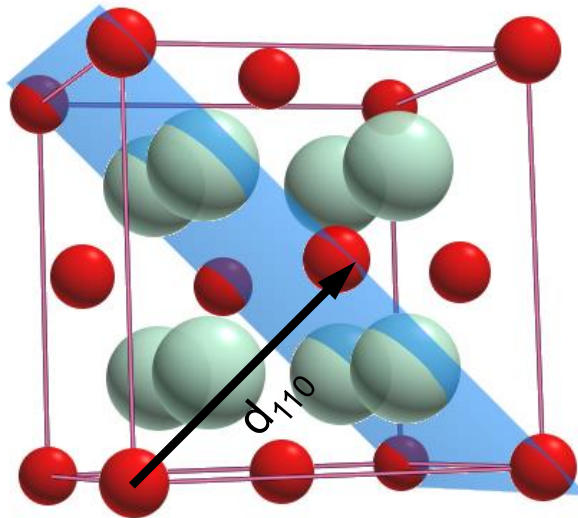
Bravais lattice	Parameters	Simple (P)	Volume centered (I)	Base centered (C)	Face centered (F)
Triclinic	$a_1 \neq a_2 \neq a_3$ $\alpha_{12} \neq \alpha_{23} \neq \alpha_{31}$				
Monoclinic	$a_1 \neq a_2 \neq a_3$ $\alpha_{23} = \alpha_{31} = 90^\circ$ $\alpha_{12} \neq 90^\circ$				
Orthorhombic	$a_1 \neq a_2 \neq a_3$ $\alpha_{12} = \alpha_{23} = \alpha_{31} = 90^\circ$				
Tetragonal	$a_1 = a_2 \neq a_3$ $\alpha_{12} = \alpha_{23} = \alpha_{31} = 90^\circ$				
Trigonal	$a_1 = a_2 = a_3$ $\alpha_{12} = \alpha_{23} = \alpha_{31} < 120^\circ$				
Cubic	$a_1 = a_2 = a_3$ $\alpha_{12} = \alpha_{23} = \alpha_{31} = 90^\circ$				
Hexagonal	$a_1 = a_2 \neq a_3$ $\alpha_{12} = 120^\circ$ $\alpha_{23} = \alpha_{31} = 90^\circ$				

Crystal systems and Bravais lattices

Bravais lattice	Parameters	Simple (P)	Volume centered (I)	Base centered (C)	Face centered (F)
Triclinic	$a_1 \neq a_2 \neq a_3$ $\alpha_{12} \neq \alpha_{23} \neq \alpha_{31}$				
Monoclinic	$a_1 \neq a_2 \neq a_3$ $\alpha_{23} = \alpha_{31} = 90^\circ$ $\alpha_{12} \neq 90^\circ$				
Orthorhombic	$a_1 \neq a_2 \neq a_3$ $\alpha_{12} = \alpha_{23} = \alpha_{31} = 90^\circ$				
Tetragonal	$a_1 = a_2 \neq a_3$ $\alpha_{12} = \alpha_{23} = \alpha_{31} = 90^\circ$				
Trigonal	$a_1 = a_2 = a_3$ $\alpha_{12} = \alpha_{23} = \alpha_{31} < 120^\circ$				
Cubic	$a_1 = a_2 = a_3$ $\alpha_{12} = \alpha_{23} = \alpha_{31} = 90^\circ$				
Hexagonal	$a_1 = a_2 \neq a_3$ $\alpha_{12} = 120^\circ$ $\alpha_{23} = \alpha_{31} = 90^\circ$				

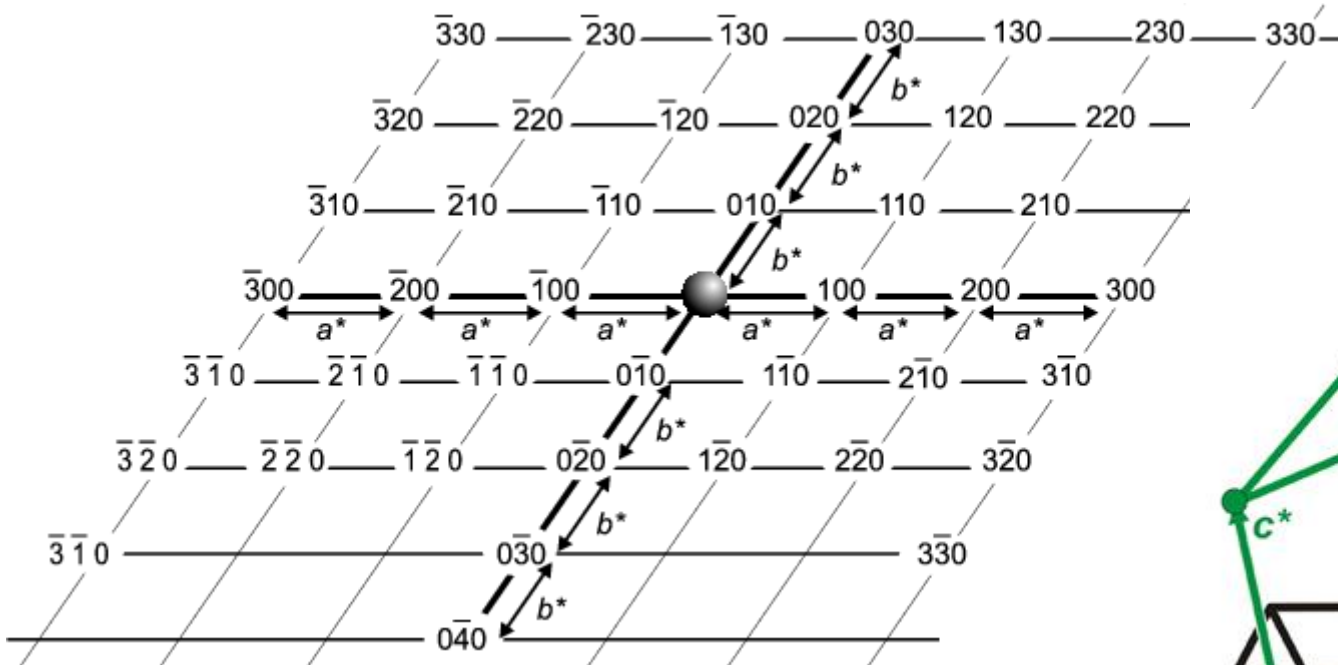


Miller indices (hkl)



Miller indices represent the lattice planes. Peaks in a diffraction pattern can be assigned to planes of the crystal

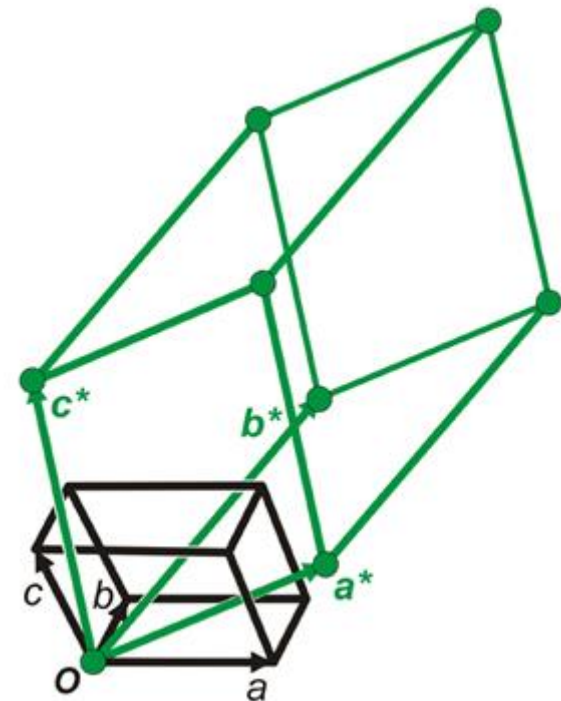
Reciprocal space



$$\mathbf{d}^* = h\mathbf{a}^* + k\mathbf{b}^* + l\mathbf{c}^*$$

$$1/d = d^*$$

$$\mathbf{a}^* = \frac{\mathbf{b} \times \mathbf{c}}{V}; \quad \mathbf{b}^* = \frac{\mathbf{c} \times \mathbf{a}}{V}; \quad \mathbf{c}^* = \frac{\mathbf{a} \times \mathbf{b}}{V};$$



Miller indices (hkl) and d-spacing

Cubic:

$$\frac{1}{d^2} = \frac{h^2 + k^2 + l^2}{a^2}$$

Tetragonal:

$$\frac{1}{d^2} = \frac{h^2 + k^2}{a^2} + \frac{l^2}{c^2}$$

Hexagonal:

$$\frac{1}{d^2} = \frac{4}{3} \left(\frac{h^2 + hk + k^2}{a^2} \right) + \frac{l^2}{c^2}$$

Rhombohedral:

$$\frac{1}{d^2} = \frac{(h^2 + k^2 + l^2) \sin^2 \alpha + 2(hk + kl + hl)(\cos^2 \alpha - \cos \alpha)}{a^2(1 - 3 \cos^2 \alpha + 2 \cos^3 \alpha)}$$

Orthorhombic:

$$\frac{1}{d^2} = \frac{h^2}{a^2} + \frac{k^2}{b^2} + \frac{l^2}{c^2}$$

Monoclinic:

$$\frac{1}{d^2} = \frac{1}{\sin^2 \beta} \left(\frac{h^2}{a^2} + \frac{k^2 \sin^2 \beta}{b^2} + \frac{l^2}{c^2} - \frac{2hl \cos \beta}{ac} \right)$$

Systematic absences

TABLE 4.1.8. Determination of Lattice Type from General Reflections, hkl

Condition for possible reflection ⁽¹⁾	Lattice type	Symbol
$h+k=2n$	Centred on the C-face (001)	C
$k+l=2n$	Centred on the A-face (100)	A
$l+h=2n$	Centred on the B-face (010)	B
h, k, l all odd or all even	Centred on all faces	F
$h+k+l=2n$	Body centred	I
$\begin{cases} -h+k+l=3n^{(2)} \\ +h-k+l=3n^{(2)} \end{cases}$	Obverse position } rhombohedral Reverse position } lattice ⁽³⁾	R
$h-k=3n$	Hexagonal. Triple unit cell as in Fig. 2.5.2(a)	H ⁽⁴⁾
No restriction	Primitive	P ⁽⁵⁾

⁽¹⁾ The symbol n stands here for any integer.

⁽²⁾ These conditions refer to indexing on hexagonal axes which are always used both for hexagonal crystals and, in the first instance, for trigonal crystals, although some of the latter may turn out to be more simply described on rhombohedral axes.

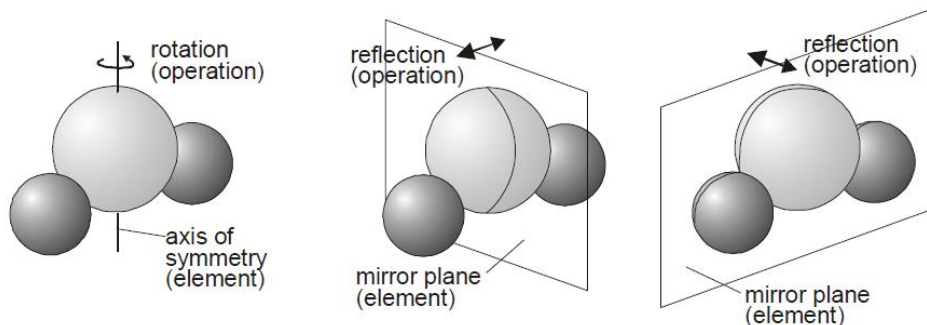
⁽³⁾ For definition of "obverse" and "reverse" see section 2.5, Fig. 2.5.3.

⁽⁴⁾ The symbol H is dropped in the present volume for systematic description (see, however, section 2.5).

⁽⁵⁾ The symbol P is applied in the present work also to the primitive hexagonal lattice which was designated by the symbol C in the former *International Tables* (1935). See Note 7, Table 2.2.1.

Rotary-Inversion Symmetry

Symmetry operation	Symmetry elements
Identity	----
Rotation by $360^\circ/n$	n-fold axis
Reflection	mirror plane
Inversion	point



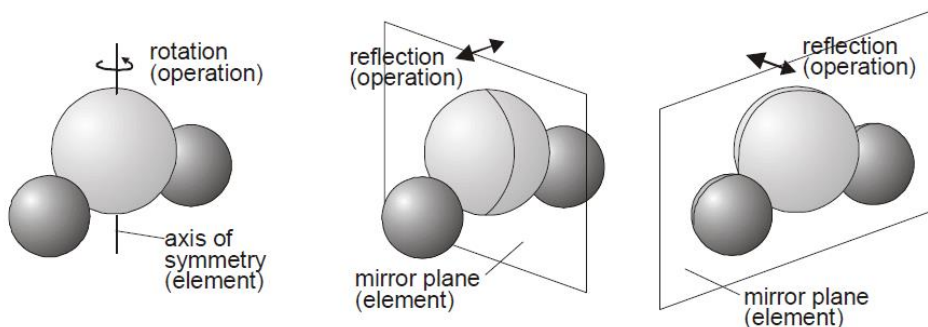
Translation
(Bravais lattice)



screw axis
glide plane

Rotary-Inversion Symmetry

Symmetry operation	Symmetry elements
Identity	----
Rotation by $360^\circ/n$	n-fold axis
Reflection	mirror plane
Inversion	point



Translation
(Bravais lattice)



**230 space
groups**
e.g. *Pm3m**

*<http://img.chem.ucl.ac.uk/sgp/misc/notation.htm>

Space groups

Triclinic: e.g. $P\bar{1}$

1. An inversion centre (presence or absence)

Monoclinic: e.g. $P2$, Pm , $P2/m$

1. A symmetry with respect to the unique axis direction (b or c)

Orthorhombic: e.g. $P222$, $Pmm2$ (or $Pm2m$ or $P2mm$), $Pmmm$

1. A symmetry with respect to the a axis
2. A symmetry with respect to the b axis
3. A symmetry with respect to the c axis

Tetragonal: e.g. $P4$, $P\bar{4}$, $P4/m$, $P422$, $P4mm$, $P\bar{4}2m$ (or $P4m2$), $P4/mmm$

1. The 4-fold symmetry parallel to the c axis
2. The symmetry with respect to both the x and y axes
3. The symmetry with respect to the face diagonals (1 1 0)

Space groups

Trigonal & Rhombohedral: e.g. $P3$, $P-3$, $P321$, $P312$, $P3m1$, $P31m$, $P-3m1$, $P-31m$

1. The 3-fold symmetry parallel to the c axis
2. The symmetry with respect to the a and b axes
3. The additional symmetry elements

Hexagonal: e.g. $P6$, $P-6$, $P6/m$, $P622$, $P6mm$, $P-62m$ (or $P-6m2$), $P6/mmm$

1. The 6-fold symmetry parallel to the c axis
2. The symmetry with respect to the a and b axes
3. The additional symmetry elements

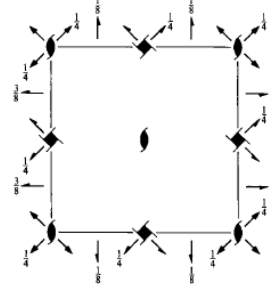
Cubic: e.g. $P23$, $Pm-3$, $P432$, $P-43m$, $Pm3m$

1. The symmetry with respect to the a , b , and c axes
2. The 3-fold symmetry of the body diagonals (1 1 1)
3. The symmetry with respect to the face diagonals (1 1 0)

Tables for X-ray Crystallography

 $P4_32_12$ D_4^8

No. 96

Origin on $2[110]$ at $2, 1(1, 2)$ Asymmetric unit $0 \leq x \leq 1; 0 \leq y \leq 1; 0 \leq z \leq \frac{1}{4}$

Symmetry operations

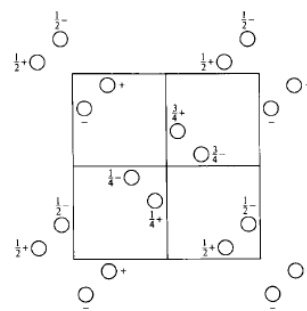
$$\begin{array}{llll} (1) 1 & (2) 2(0, 0, \frac{1}{2}) & 0, 0, z & (3) 4'(0, 0, \frac{1}{2}) & 0, \frac{1}{2}, z \\ (5) 2(0, \frac{1}{2}, 0) & (6) 2(\frac{1}{2}, 0, 0) & x, \frac{1}{2}, \frac{1}{2} & (7) 2 & x, x, 0 \\ & & & (8) 2 & x, \bar{x}, \frac{1}{2} \end{array}$$

422

Tetragonal

CONTINUED

No. 96

 $P4_32_12$ Patterson symmetry $P4/mmm$ Generators selected (1); $t(1, 0, 0); t(0, 1, 0); t(0, 0, 1)$; (2); (3); (5)

Positions

Multiplicity,
Wyckoff letter,
Site symmetry

Coordinates

Reflection conditions

$$\begin{array}{llll} 8 & b & 1 & (1) x, y, z \\ & & & (2) \bar{x}, \bar{y}, z + \frac{1}{2} \\ & & & (5) \bar{x} + \frac{1}{2}, y + \frac{1}{2}, \bar{z} + \frac{1}{2} \\ & & & (6) x + \frac{1}{2}, \bar{y} + \frac{1}{2}, \bar{z} + \frac{1}{2} \\ & & & (7) y, x, \bar{z} \\ & & & (8) \bar{y}, \bar{x}, \bar{z} + \frac{1}{2} \end{array}$$

General:

$$\begin{array}{l} 00l : l = 4n \\ h00 : h = 2n \end{array}$$

$$4 \quad a \quad . . 2 \quad x, x, 0 \quad \bar{x}, \bar{x}, \frac{1}{2} \quad \bar{x} + \frac{1}{2}, x + \frac{1}{2}, \frac{1}{2} \quad x + \frac{1}{2}, \bar{x} + \frac{1}{2}, \frac{1}{2}$$

Special: as above, plus
 $0kl : l = 2n + 1$
or $2k + l = 4n$

Symmetry of special projections

Along [001] $p4gm$

$$\mathbf{a}' = \mathbf{a} \quad \mathbf{b}' = \mathbf{b}$$

Origin at $0, \frac{1}{2}, z$ Along [100] $p2gg$

$$\mathbf{a}' = \mathbf{b} \quad \mathbf{b}' = \mathbf{c}$$

Origin at $x, \frac{1}{2}, \frac{1}{8}$ Along [110] $p2gm$

$$\mathbf{a}' = \frac{1}{2}(-\mathbf{a} + \mathbf{b}) \quad \mathbf{b}' = \mathbf{c}$$

Origin at $x, x, 0$

Maximal non-isomorphic subgroups

$$\begin{array}{ll} \text{I} & [2] P4_311(P4_3, 78) \quad 1; 2; 3; 4 \\ & [2] P2_112(C222_1, 20) \quad 1; 2; 7; 8 \\ & [2] P2_12_1(P2_12_1, 19) \quad 1; 2; 5; 6 \end{array}$$

IIa none

IIb none

Maximal isomorphic subgroups of lowest index

$$\text{IIc} \quad [3] P4_32_2(\mathbf{c}' = 3\mathbf{c}) (92); [5] P4_32_1(\mathbf{c}' = 5\mathbf{c}) (96); [9] P4_32_2(\mathbf{a}' = 3\mathbf{a}, \mathbf{b}' = 3\mathbf{b}) (96)$$

Minimal non-isomorphic supergroups

$$\text{I} \quad [3] P4_332(212)$$

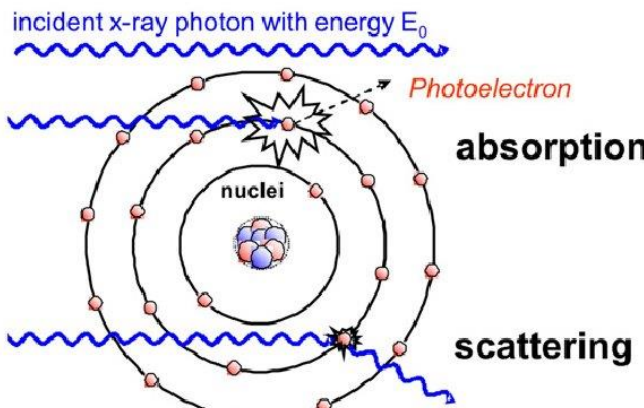
$$\text{II} \quad [2] C4_322(P4_322, 95); [2] I4_122(98); [2] P4_32_2(\mathbf{c}' = \frac{1}{3}\mathbf{c}) (94)$$

Brief history of XRD

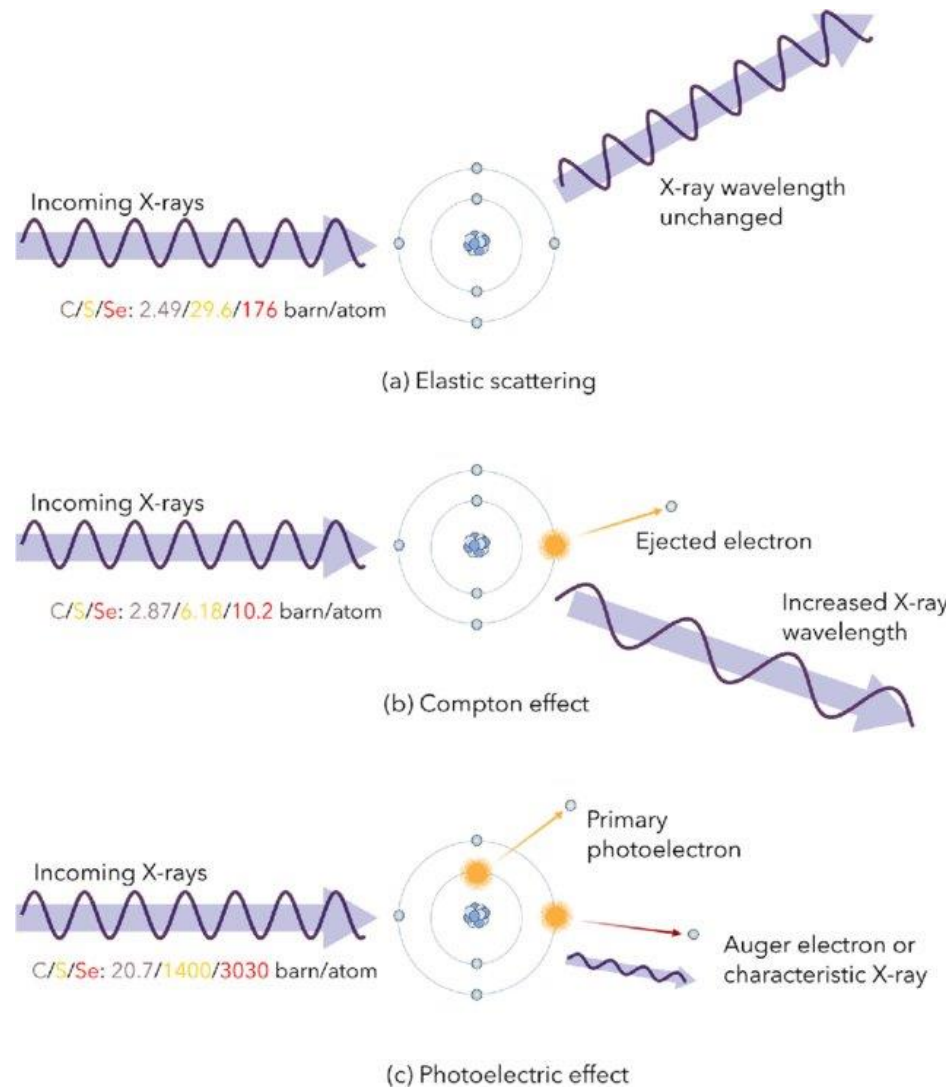
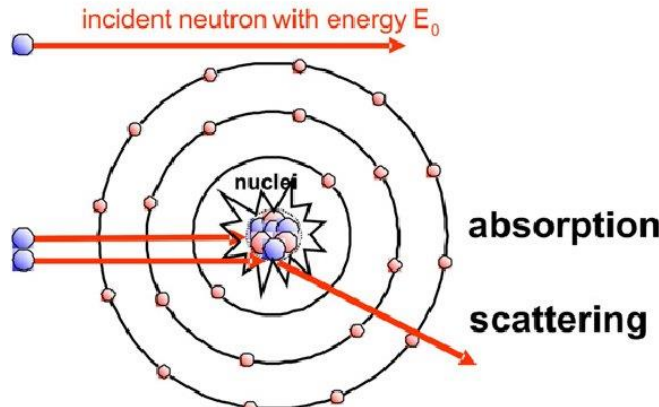
- 1895- Wilhelm Röntgen publishes the discovery of X-rays
- 1912- Maxwell von Laue observes diffraction of X-rays from a crystal
- 1913- Lawrence Bragg and William Henry Bragg solve the first crystal structure from X-ray diffraction data

Elastic scattering

(a) X-rays

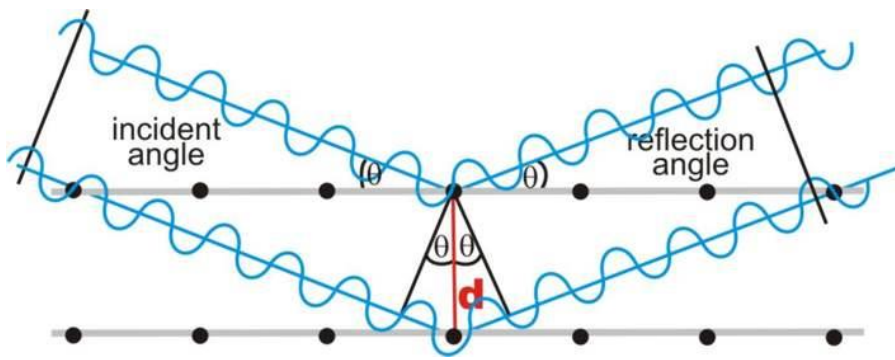


(b) neutrons

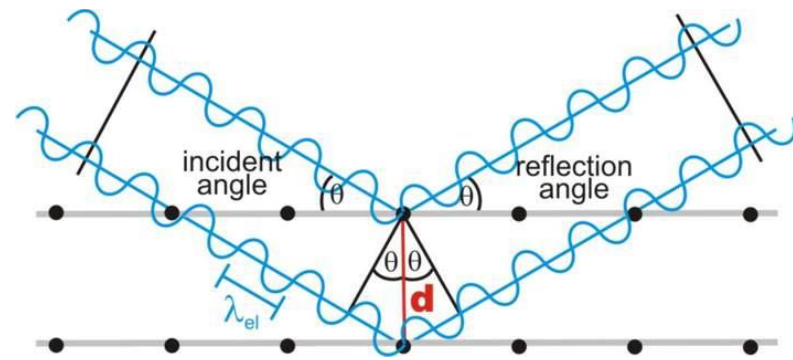


Bragg's Law

Elastic scattering phenomenon that occurs when a plane wave interacts with an obstacle or a slit whose size is approximately that of the wavelength



Destructive interference (out of phase).



Constructive interference (in phase).

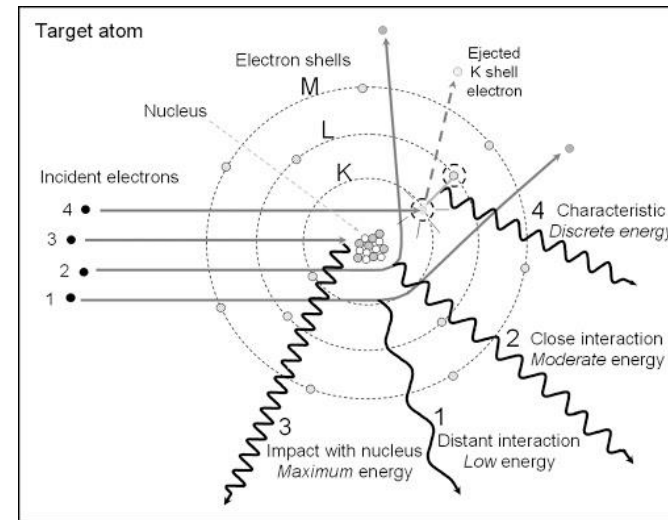
$$\text{Bragg's Law } n\lambda = 2ds\sin\theta$$

X-ray light source

Particle accelerator (synchrotron source):
Electrons accelerated at velocity close to the speed of light emit electromagnetic radiation in the region of X-rays.

- Tunable wavelength
- High brilliance (many photons of a given wavelength and direction)
- X-rays: very high resolution

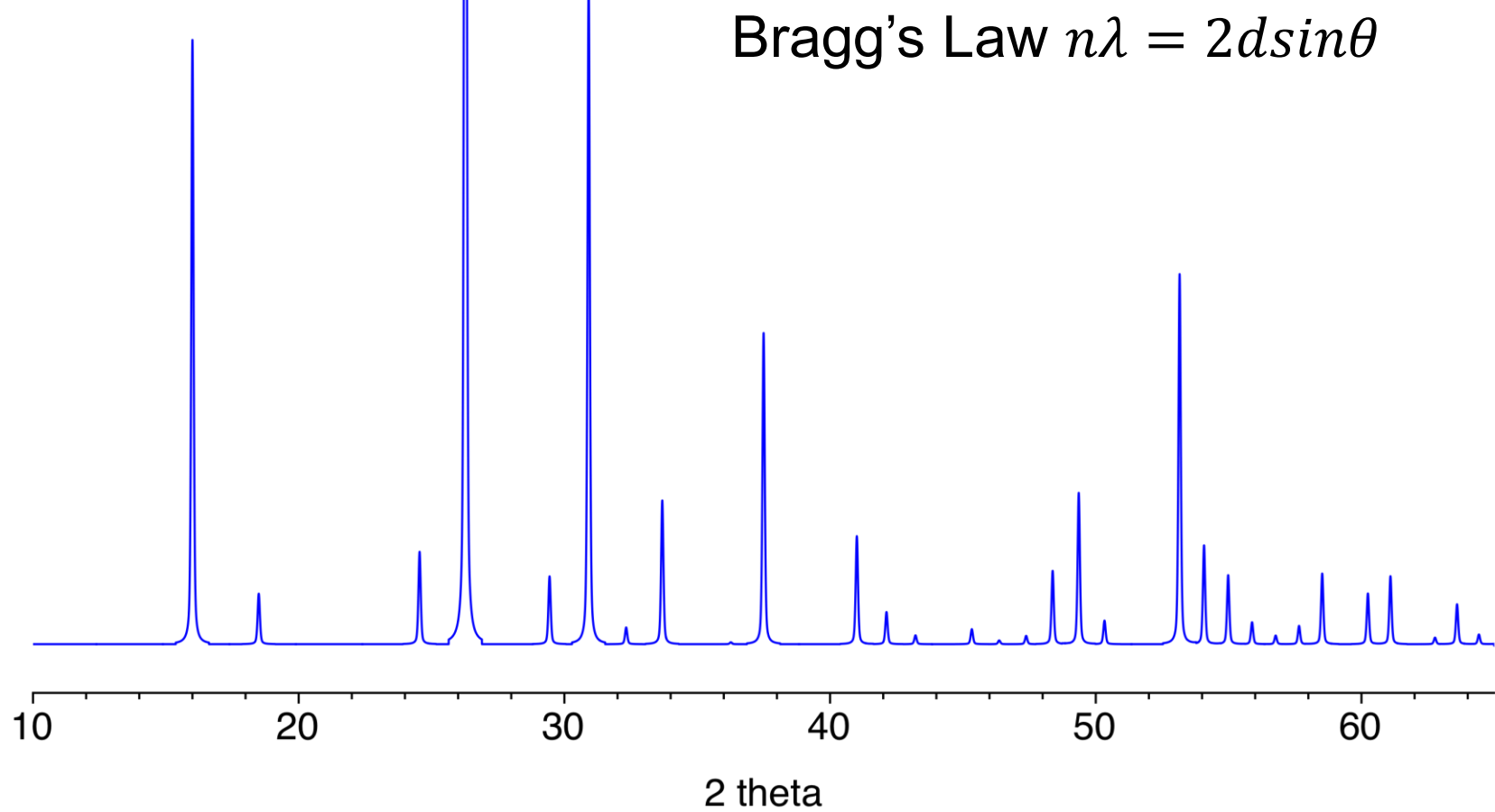
In-house diffraction: Energy released when an electron from an outer shell “fills the gap” left by an inner shell electron that has been ionized. $K\alpha$ Cu (1.5418 Å) is the most common



Comparison of different radiations

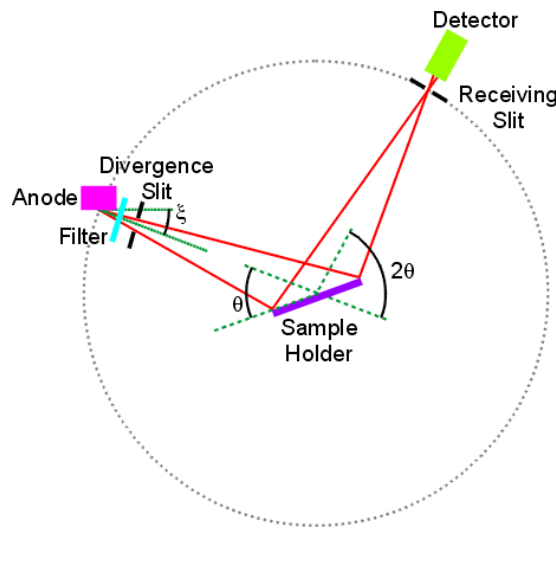
	X-ray (powder)	Electrons	Neutrons (powder)
Data collection	easy	Less easy	difficult
Crystallite size	µm	nm	µm
Lattice parameters	precise	approximate	precise
Intensities	kinematical	dynamical	kinematical
Overlap	yes	no	yes
Image	no	yes	no
Magnetic moment	no	yes	yes
Scattering power against Z	smooth	smooth	irregular

X-ray Powder Diffraction

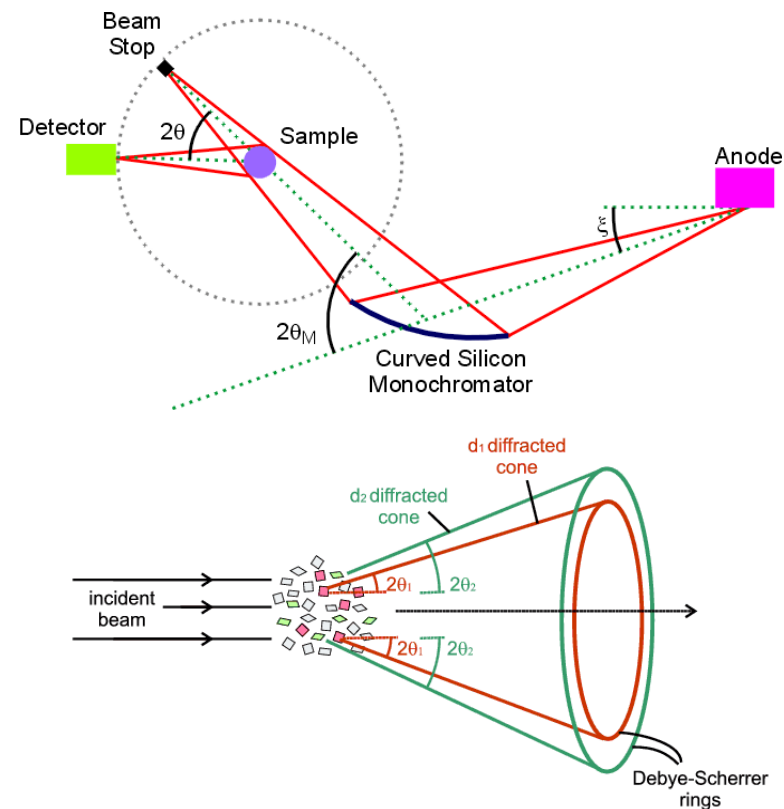


Diffraction geometry

The Bragg-Brentano (reflection) geometry needs the simultaneous, equiaxial move of the anode and the detector (2θ) to provide the constant irradiated volume from a sample



The Debye-Scherrer (transmission) geometry



Structure factor

$$F_{hkl} = \sum_j f_j \cdot e^{i2\pi(hx_j + ky_j + lz_j)} = |F_{hkl}| \cdot e^{i\phi_{hkl}}$$

Structure factor phases are lost in diffraction data

From the Structure Factor to Measured Intensities

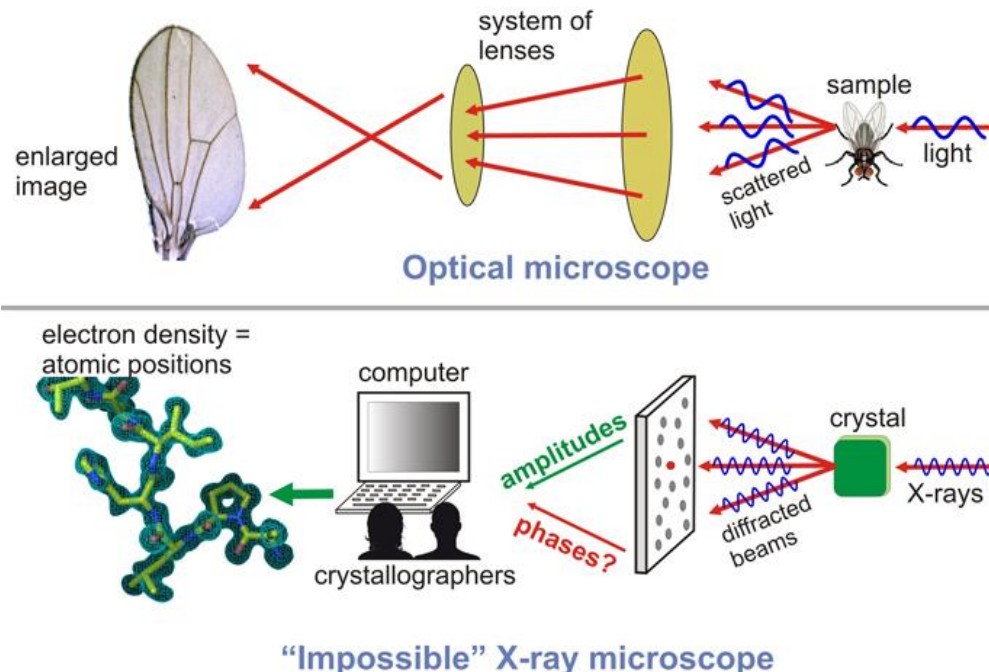
$$I_{\text{obs}}(hkl) = c j P L A |F_{\text{obs}}(hkl)|^2$$

- multiplicity, j
- the polarization factor, P
- the Lorentz factor, L
- X-ray absorption, A
- temperature

Structure factor

$$F_{hkl} = \sum_j f_j \cdot e^{i2\pi(hx_j + ky_j + lz_j)} = |F_{hkl}| \cdot e^{i\phi_{hkl}}$$

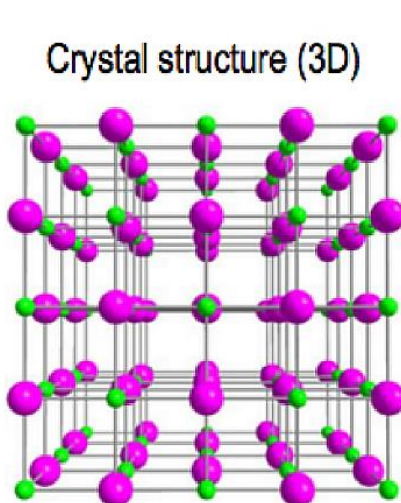
Structure factor phases are lost in diffraction data



Structure factor

$$F_{hkl} = \sum_j f_j \cdot e^{i2\pi(hx_j + ky_j + lz_j)} = |F_{hkl}| \cdot e^{i\phi_{hkl}}$$

Structure factor phases are lost in diffraction data

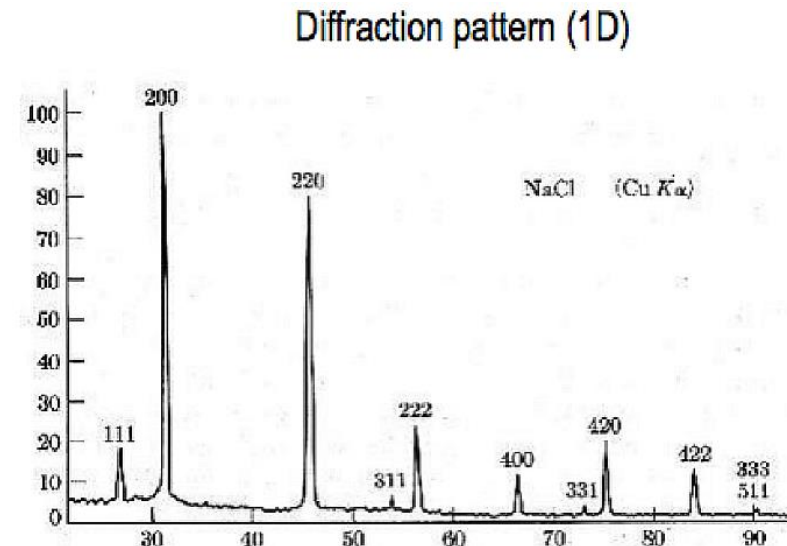


$$F(\mathbf{h}) = \int_{cell} \rho(\mathbf{x}) \exp(2\pi i \mathbf{h} \cdot \mathbf{x}) d\mathbf{v}$$

Diffraction experiment

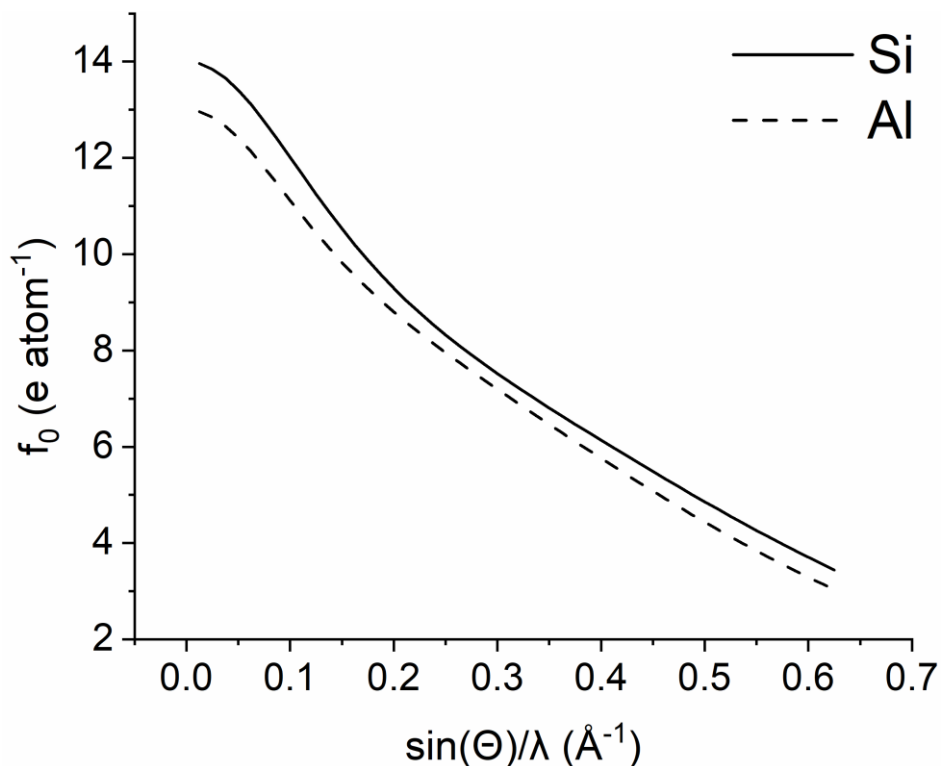
$$\rho(\mathbf{x}) = \frac{1}{V} \sum_{\mathbf{h}} F(\mathbf{h}) \exp(-2\pi i \mathbf{h} \cdot \mathbf{x})$$

Structure solution



X-ray Atomic Form Factor

Atomic form factor represents the scattering power of specific element regardless its positioning or symmetry. It depends only on number of electrons, radiation energy and Debye-Waller factor (2Θ)



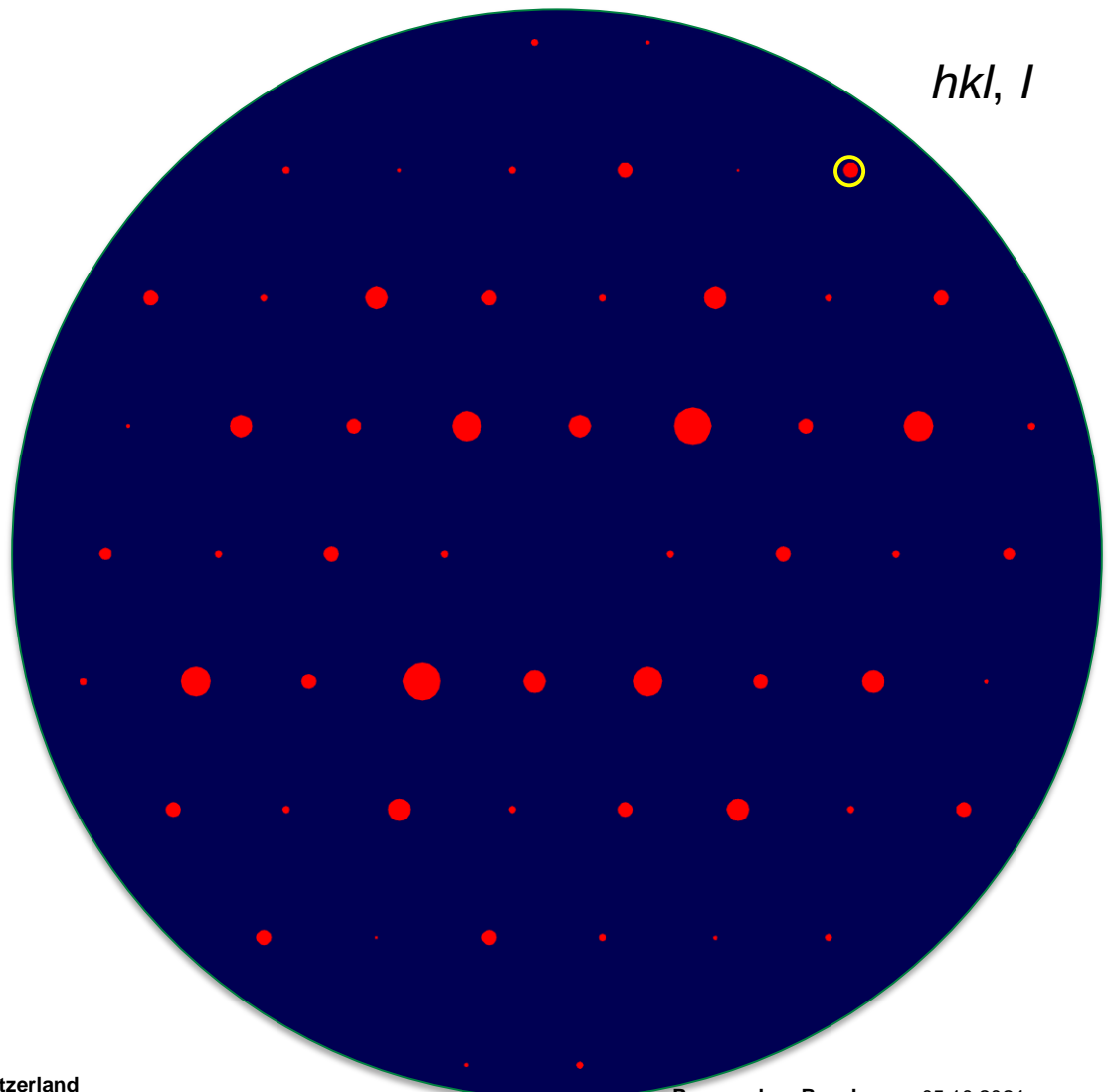
Silicon and aluminum demonstrate similar atomic number ($Z=14$ and 13) and are difficult to be distinguished

X-ray Single-crystal Diffraction

X-rays



$10^6 \mu\text{m}^3$

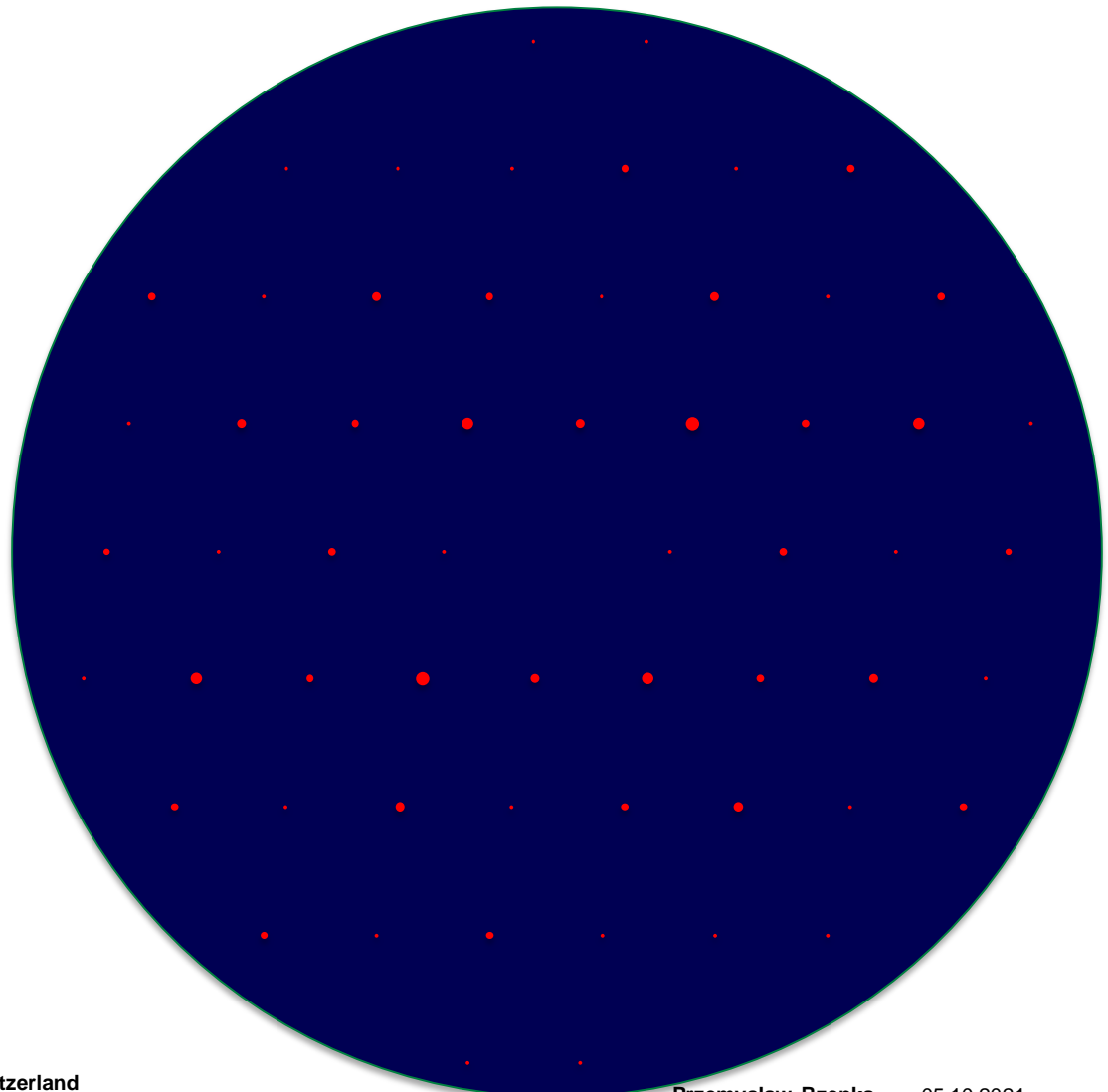


X-ray Powder Diffraction

X-rays

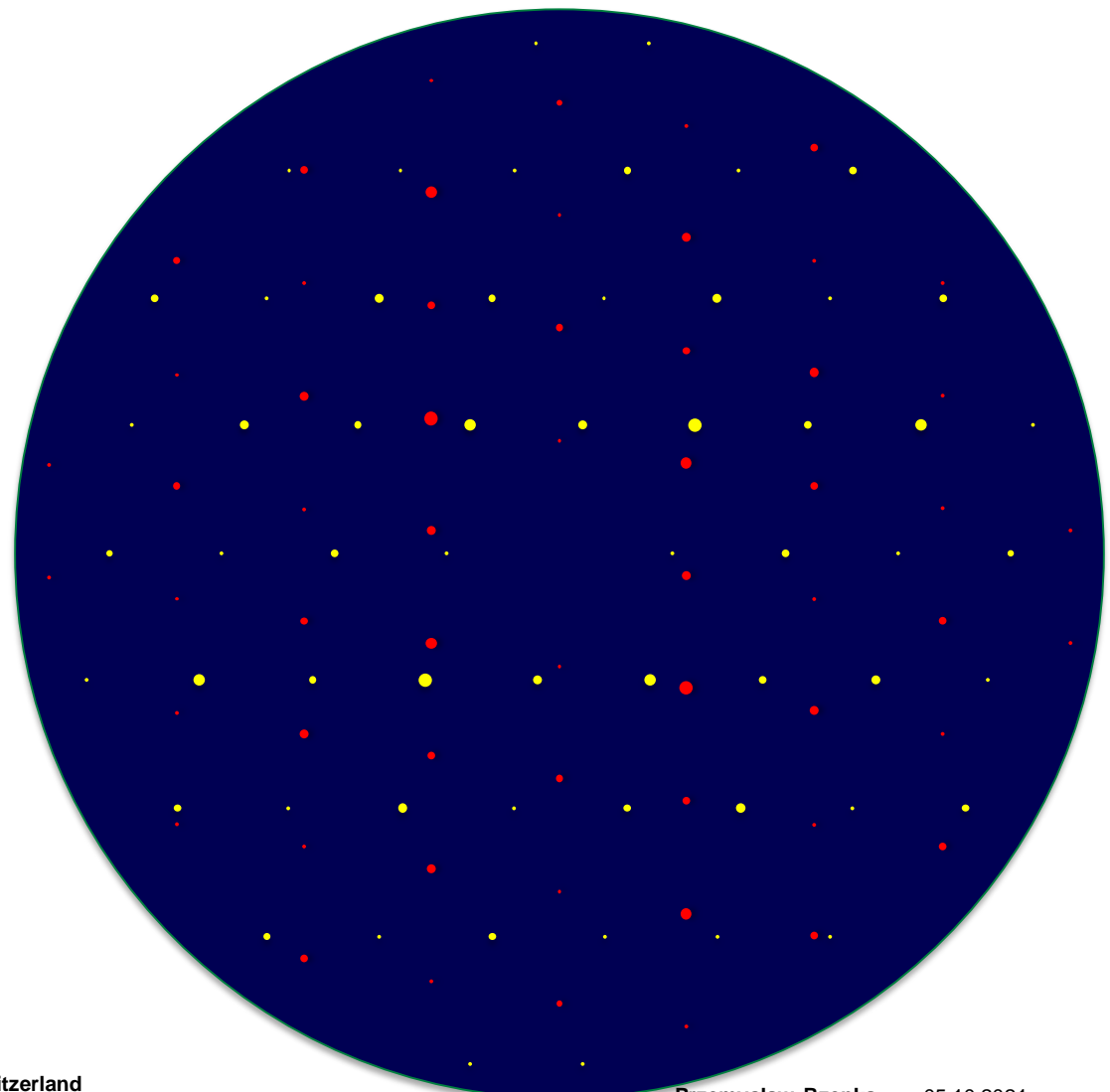


$1 \mu\text{m}^3$



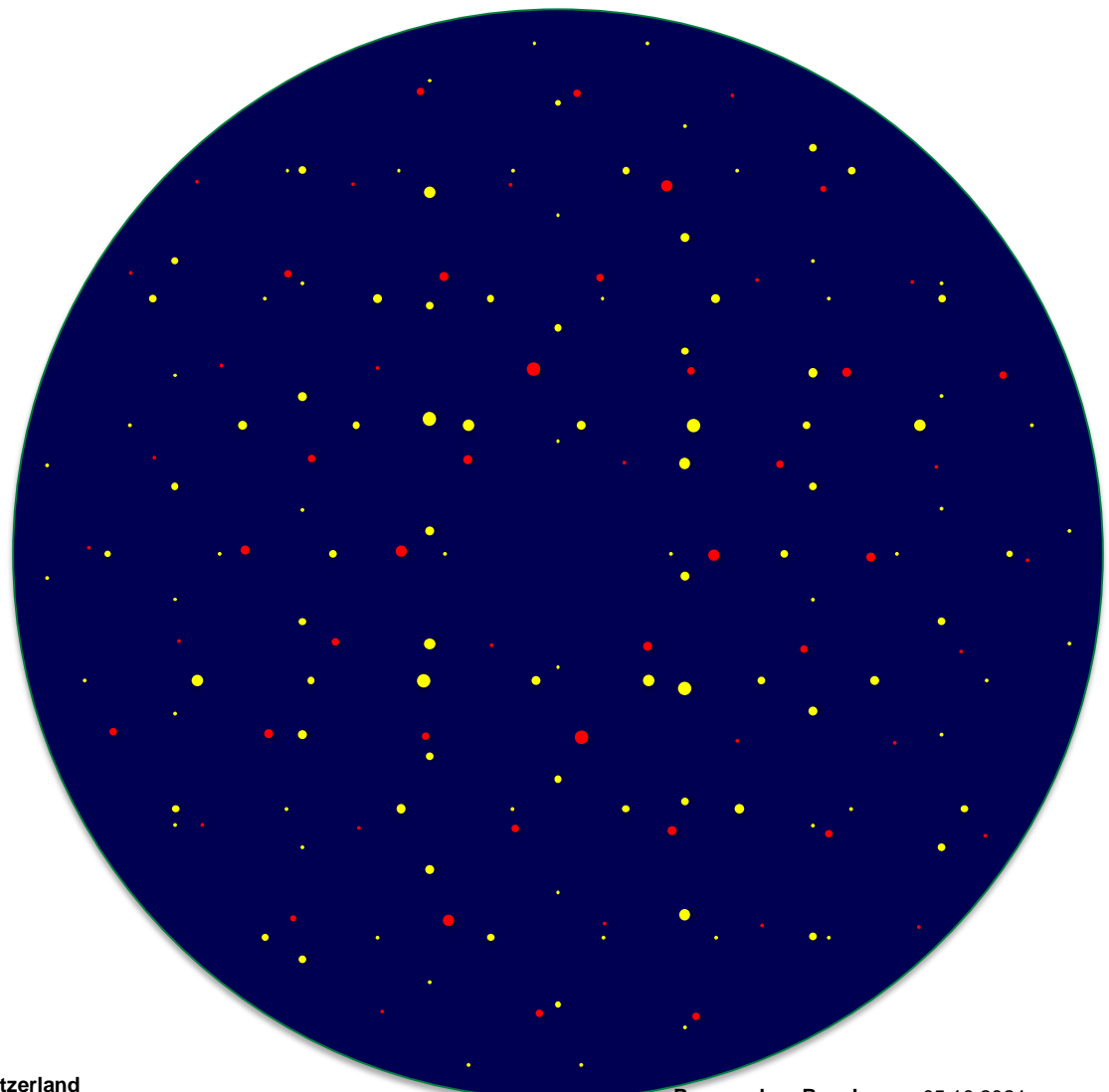
X-ray Powder Diffraction

X-rays



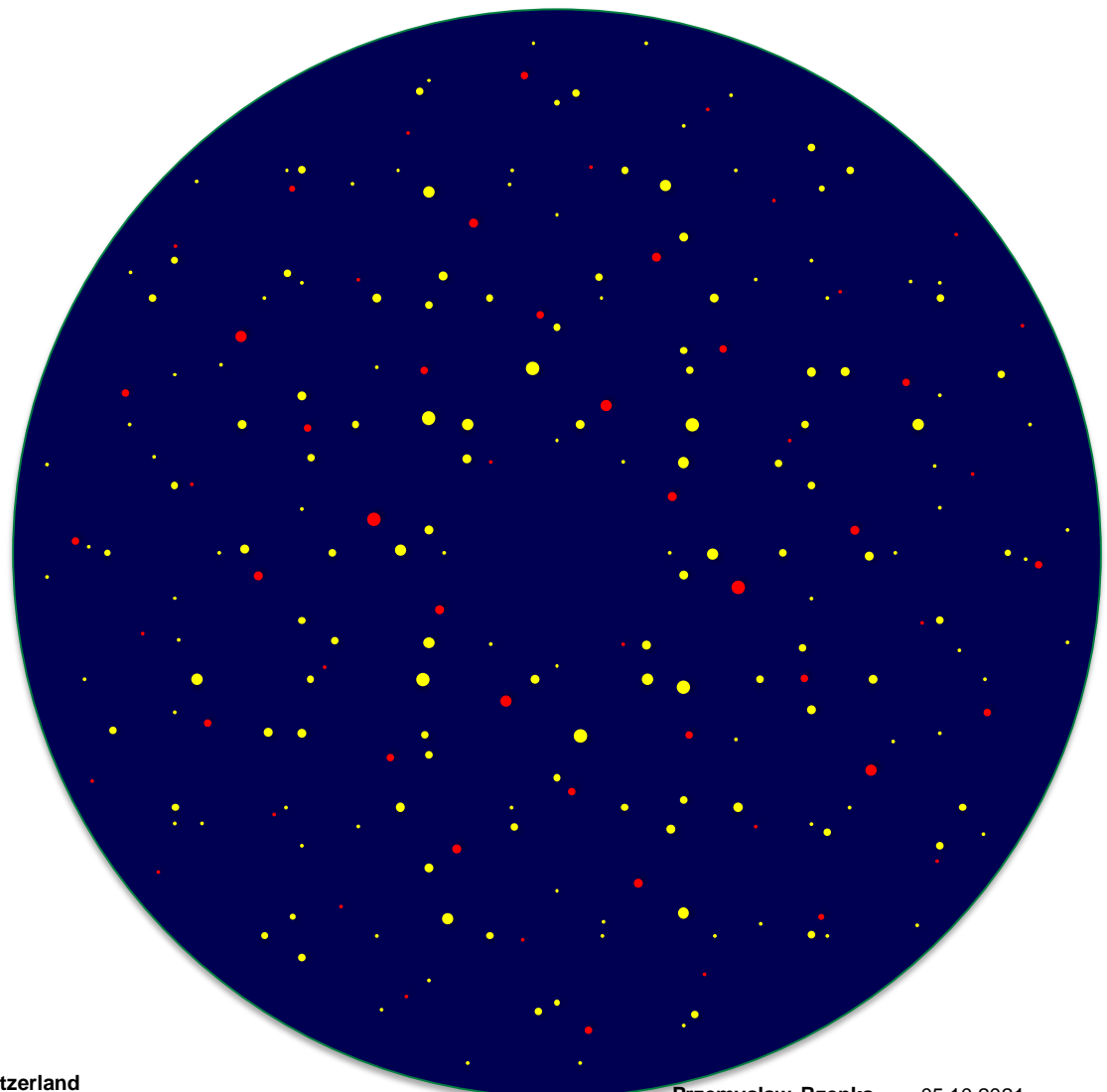
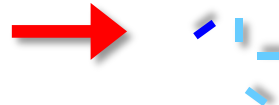
X-ray Powder Diffraction

X-rays



X-ray Powder Diffraction

X-rays



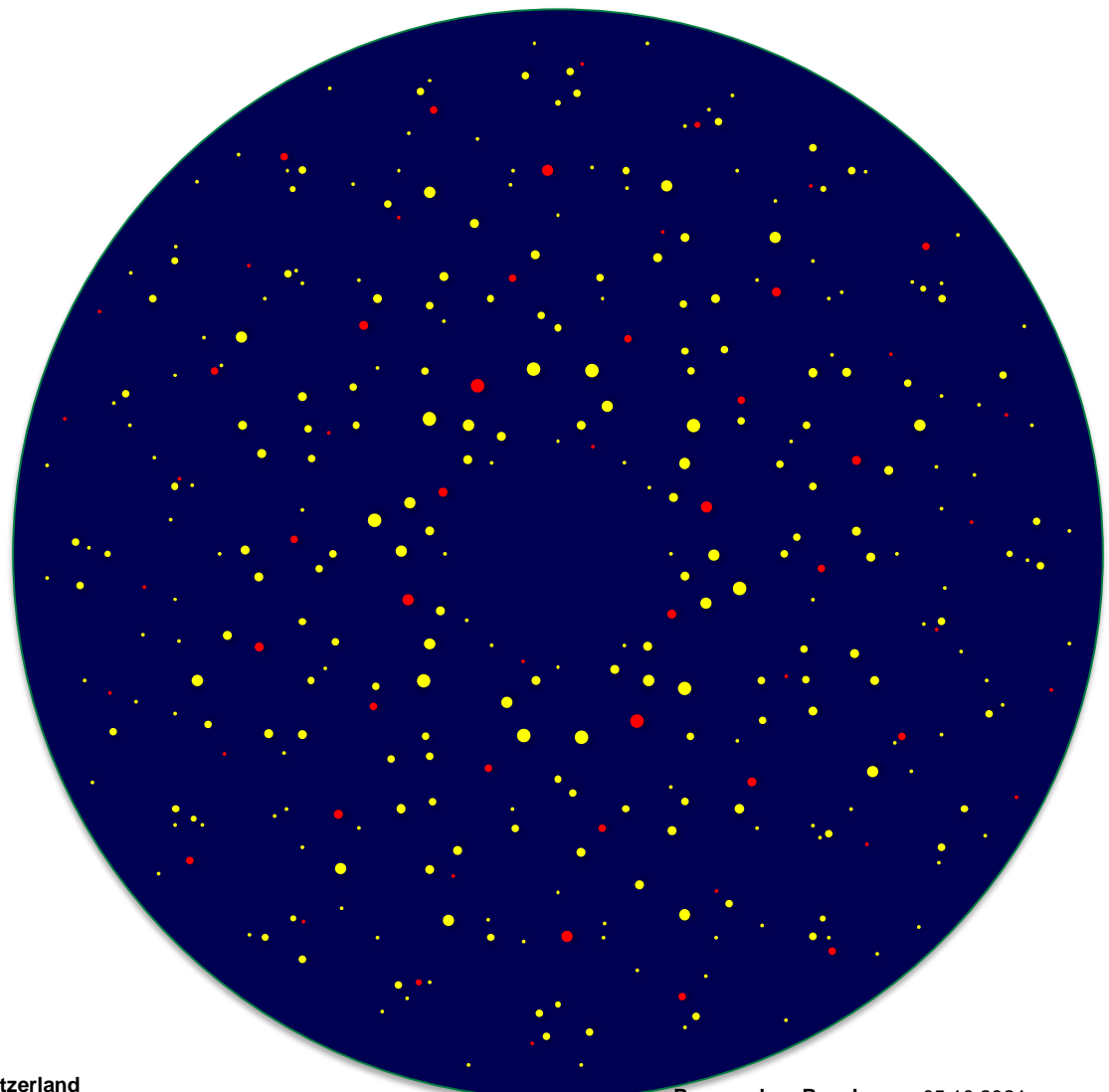
X-ray Powder Diffraction

X-rays



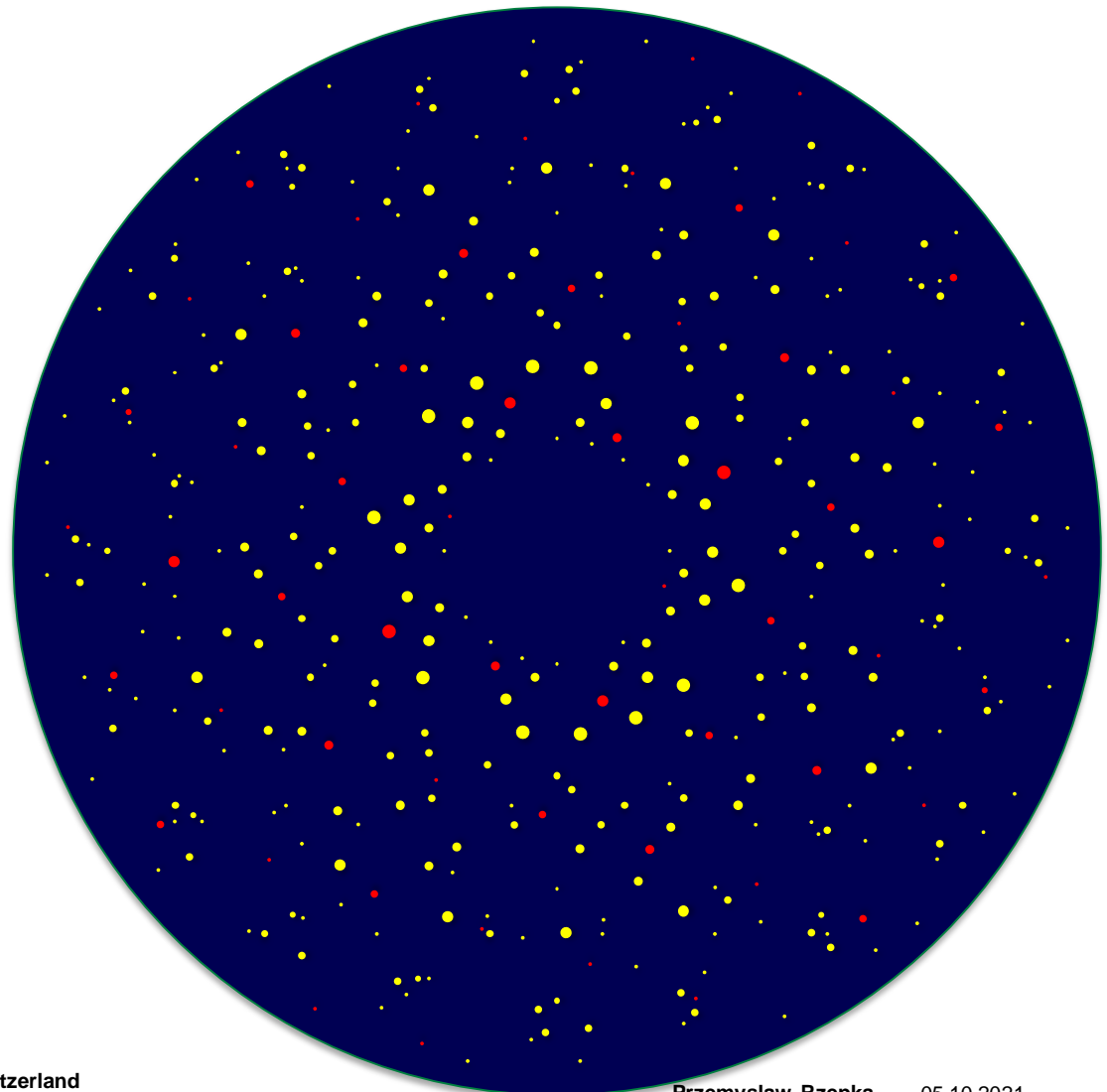
X-ray Powder Diffraction

X-rays



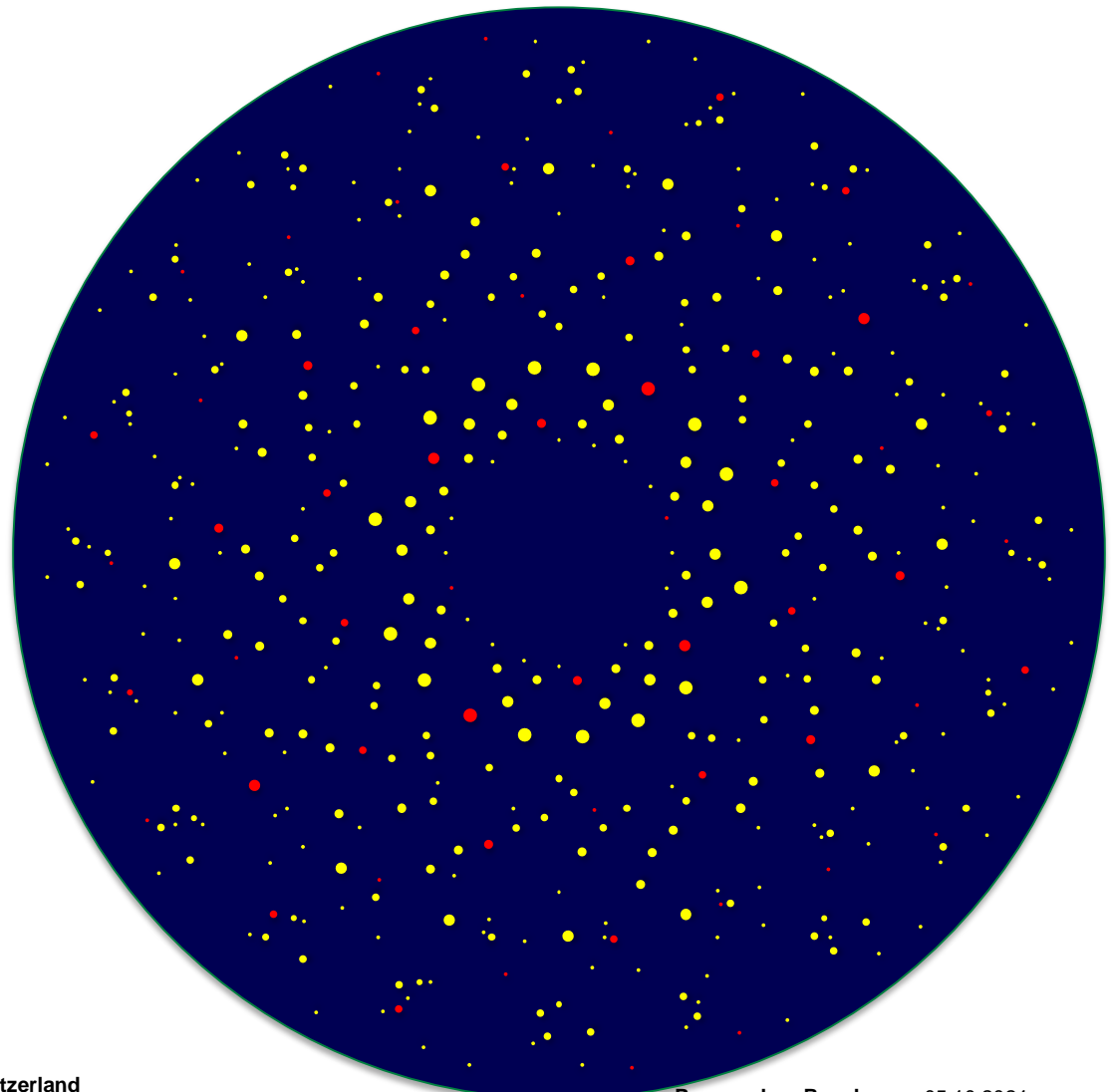
X-ray Powder Diffraction

X-rays



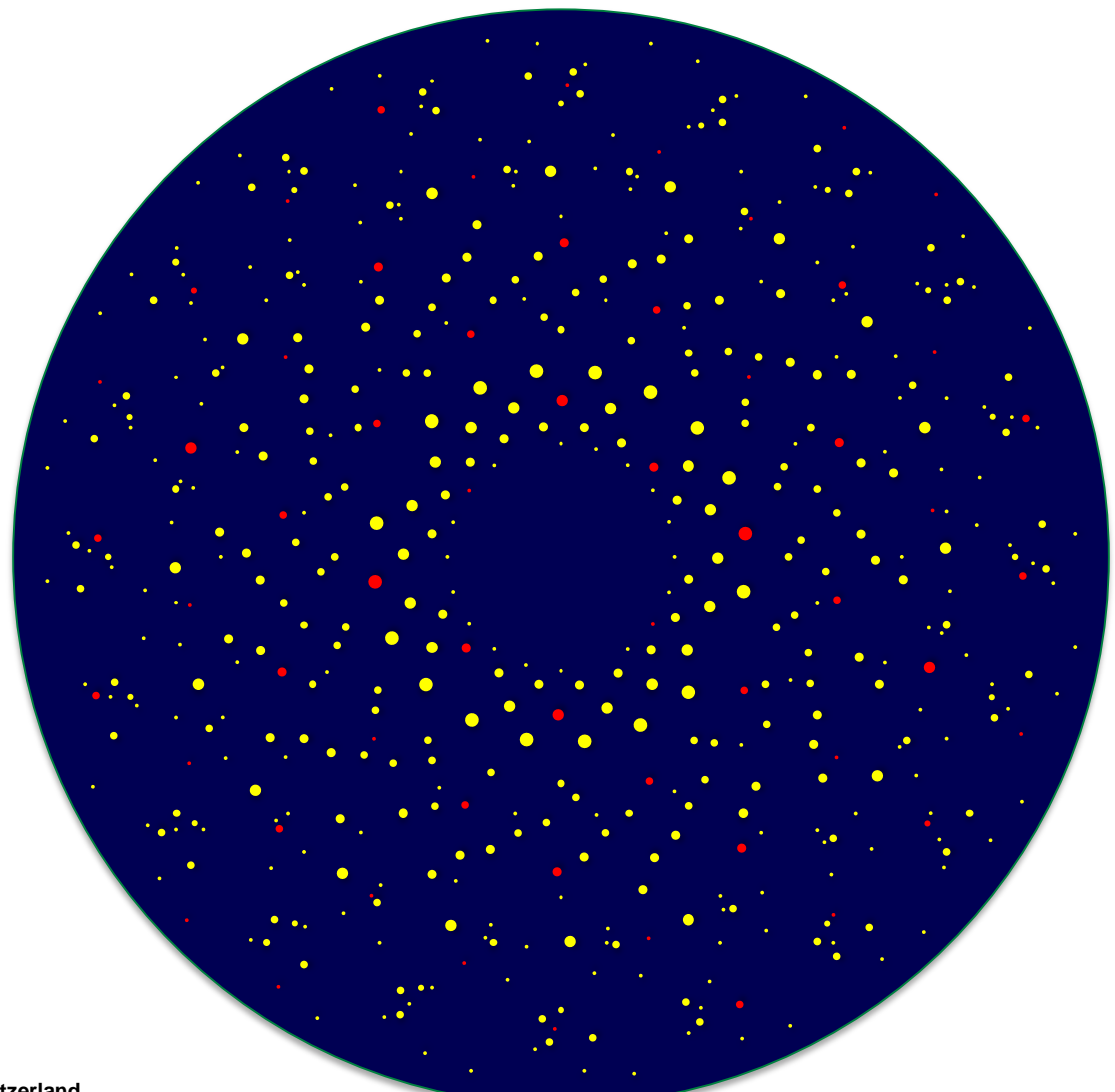
X-ray Powder Diffraction

X-rays

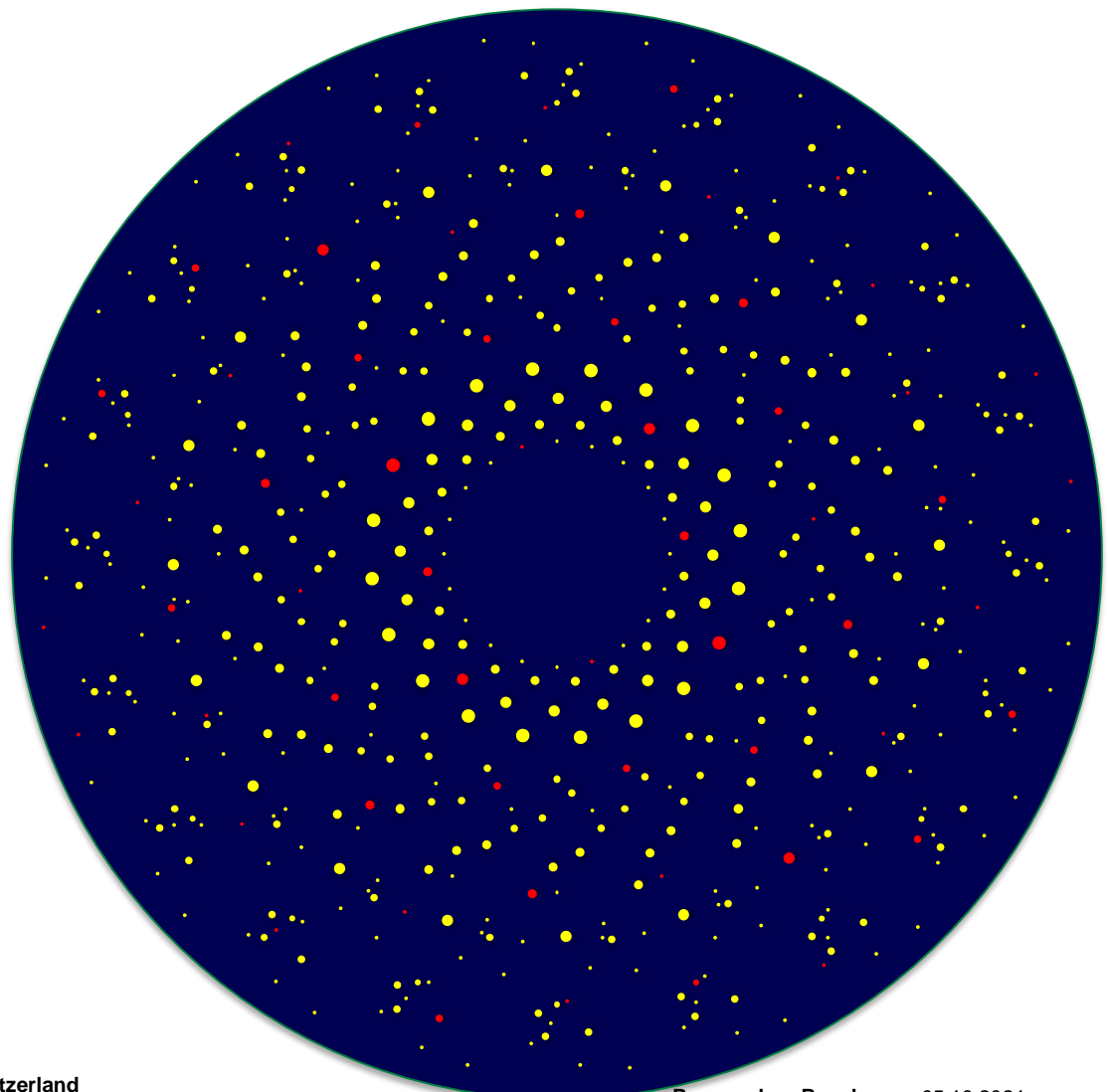
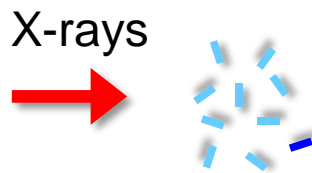


X-ray Powder Diffraction

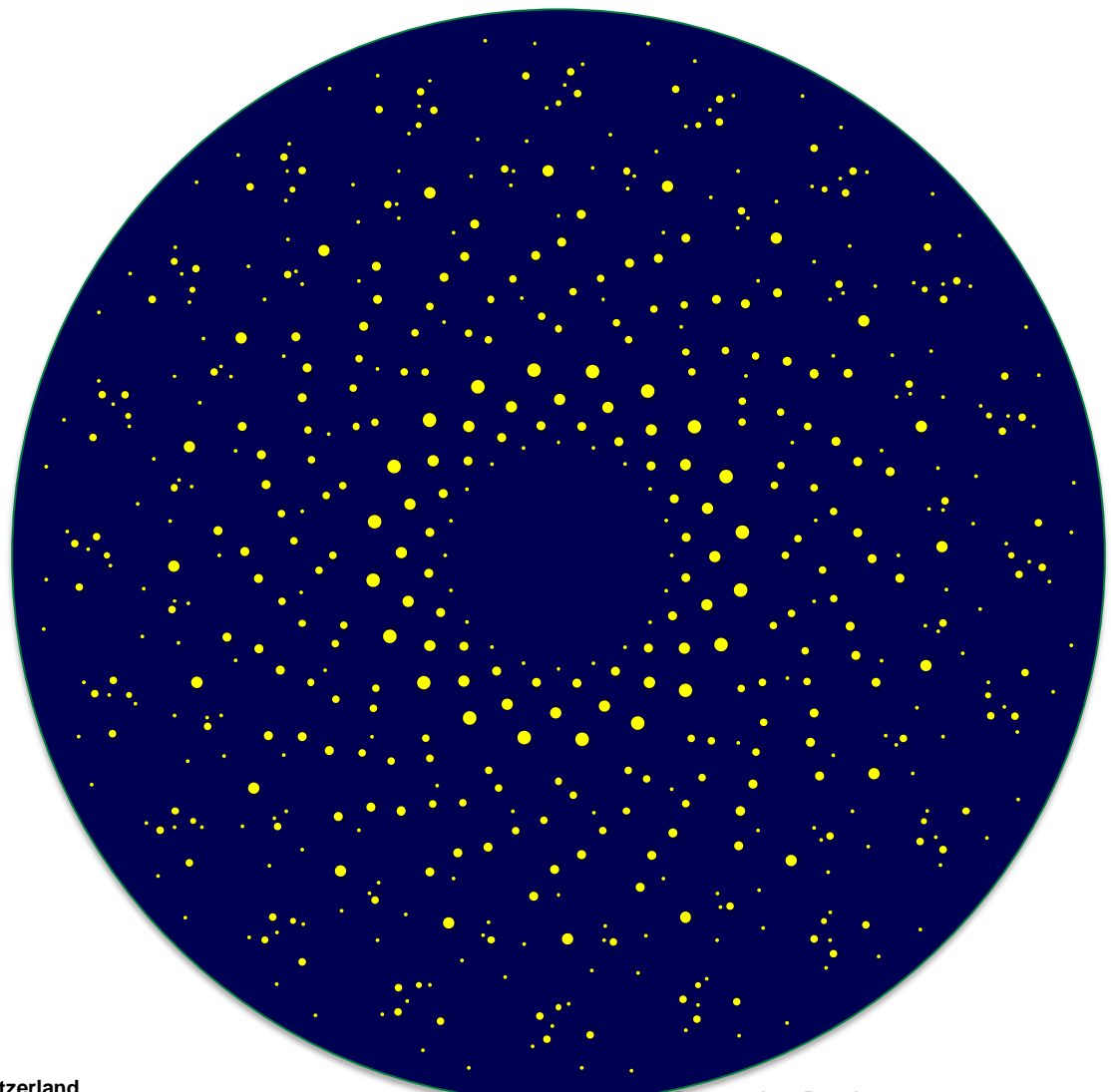
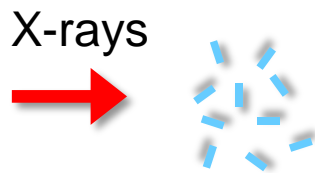
X-rays



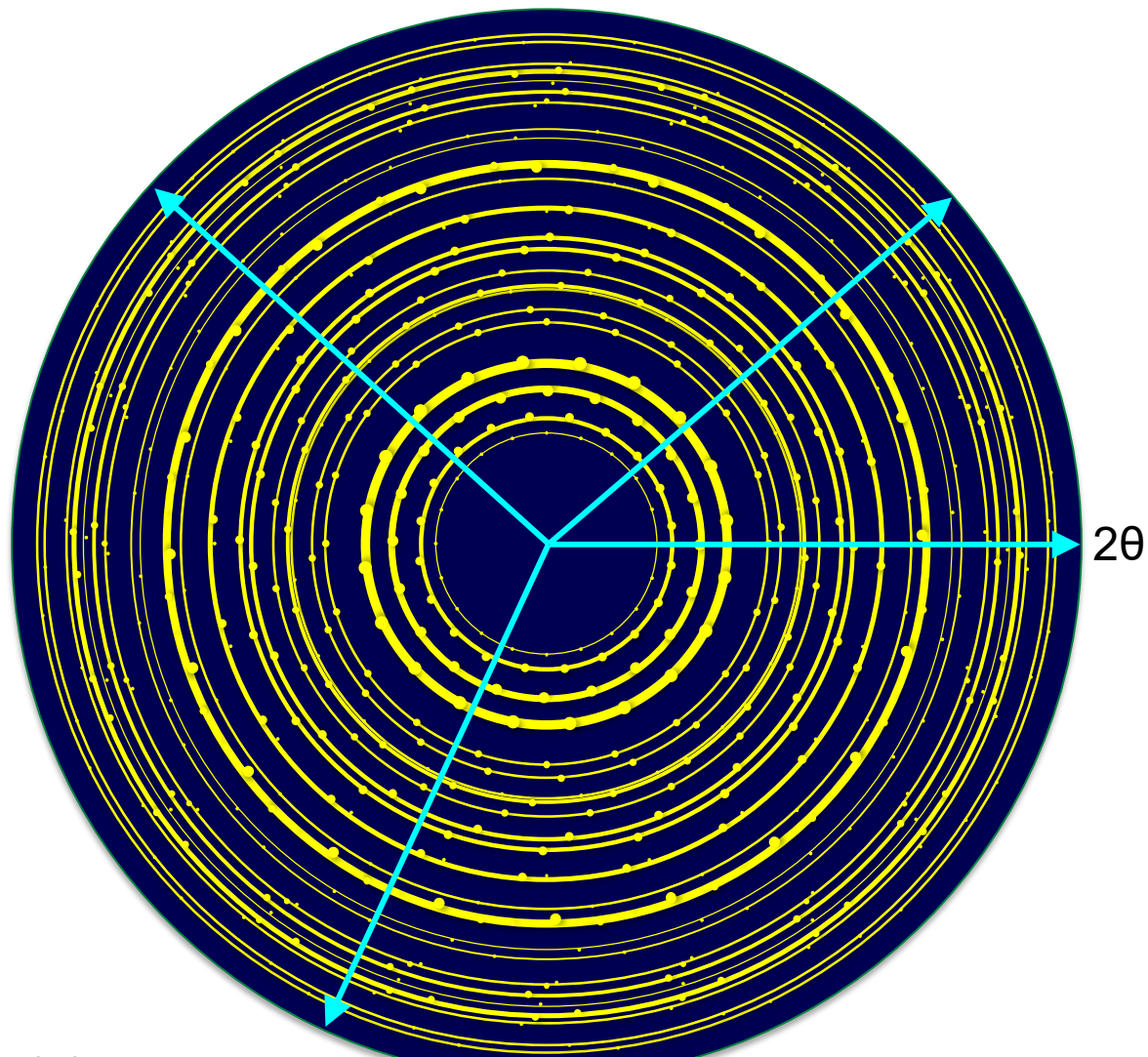
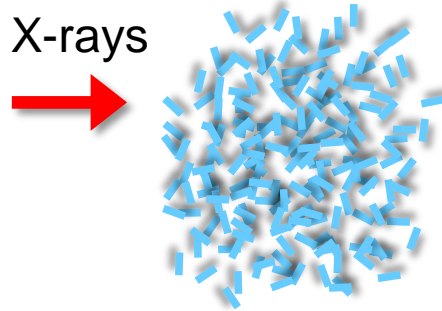
X-ray Powder Diffraction



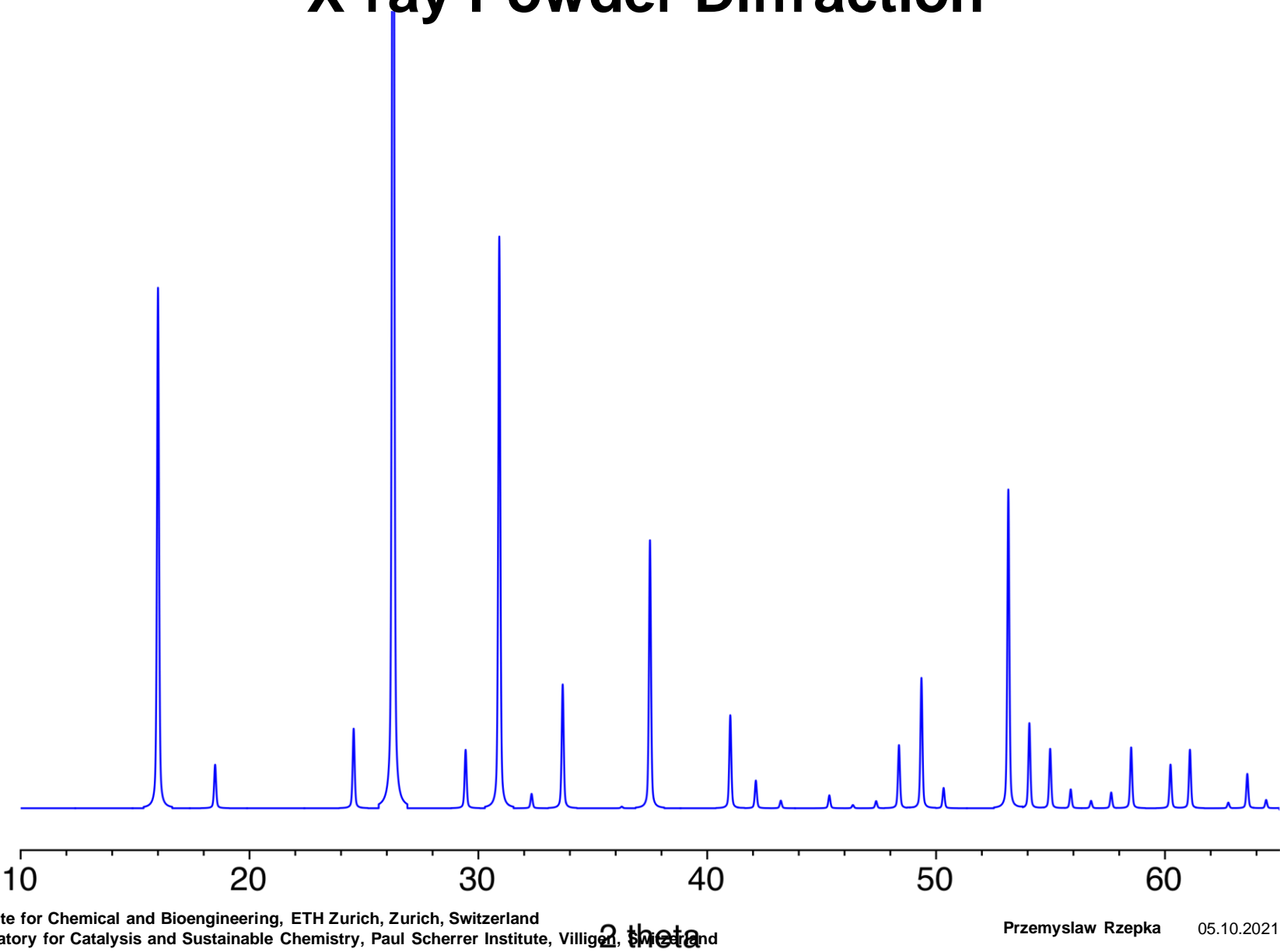
X-ray Powder Diffraction



X-ray Powder Diffraction

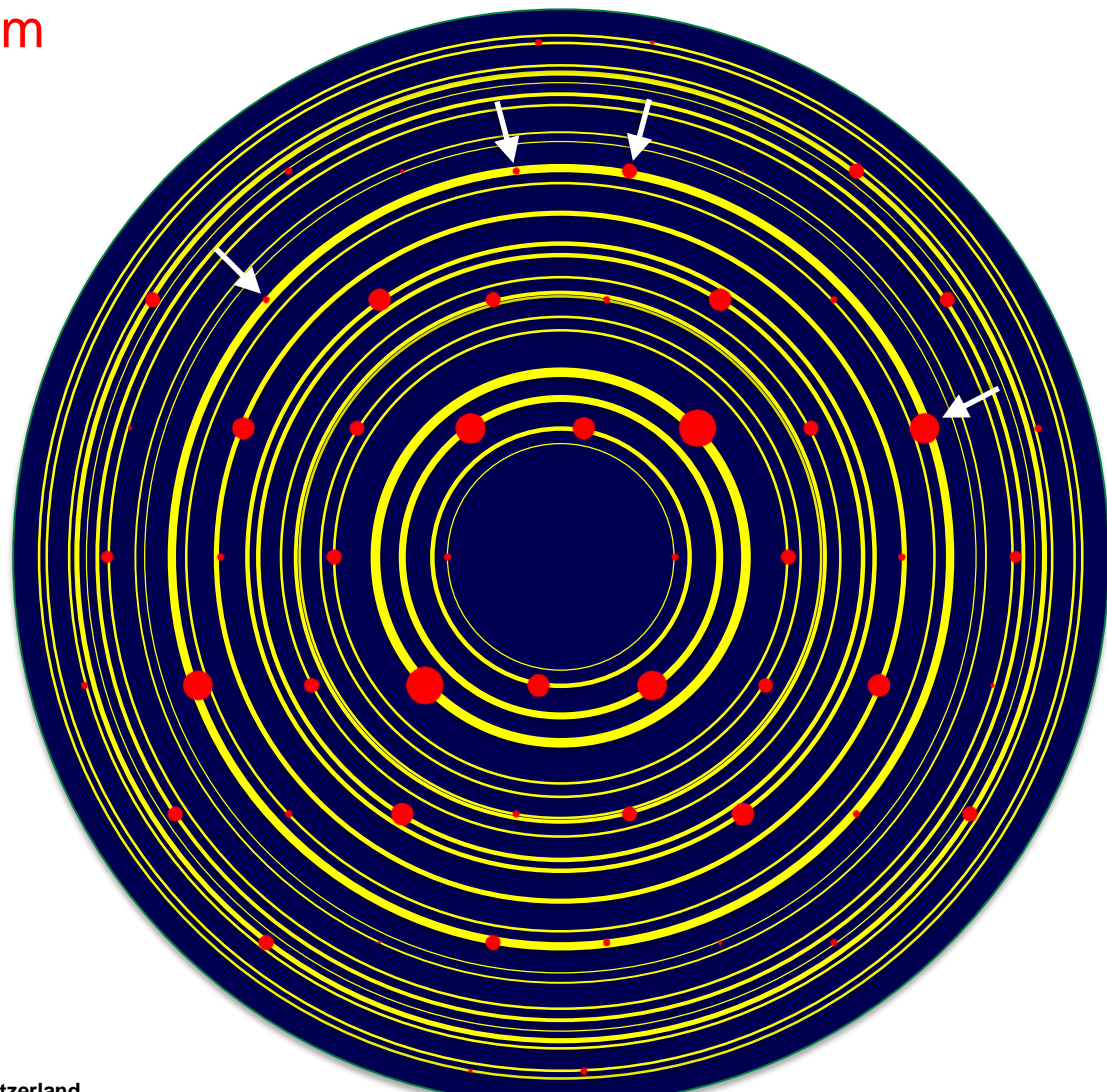
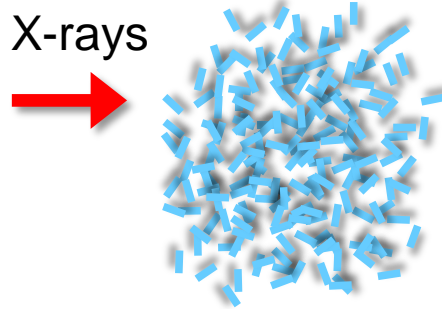


X-ray Powder Diffraction



X-ray Powder Diffraction

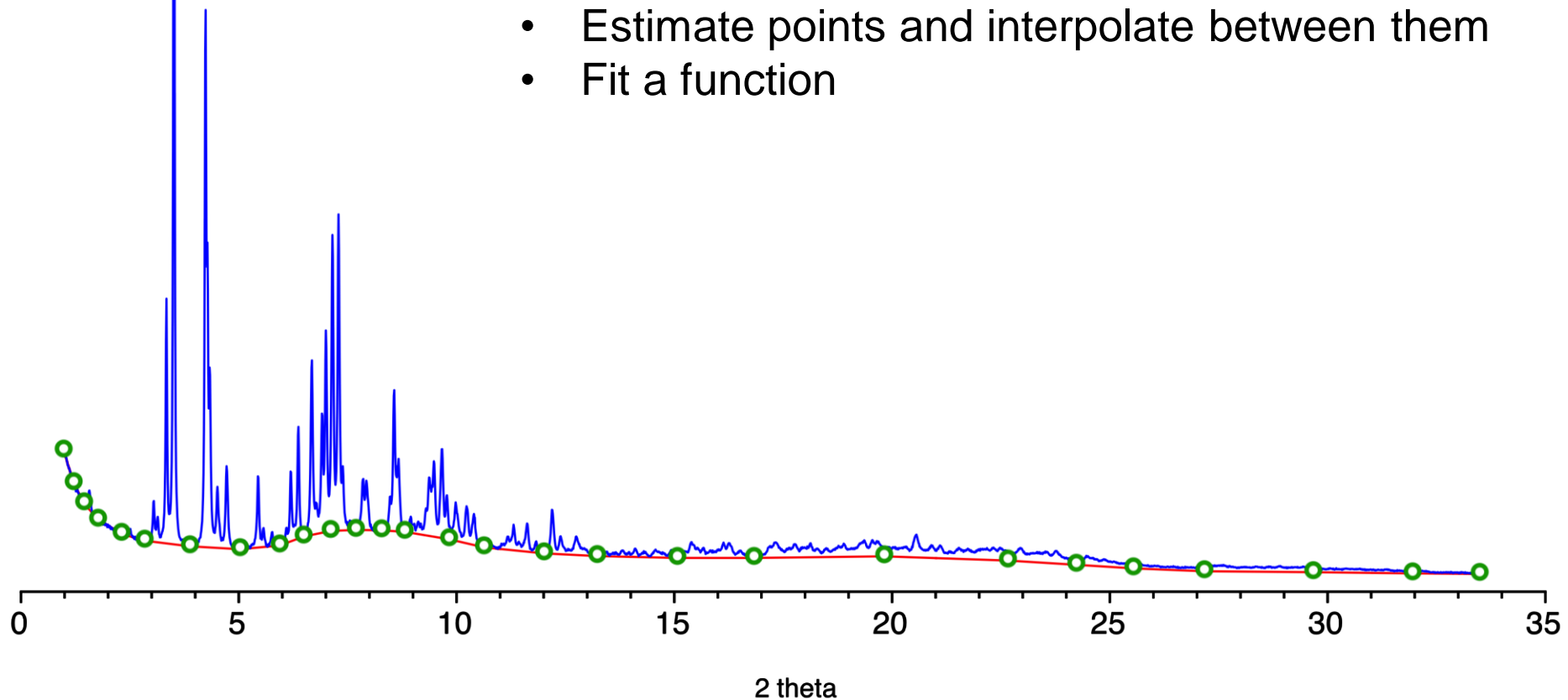
Reflection Overlap Problem



Indexing an XPD Pattern

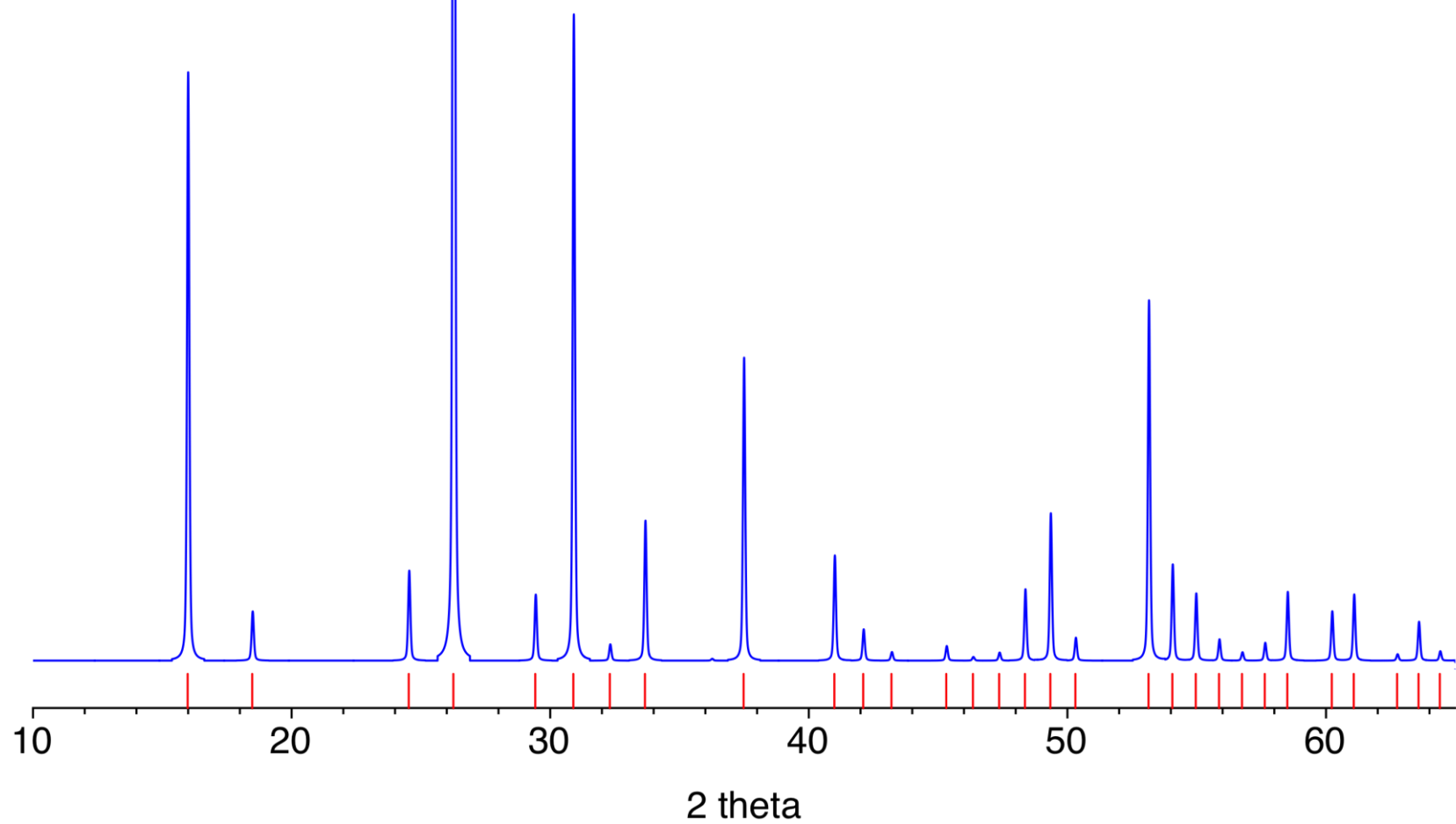
The determination of the background

- Assume flat background
- Measure an empty sample holder
- Estimate points and interpolate between them
- Fit a function



Indexing an XPD Pattern

Peak positions search



Indexing an XPD Pattern

Relationship between 2θ and d -spacing

Bragg's Law $\lambda = 2d_{hkl} \sin\theta_{hkl}$

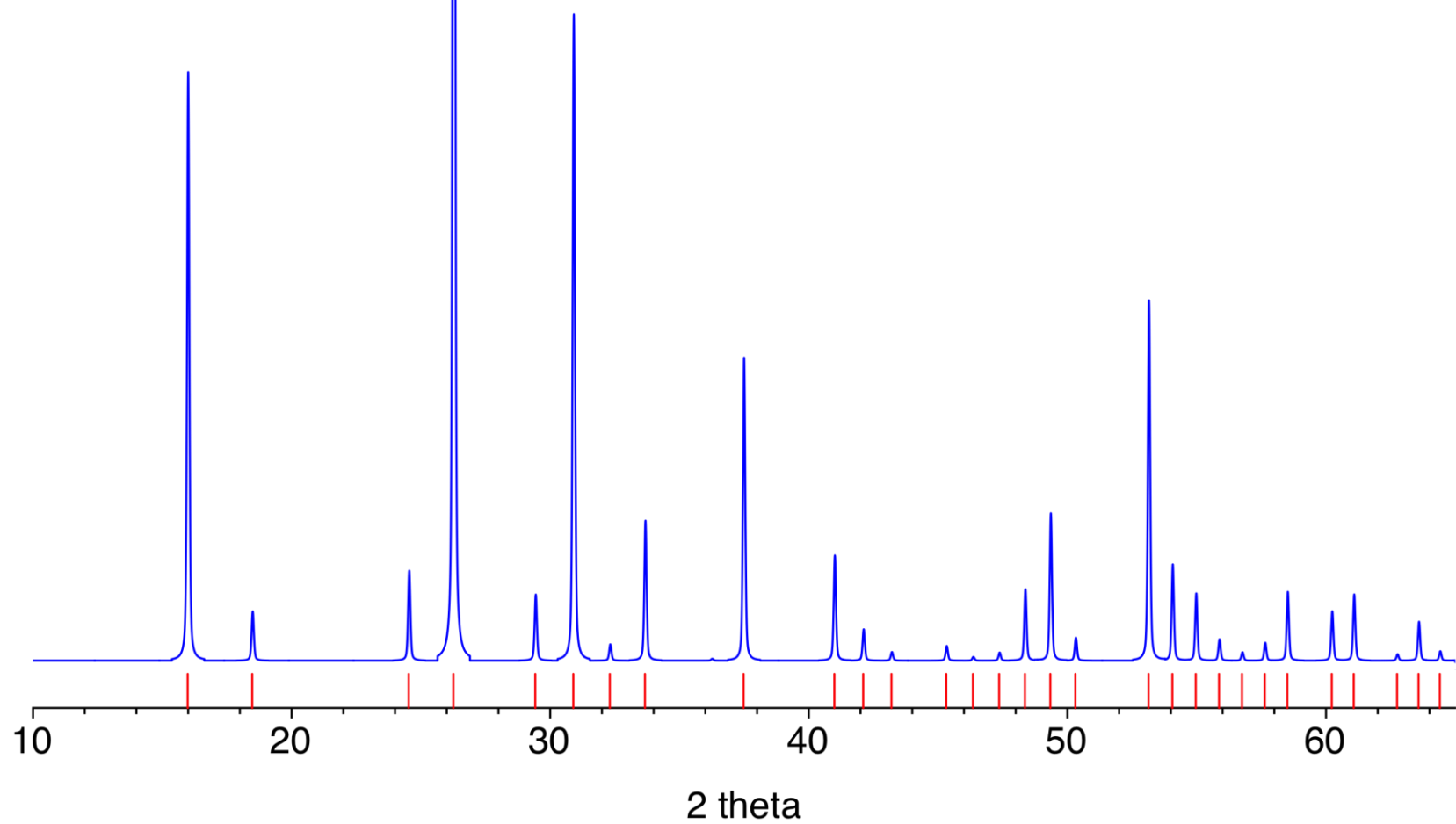
$$d_{hkl} = \frac{\lambda}{2 \sin\theta_{hkl}}$$

Relationship between d -spacing and lattice parameters

Cubic example $d_{hkl}^2 = \frac{a^2}{h^2 + k^2 + l^2}$

Indexing an XPD Pattern

Peak positions search



Indexing an XPD Pattern

$$d_{hkl}^2 = \frac{\lambda^2}{4\sin^2 \theta_{hkl}} = \frac{a^2}{h^2 + k^2 + l^2} \quad \rightarrow \quad \sin^2 \theta_{hkl} = \left(\frac{\lambda^2}{4a^2} \right) (h^2 + k^2 + l^2)$$

Indexing an XPD Pattern

$$d_{hkl}^2 = \frac{\lambda^2}{4\sin^2 \theta_{hkl}} = \frac{a^2}{h^2 + k^2 + l^2} \quad \rightarrow \quad \sin^2 \theta_{hkl} = \left(\frac{\lambda^2}{4a^2} \right) (h^2 + k^2 + l^2)$$

2θ (°)
16.00
18.50
24.55
26.28
29.44
30.91
32.33
33.68
37.50
41.01
42.12
43.22
45.34

Indexing an XPD Pattern

$$d_{hkl}^2 = \frac{\lambda^2}{4\sin^2 \theta_{hkl}} = \frac{a^2}{h^2 + k^2 + l^2} \quad \rightarrow \quad \sin^2 \theta_{hkl} = \left(\frac{\lambda^2}{4a^2} \right) (h^2 + k^2 + l^2)$$

2θ (°)	$\sin^2 \theta$
16.00	0.01937
18.50	0.02583
24.55	0.04520
26.28	0.05166
29.44	0.06457
30.91	0.07103
32.33	0.07749
33.68	0.08395
37.50	0.10332
41.01	0.12269
42.12	0.12915
43.22	0.13561
45.34	0.14852

$$\frac{\sin^2 \theta_2}{\sin^2 \theta_1} = \frac{(h_2^2 + k_2^2 + l_2^2)}{(h_1^2 + k_1^2 + l_1^2)}$$

Indexing an XPD Pattern

$$d_{hkl}^2 = \frac{\lambda^2}{4\sin^2 \theta_{hkl}} = \frac{a^2}{h^2 + k^2 + l^2} \quad \rightarrow \quad \sin^2 \theta_{hkl} = \left(\frac{\lambda^2}{4a^2} \right) (h^2 + k^2 + l^2)$$

2θ (°)	$\sin^2 \theta$	ratio
16.00	0.01937	1.00
18.50	0.02583	1.33
24.55	0.04520	2.33
26.28	0.05166	2.67
29.44	0.06457	3.33
30.91	0.07103	3.66
32.33	0.07749	4.00
33.68	0.08395	4.33
37.50	0.10332	5.33
41.01	0.12269	6.33
42.12	0.12915	6.67
43.22	0.13561	7.00
45.34	0.14852	7.66

Indexing an XPD Pattern

$$d_{hkl}^2 = \frac{\lambda^2}{4 \sin^2 \theta_{hkl}} = \frac{a^2}{h^2 + k^2 + l^2} \quad \rightarrow \quad \sin^2 \theta_{hkl} = \left(\frac{\lambda^2}{4a^2} \right) (h^2 + k^2 + l^2)$$

2θ (°)	$\sin^2 \theta$	ratio	integers
16.00	0.01937	1.00	3
18.50	0.02583	1.33	4
24.55	0.04520	2.33	7
26.28	0.05166	2.67	8
29.44	0.06457	3.33	10
30.91	0.07103	3.66	11
32.33	0.07749	4.00	12
33.68	0.08395	4.33	13
37.50	0.10332	5.33	16
41.01	0.12269	6.33	19
42.12	0.12915	6.67	20
43.22	0.13561	7.00	21
45.34	0.14852	7.66	23

Indexing an XPD Pattern

$$d_{hkl}^2 = \frac{\lambda^2}{4\sin^2 \theta_{hkl}} = \frac{a^2}{h^2 + k^2 + l^2} \quad \rightarrow \quad \sin^2 \theta_{hkl} = \left(\frac{\lambda^2}{4a^2} \right) (h^2 + k^2 + l^2)$$

2θ ($^\circ$)	$\sin^2 \theta$	ratio	integers	$h^2 + k^2 + l^2$	hkl
16.00	0.01937	1.00	3	6	211
18.50	0.02583	1.33	4	8	220
24.55	0.04520	2.33	7	14	321
26.28	0.05166	2.67	8	16	400
29.44	0.06457	3.33	10	20	420
30.91	0.07103	3.66	11	22	332
32.33	0.07749	4.00	12	24	422
33.68	0.08395	4.33	13	26	431
37.50	0.10332	5.33	16	32	440
41.01	0.12269	6.33	19	38	532, 611
42.12	0.12915	6.67	20	40	620
43.22	0.13561	7.00	21	42	541
45.34	0.14852	7.66	23	46	631

Indexing an XPD Pattern

$$d_{hkl}^2 = \frac{\lambda^2}{4\sin^2 \theta_{hkl}} = \frac{a^2}{h^2 + k^2 + l^2} \quad \rightarrow \quad \sin^2 \theta_{hkl} = \left(\frac{\lambda^2}{4a^2} \right) (h^2 + k^2 + l^2)$$

$2\theta (\circ)$	$\sin^2 \theta$	ratio	integers	$h^2 + k^2 + l^2$	hkl	$a (\text{\AA})$
16.00	0.01937	1.00	3	6	211	13.5567
18.50	0.02583	1.33	4	8	220	13.5564
24.55	0.04520	2.33	7	14	321	13.5567
26.28	0.05166	2.67	8	16	400	13.5563
29.44	0.06457	3.33	10	20	420	13.5566
30.91	0.07103	3.66	11	22	332	13.5566
32.33	0.07749	4.00	12	24	422	13.5563
33.68	0.08395	4.33	13	26	431	13.5565
37.50	0.10332	5.33	16	32	440	13.5565
41.01	0.12269	6.33	19	38	532, 611	13.5564
42.12	0.12915	6.67	20	40	620	13.5565
43.22	0.13561	7.00	21	42	541	13.5565
45.34	0.14852	7.66	23	46	631	13.5565

Indexing an XPD Pattern

$$d_{hkl}^2 = \frac{\lambda^2}{4\sin^2 \theta_{hkl}} = \frac{a^2}{h^2 + k^2 + l^2} \quad \rightarrow \quad \sin^2 \theta_{hkl} = \left(\frac{\lambda^2}{4a^2} \right) (h^2 + k^2 + l^2)$$

2θ (°)	hkl
16.00	211
18.50	220
24.55	321
26.28	400
29.44	420
30.91	332
32.33	422
33.68	431
37.50	440
41.01	532, 611
42.12	620
43.22	541
45.34	631

Lattice parameter
 $a = 13.5565$ Å

Centered?

- P : no conditions on hkl
 - I : $h + k + l = 2n$
 - F : $\begin{cases} h + k = 2n \\ h + l = 2n \\ k + l = 2n \end{cases}$
- hkl all
even or all
odd

Indexing an XPD Pattern

$$d_{hkl}^2 = \frac{\lambda^2}{4\sin^2 \theta_{hkl}} = \frac{a^2}{h^2 + k^2 + l^2} \quad \rightarrow \quad \sin^2 \theta_{hkl} = \left(\frac{\lambda^2}{4a^2} \right) (h^2 + k^2 + l^2)$$

2θ (°)	hkl
16.00	211
18.50	220
24.55	321
26.28	400
29.44	420
30.91	332
32.33	422
33.68	431
37.50	440
41.01	532, 611
42.12	620
43.22	541
45.34	631

Lattice parameter

$$a = 13.5565 \text{ \AA}$$

Centered?

P: no conditions on hkl

→ I: $h + k + l = 2n$

F: $\begin{cases} h + k = 2n \\ h + l = 2n \\ k + l = 2n \end{cases}$

hkl all
even or all
odd

Indexing an XPD Pattern

$$d_{hkl}^2 = \frac{\lambda^2}{4\sin^2 \theta_{hkl}} = \frac{a^2}{h^2 + k^2 + l^2} \quad \rightarrow \quad \sin^2 \theta_{hkl} = \left(\frac{\lambda^2}{4a^2} \right) (h^2 + k^2 + l^2)$$

$2\theta (\circ)$
38.46
55.54
69.58
82.46
94.94
107.64
121.36

Exercise 1 (send answers to
przepka@ethz.ch):

1. Index listed peaks if you know the structure is cubic
2. What is lattice parameter a if $\lambda=1.54\text{\AA}$?
3. What is centering?

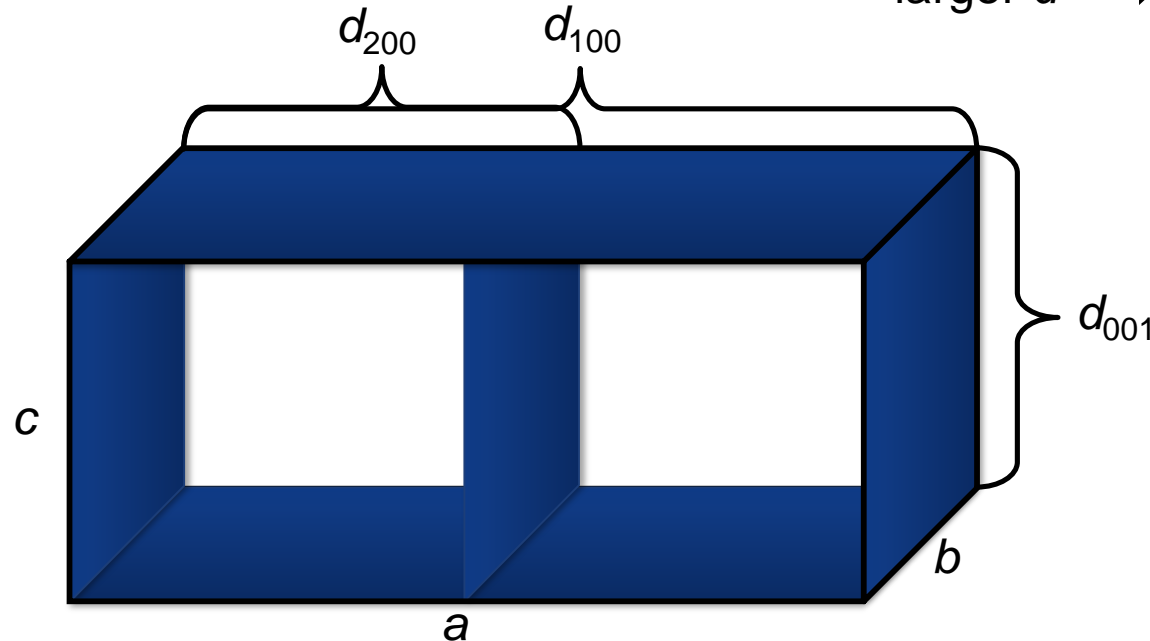
Reflection position

Parameters affecting reflection positions

- unit cell parameters
- zero point of the detector
- sample displacement

$$\boxed{d} = 2d_{hkl} \sin q_{hkl}$$

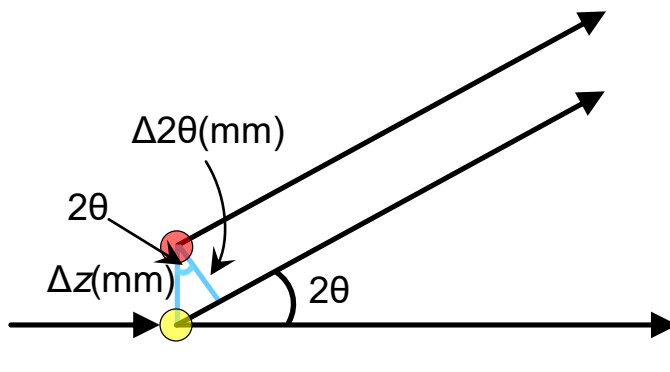
smaller $d \rightarrow$ larger 2θ
larger $d \rightarrow$ smaller 2θ



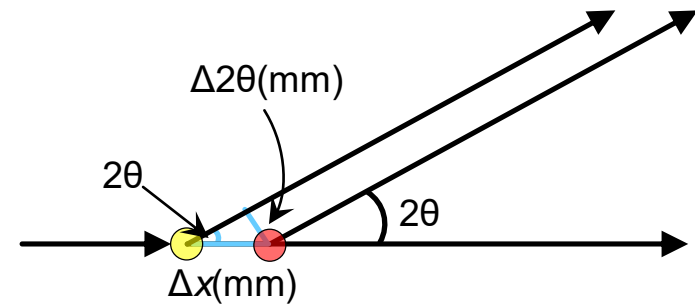
Reflection position

Parameters affecting reflection positions

- unit cell parameters
- zero point of the detector
- sample displacement (capillary)



$$\cos(2\theta) = \Delta 2\theta / \Delta z$$
$$\Delta 2\theta = \Delta z \cos(2\theta)$$



$$\sin(2\theta) = \Delta 2\theta / \Delta x$$
$$\Delta 2\theta = \Delta x \sin(2\theta)$$

Crystalline size

Peak width (B) is inversely proportional to crystallite size (L)

Scherrer equation $D = \frac{K\lambda}{FWHM \cos\theta}$

D – crystalline size, K=0.9 - shape factor, λ – wavelength, FWHM – the line broadening at half the maximum intensity, θ – Bragg angle

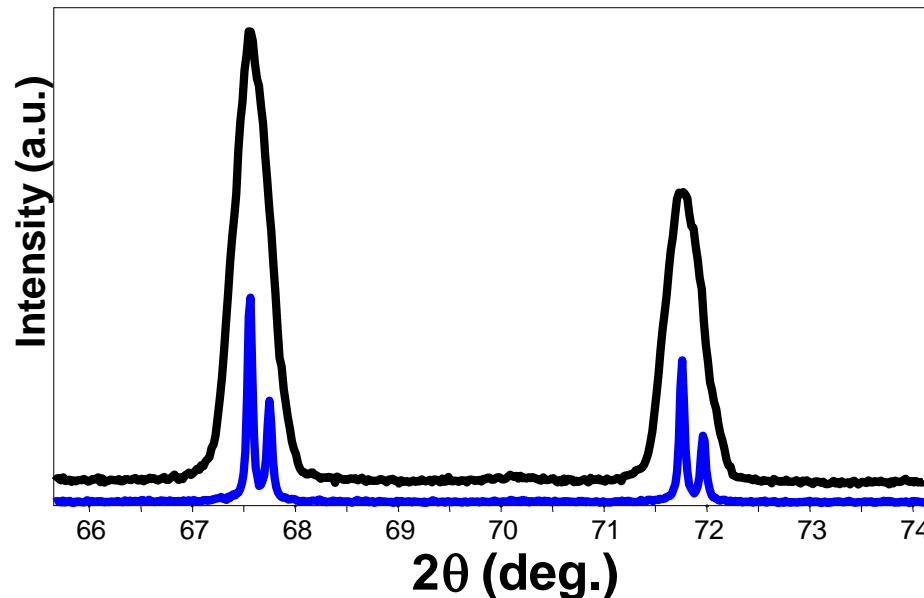
The Laue Equations describe the intensity of a diffracted peak from an **infinitely large (> 1um)** and **perfectly ordered** crystal. Deviations from the ideal (nano-sizing) create peak broadening.

Crystalline size

Peak width (B) is inversely proportional to crystallite size (L)

Scherrer equation $D = \frac{K\lambda}{FWHM \cos\theta}$

D – crystalline size, K=0.9 - shape factor, λ – wavelength, FWHM – the line broadening at half the maximum intensity, θ – Bragg angle



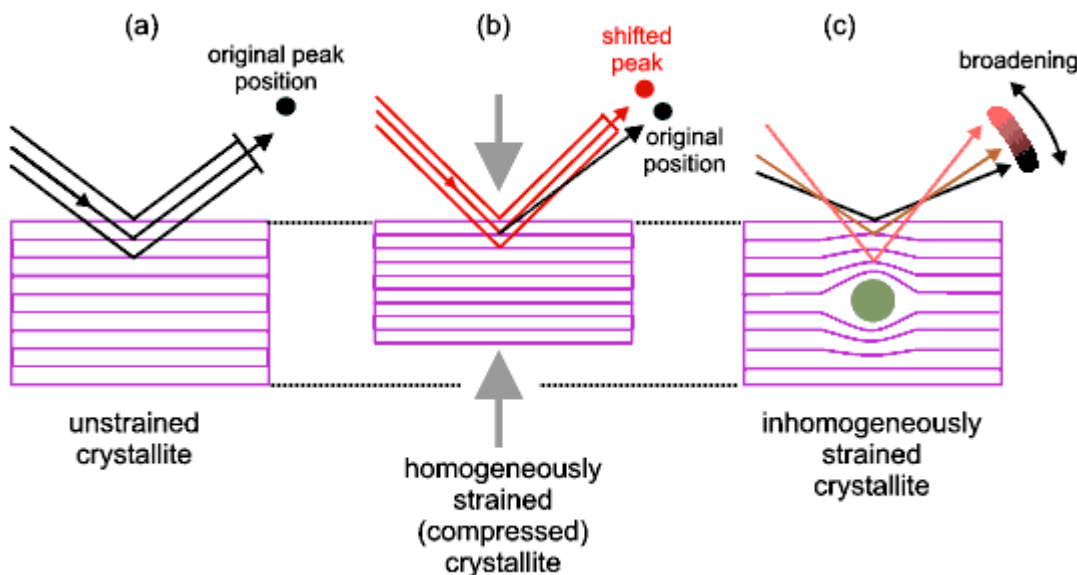
Note the instrumental contribution. Left: the same sample, different instruments.

Crystalline size

Peak width (B) is inversely proportional to crystallite size (L)

Scherrer equation $D = \frac{K\lambda}{FWHM \cos\theta}$

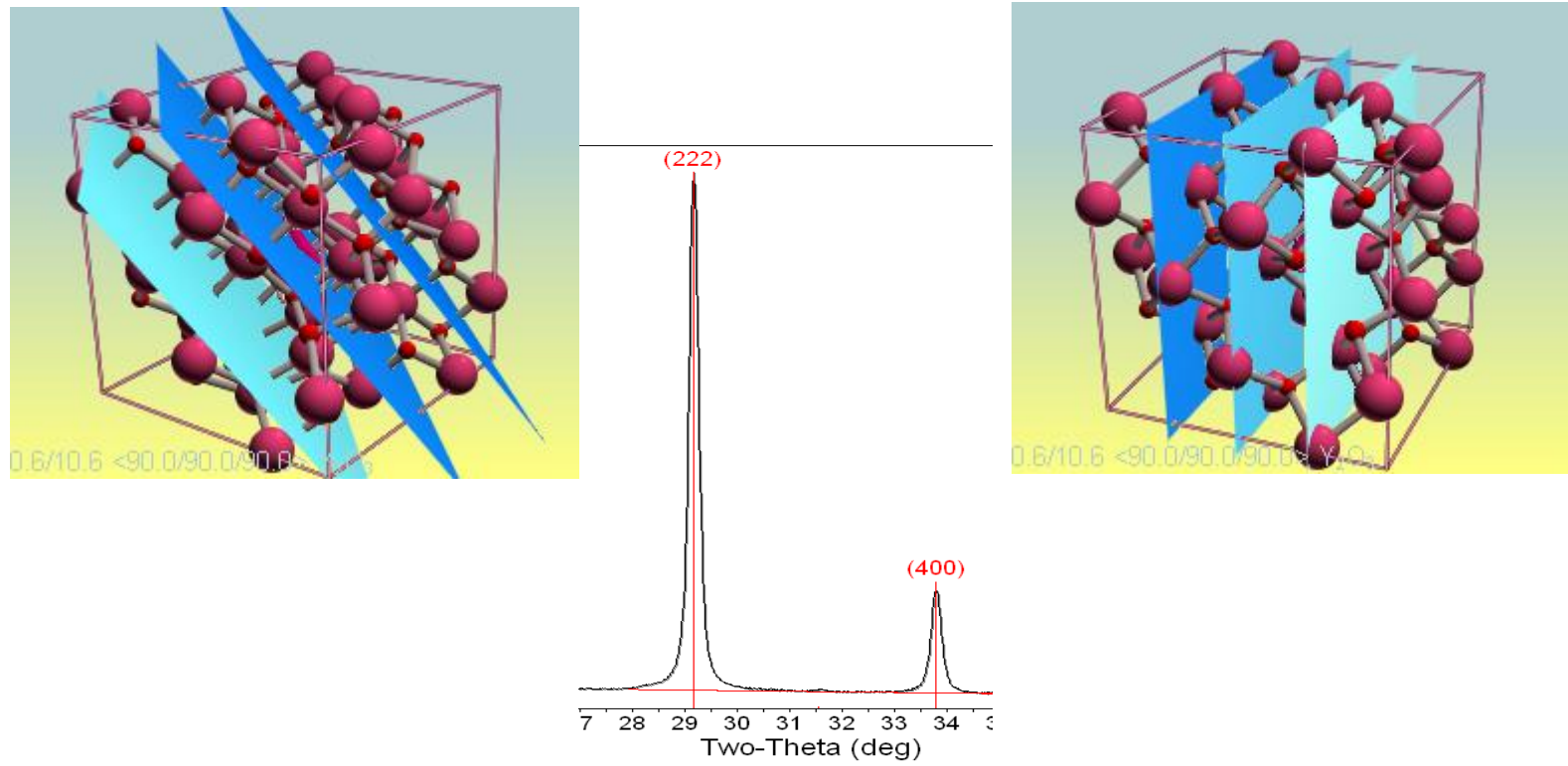
Microstrain analysis



$$FWHM = C \varepsilon \tan\theta$$

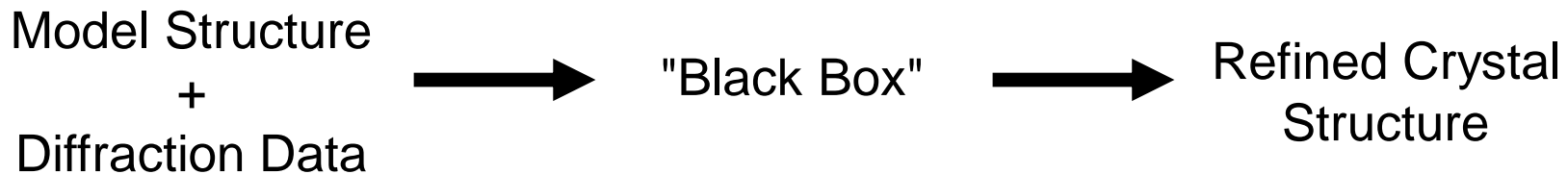
Anisotropic Size Broadening

The broadening of a single diffraction peak is the product of the crystallite dimensions in the direction perpendicular to the planes that produced the diffraction peak.



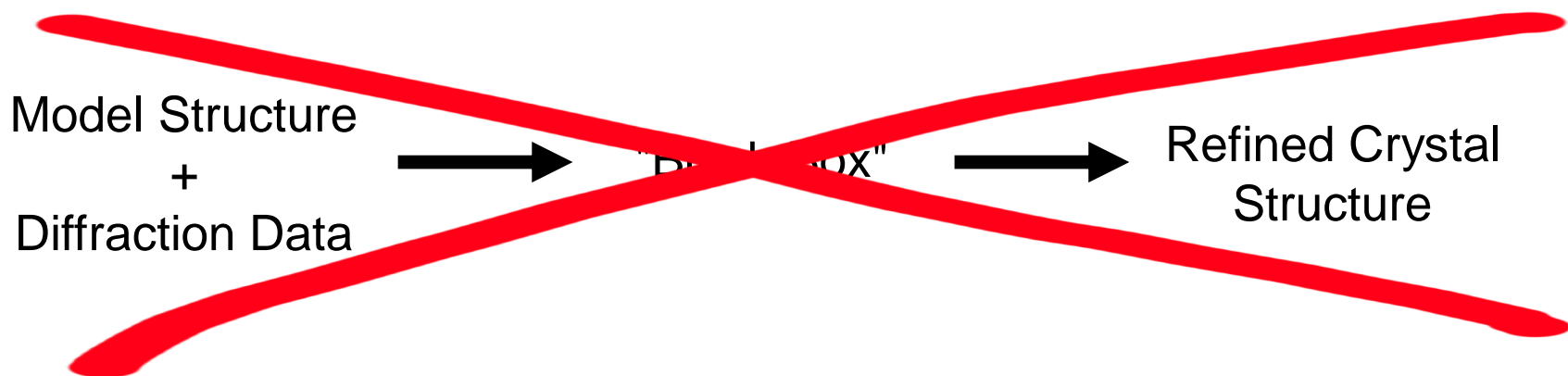
The Rietveld analysis

The Rietveld method refines user-selected parameters to minimize the difference between an experimental pattern (observed data) and a model based on the hypothesized crystal structure and instrumental parameters (calculated pattern).



The Rietveld analysis

The Rietveld method refines user-selected parameters to minimize the difference between an experimental pattern (observed data) and a model based on the hypothesized crystal structure and instrumental parameters (calculated pattern).



From intensities to structural parameters

$$\Delta = \sum_{n=1}^N \{ I_n(\text{obs}) - I_n(\text{calc}) \}^2$$

$$I(\text{calc}) = c j_{hkl} L(2\theta) P(2\theta) A(2\theta) F^2(hkl)$$

where L, P, A are the Lorentz, polarization, and absorption corrections, respectively. j is the multiplicity factor (symmetry), c is a scale factor and F is a structure factor.

$$F_{hkl} = \sum_j f_j \exp[2\pi i(hx_j + hy_j + hz_j)]$$

where f_i is atomic form factor.

bkg @ 0 0 0 0

R-Factors

$$R_{wp} = \{ \sum_i w_i \{y_i(obs) - y_i(calc)\}^2 / \{ \sum_i w_i y_i(obs)^2 \}^{1/2}$$

$$w_i^2 = 1/\sigma(y_i(obs))^2$$

$$R_{exp} = \{ (M - P) / \{ \sum_i w_i y_i(obs)^2 \}^{1/2}$$

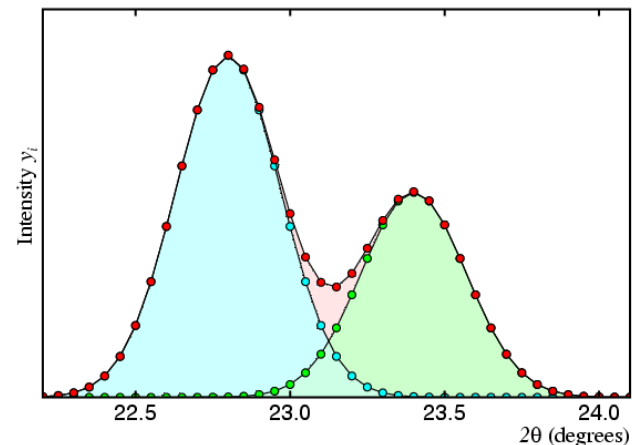
$$\chi^2 = (R_{wp}/R_{exp})^2 \text{ (goodness-of-fit)}$$

where w_i is weighting related to uncertainty σ . M – the number of data points, P – the number of parameters

Pawley and LeBail profile fitting

Parameters:

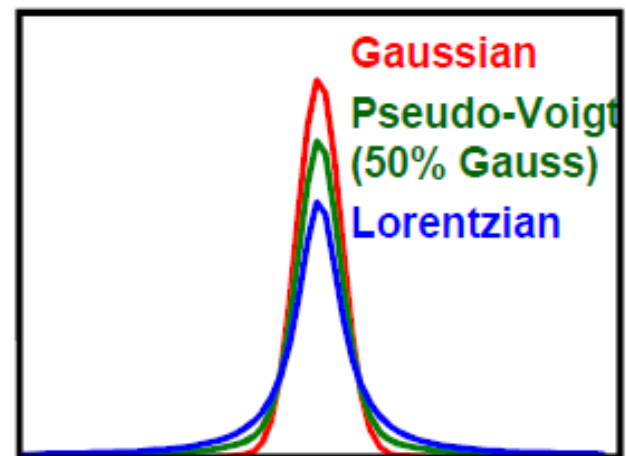
- $I(hkl)$ - Intensity of each reflection with indices hkl (only Pawley);
- $a, b, c, \alpha, \beta, \gamma$ - Unit-cell metric tensor parameters;
- $2\theta_{\text{zero}}$ - Instrumental zero error;
- U, V, W - Peak-width parameters;
- η , etc. - Other peak-shape parameters



Pseudo-Voight peak shape function:

$$I(2\theta) = I_{\text{hkl}} [\eta \mathbf{L}(2\theta - 2\theta_0) + (1 - \eta) \mathbf{G}(2\theta - 2\theta_0)]$$

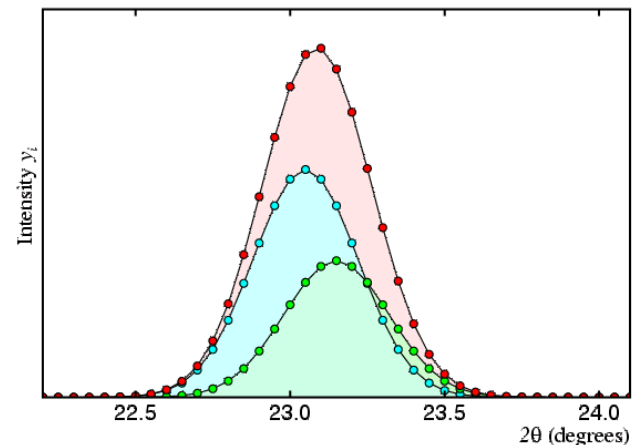
where $\mathbf{L}(2\theta - 2\theta_0)$ and $\mathbf{G}(2\theta - 2\theta_0)$ represent Lorentz and Gaussian functions, and η - the "Lorentz fraction"



Pawley and LeBail profile fitting

Parameters:

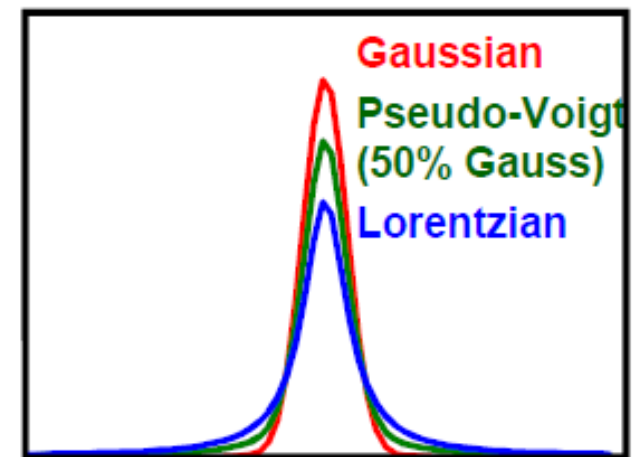
- $I(hkl)$ - Intensity of each reflection with indices hkl (only Pawley);
- $a, b, c, \alpha, \beta, \gamma$ - Unit-cell metric tensor parameters;
- $2\theta_{\text{zero}}$ - Instrumental zero error;
- U, V, W - Peak-width parameters;
- η , etc. - Other peak-shape parameters.



Pseudo-Voight peak shape function:

$$I(2\theta) = I_{\text{hkl}} [\eta \mathbf{L}(2\theta - 2\theta_0) + (1 - \eta) \mathbf{G}(2\theta - 2\theta_0)]$$

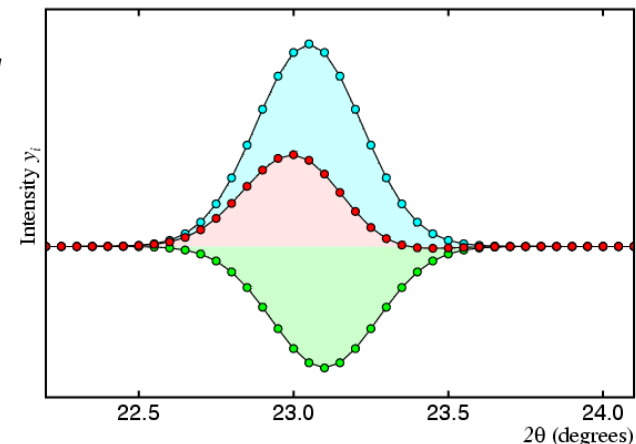
where $\mathbf{L}(2\theta - 2\theta_0)$ and $\mathbf{G}(2\theta - 2\theta_0)$ represent Lorentz and Gaussian functions, and η - the "Lorentz fraction"



Pawley and LeBail profile fitting

Parameters:

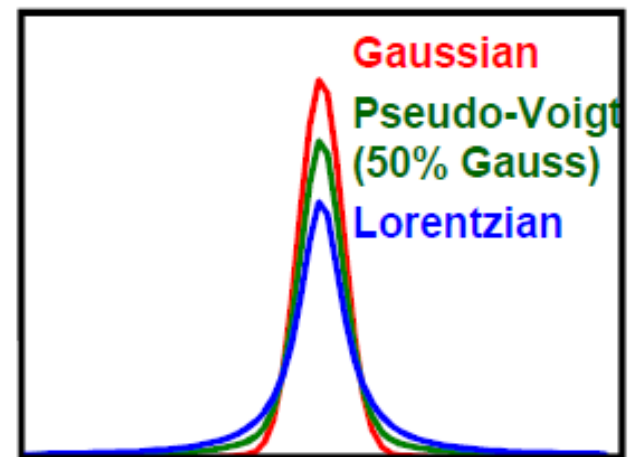
- $I(hkl)$ - Intensity of each reflection with indices hkl (only Pawley);
- $a, b, c, \alpha, \beta, \gamma$ - Unit-cell metric tensor parameters;
- $2\theta_{\text{zero}}$ - Instrumental zero error;
- U, V, W - Peak-width parameters;
- η , etc. - Other peak-shape parameters.



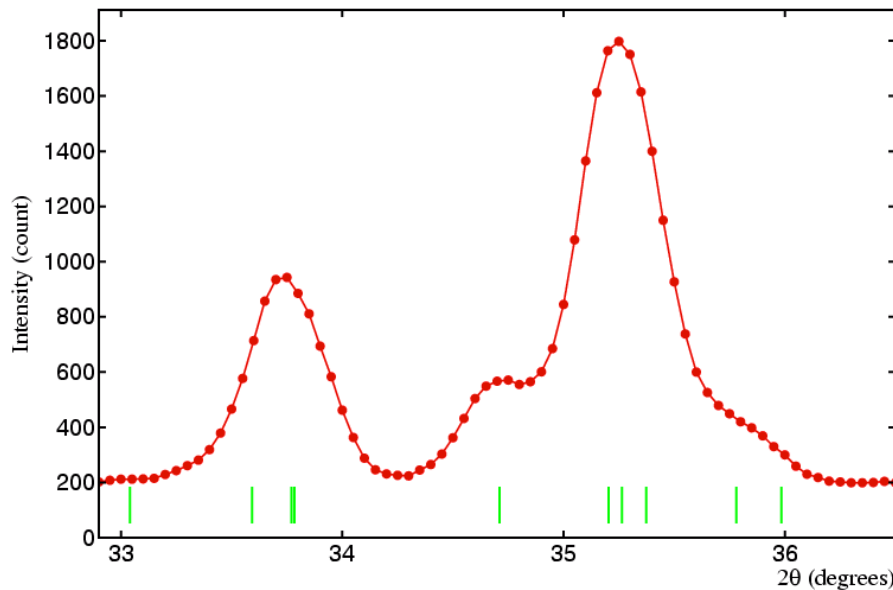
Pseudo-Voight peak shape function:

$$I(2\theta) = I_{\text{hkl}} [\eta \mathbf{L}(2\theta - 2\theta_0) + (1 - \eta) \mathbf{G}(2\theta - 2\theta_0)]$$

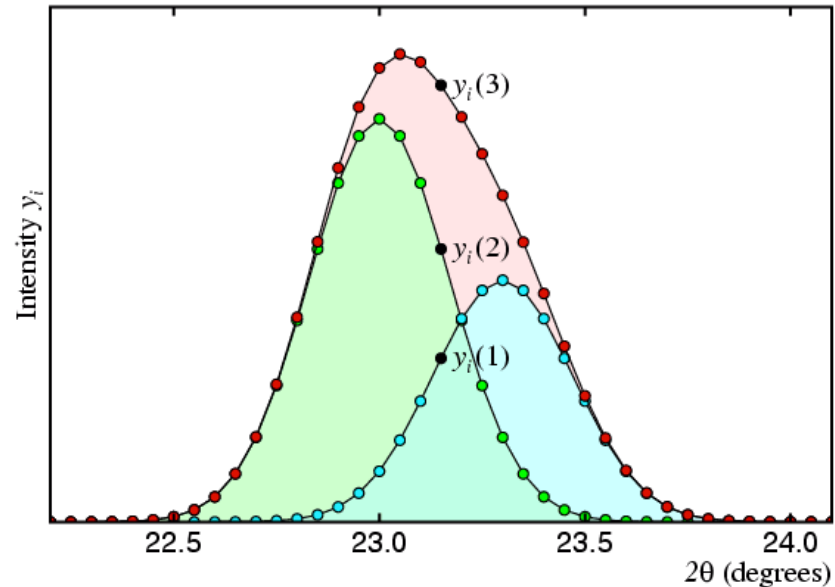
where $\mathbf{L}(2\theta - 2\theta_0)$ and $\mathbf{G}(2\theta - 2\theta_0)$ represent Lorentz and Gaussian functions, and η - the "Lorentz fraction"



Rietveld profile fitting



The detailed diffraction profile contained a lot more information than the extracted intensities of composite peaks.



The detailed profile can be fitted on a point by point basis as the summation of the profiles of all reflections to that point:

$$y_i(3) = y_i(1) + y_i(2)$$

Instrumental function

Refinement in TOPAS

```
xdd {  
!      Lam profile (wavelength)  
@      SD()  
  
@      PV_Peak_Type()  
@      Simple_Axial_Model()  
@      @ Scale  
}
```

Structure parameters

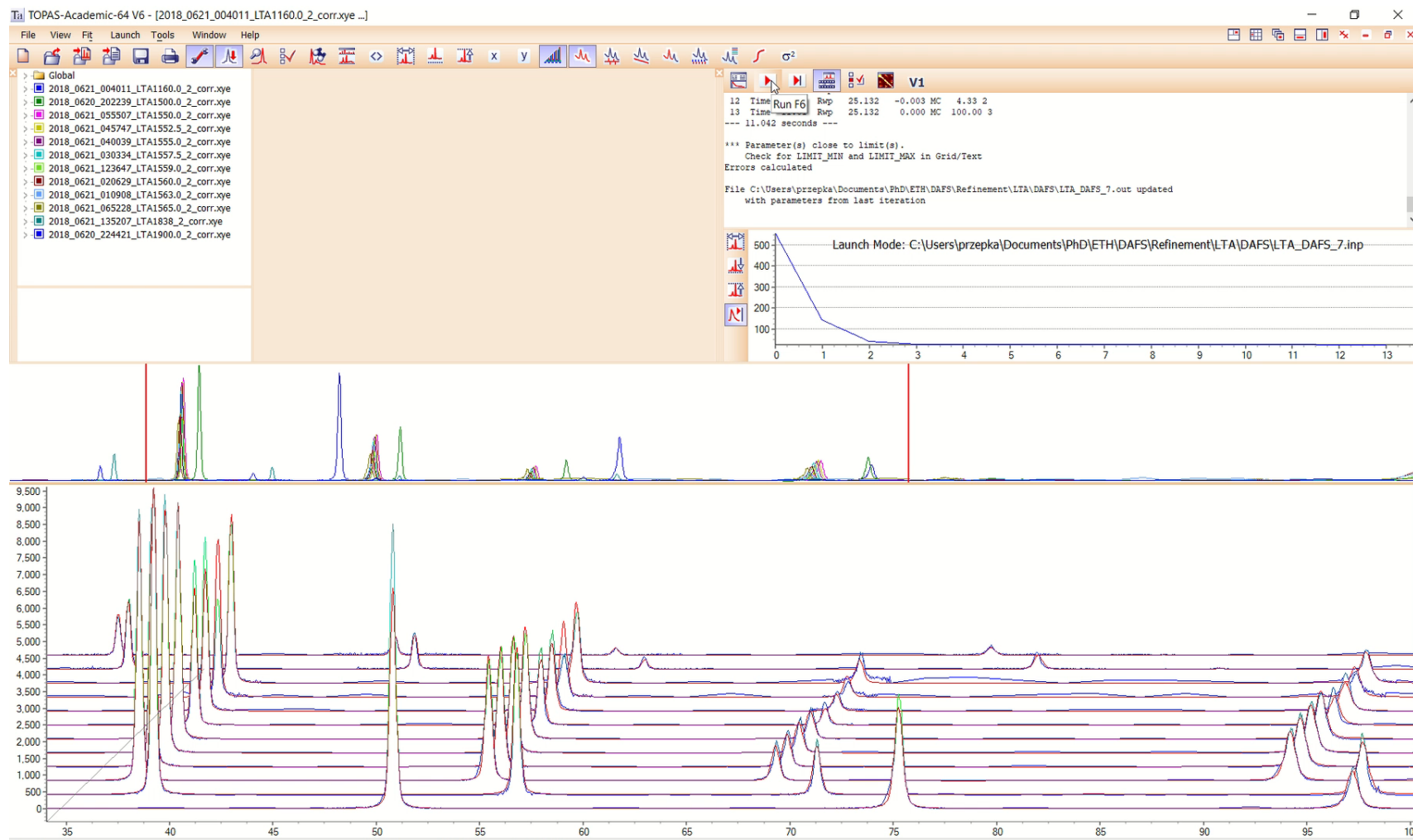
str {

@ Unit cell parameters

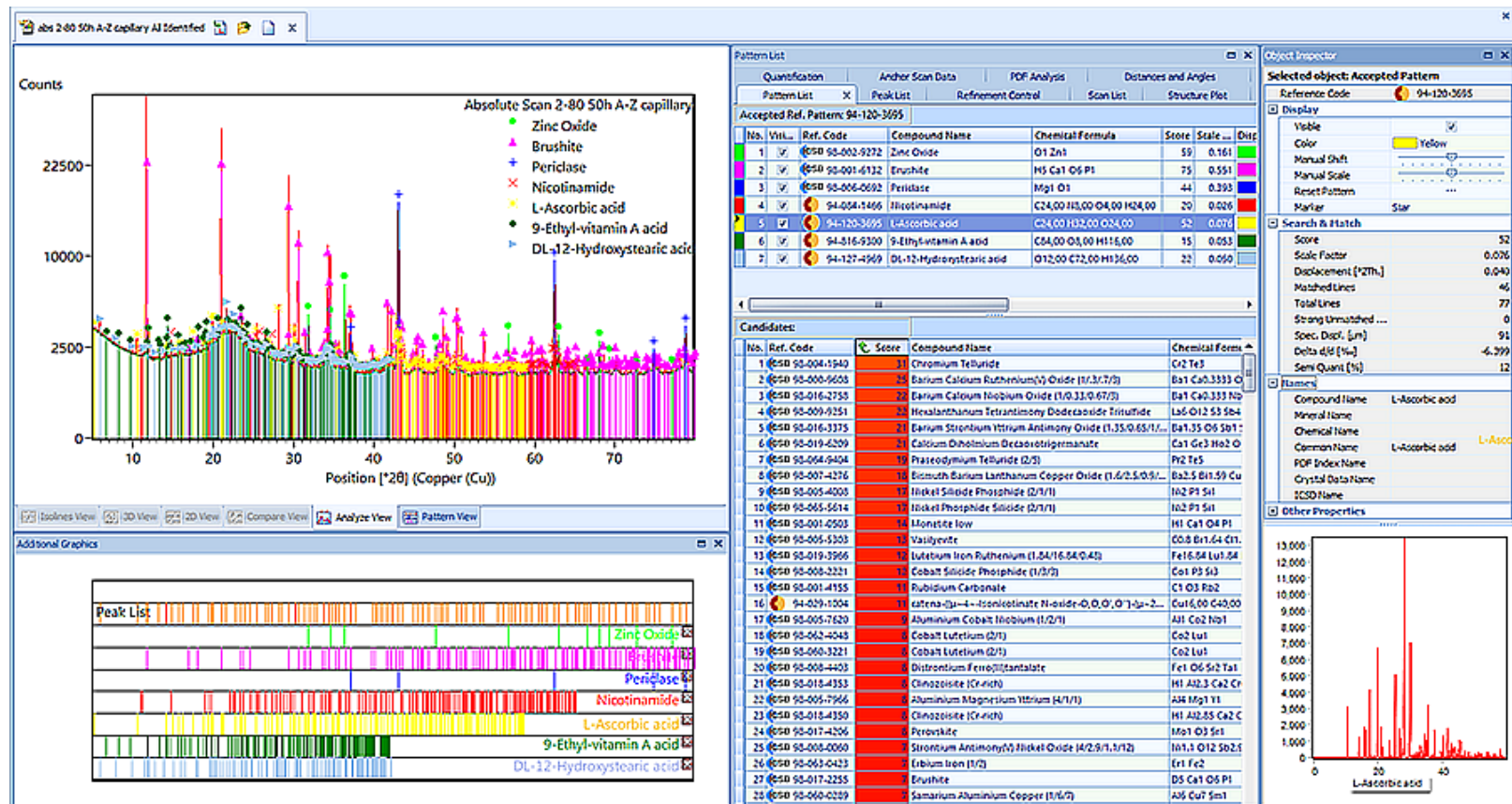
				Fractional atomic coordinates	Site Occup.	Therm. Factor
site Si(1)	num_posns	16	x 0.32281	y 0.19961	z 0.20804	occ Si 1.0 beq 1
site Si(2)	num_posns	8	x 0.08670	y 0.20129	z 0.00000	occ Si 1.0 beq 1
site Si(3)	num_posns	8	x 0.27374	y 0.00000	z 0.29371	occ Si 1.0 beq 1
site Si(4)	num_posns	4	x 0.15538	y 0.00000	z 0.00000	occ Si 1.0 beq 1
site O(8)	num_posns	4	x 0.25169	y 0.00000	z 0.50000	occ O 1.0 beq 1
site O(7)	num_posns	8	x 0.20342	y 0.00000	z 0.18745	occ O 1.0 beq 2
site O(5)	num_posns	8	x 0.10707	y 0.09088	z 0.00000	occ O 1.0 beq 2
site O(3)	num_posns	8	x 0.34246	y 0.21404	z 0.00000	occ O 1.0 beq 2
site O(6)	num_posns	4	x 0.00000	y 0.20890	z 0.00000	occ O 1.0 beq 2
site O(4)	num_posns	8	x 0.25000	y 0.25000	z 0.25000	occ O 1.0 beq 2
site O(2)	num_posns	16	x 0.38070	y 0.24571	z 0.32000	occ O 1.0 beq 2
site O(1)	num_posns	16	x 0.31646	y 0.09052	z 0.24720	occ O 1.0 beq 2

}

The Rietveld analysis



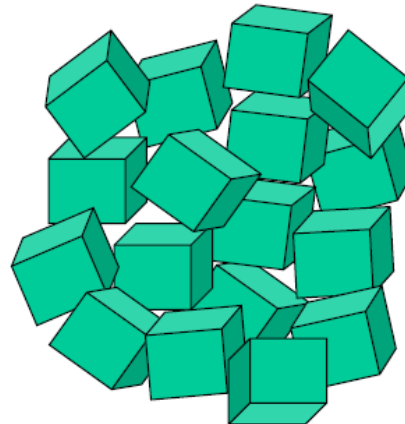
Phase identification



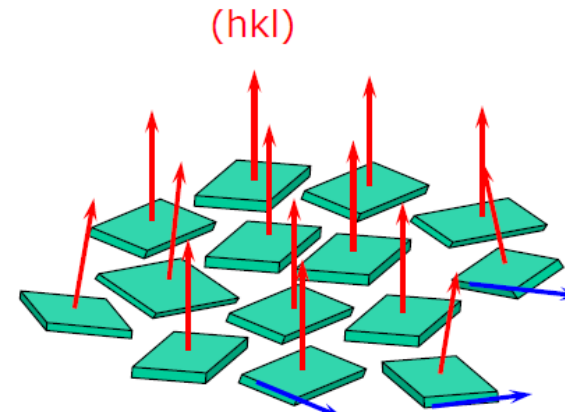
HighScore matches the peaks from collected data with database records

Sample preparation. What happens when wrong?

1. Not all crystal lattice planes present (graininess)
2. Relative intensities distribution different from expected (preferred orientation)



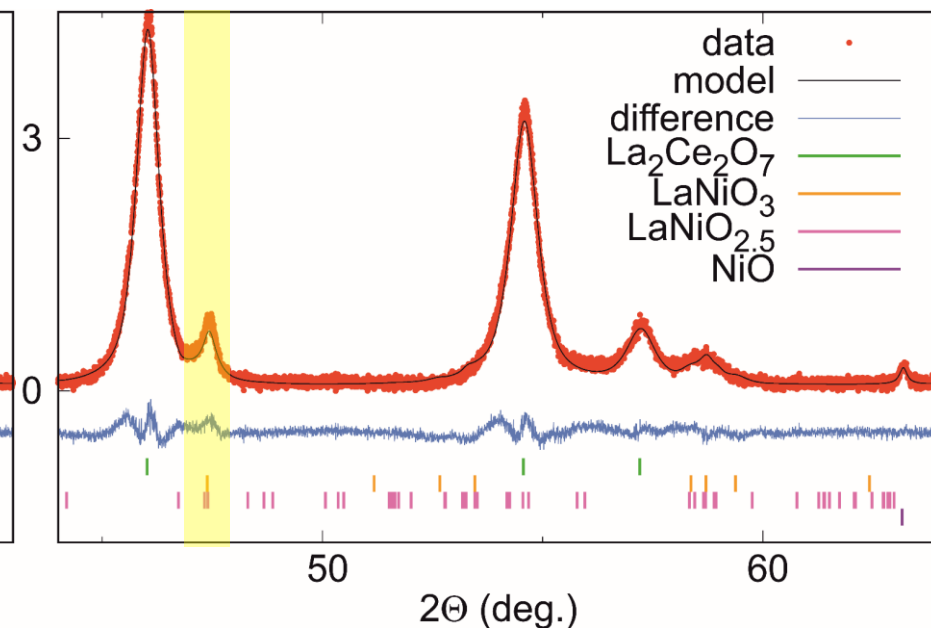
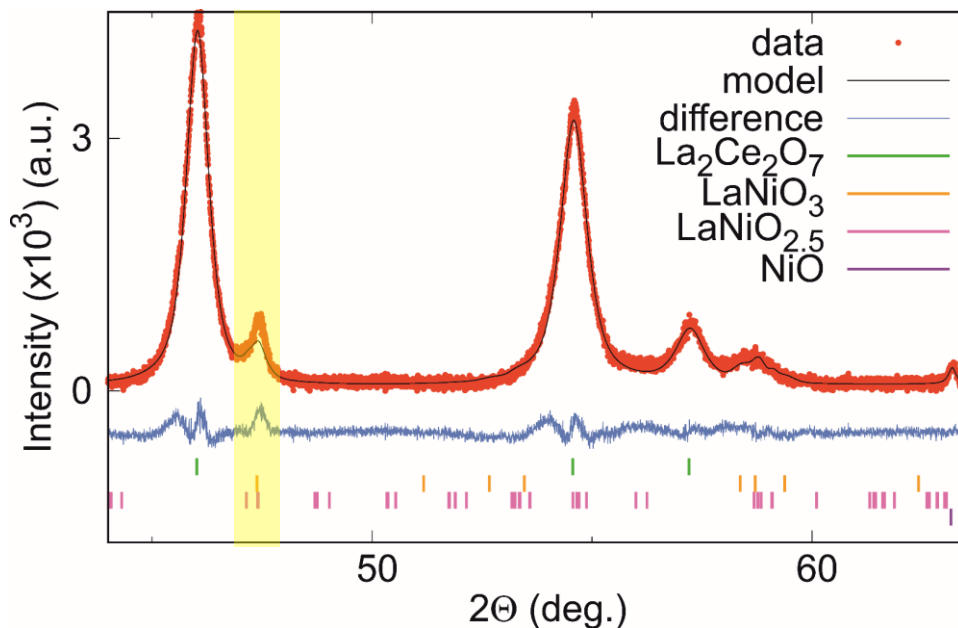
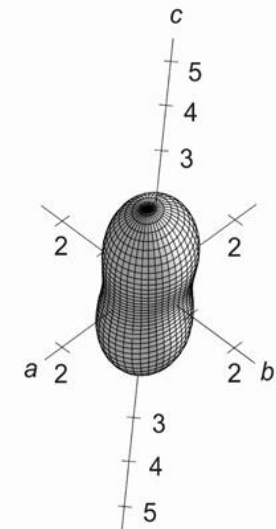
Random orientation of
crystallites (e.g. isotropic
powder)



(hkl)
[uvw]
Preferred orientation of
crystallites (typical for
plate-like crystallites)

Sample preparation

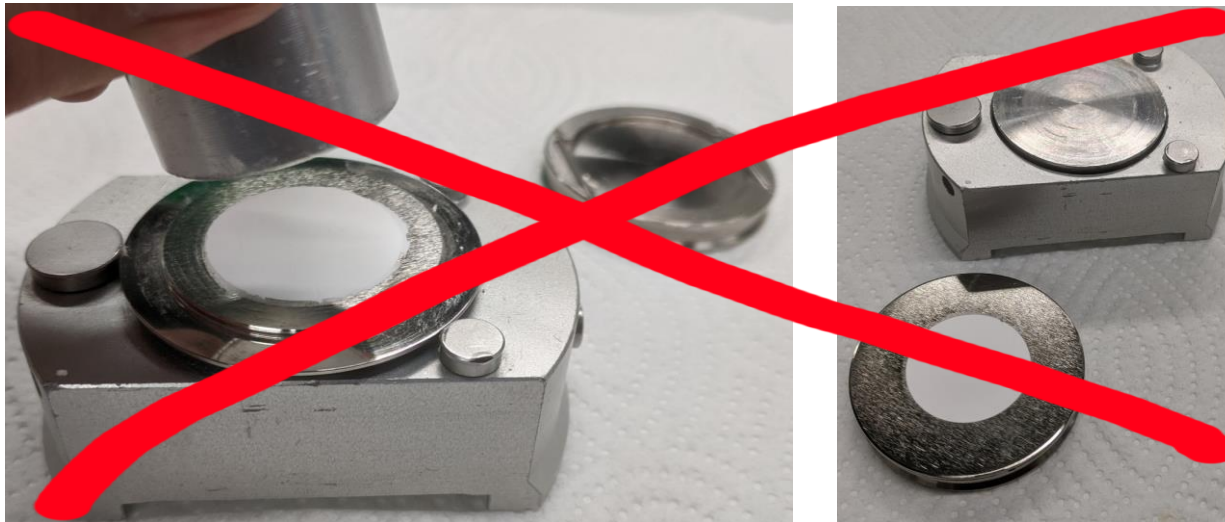
Preferred orientation may be corrected by spherical harmonics function. It compromises however the structure refinement or quantitative phase identification



Sample preparation for reflection XRD



Sample preparation for reflection XRD



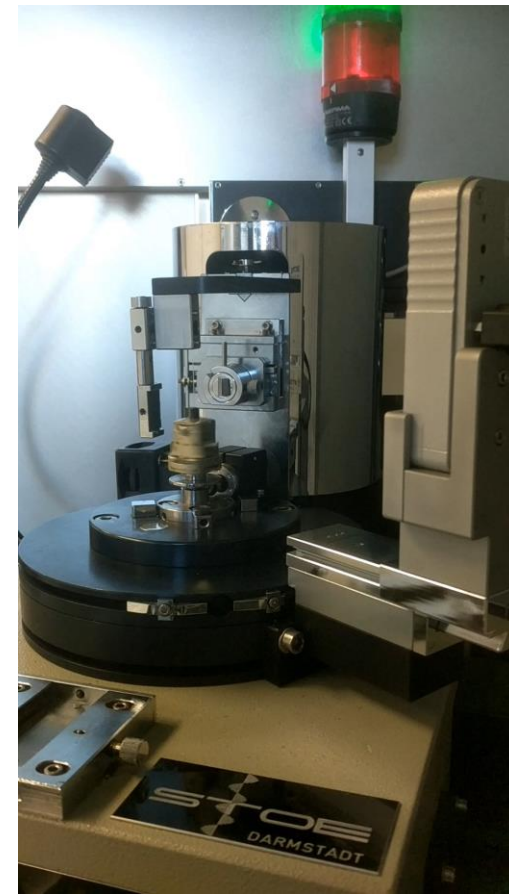
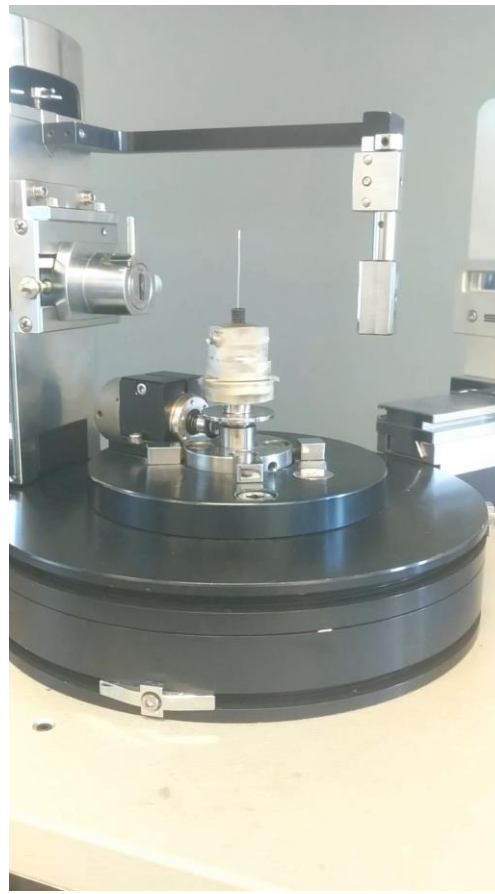
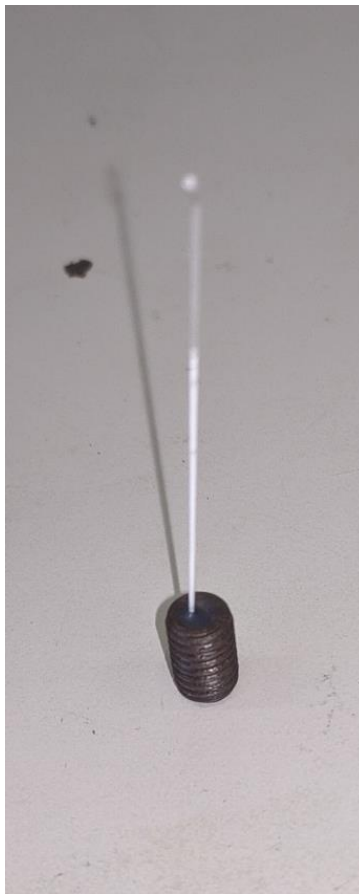
$$I/I_0 = e^{-(\mu_{tot}/\rho)x} < 1\% \text{ if } x > 0.5mm$$

I_0 (ph/s) – incident photon flux for Cu anode;
 μ_{tot} – total absorption coefficient for a zeolite;
 ρ – density of a zeolite;

Sample preparation for reflection XRD



Sample preparation for transmission XRD

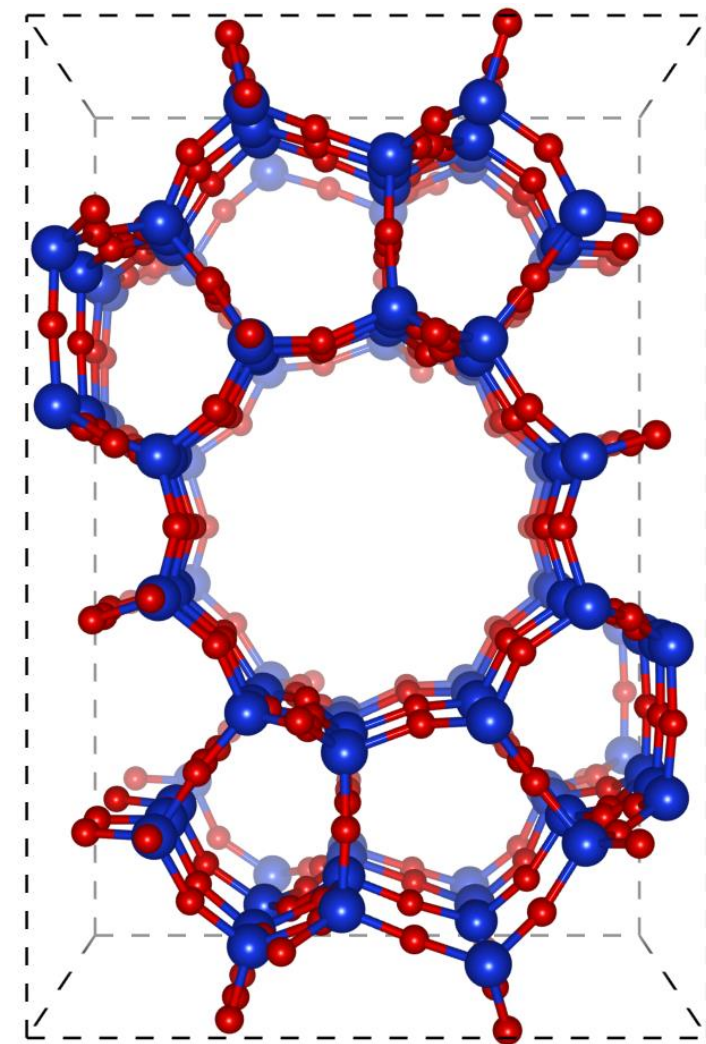
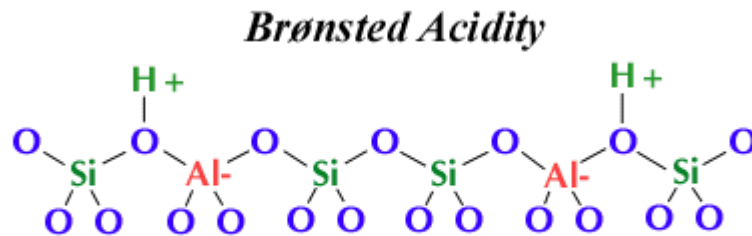


Stoe STADIP diffractometer working in Transmission-/Debye-Scherrer-geometry available for ex situ capillaries measurements

Si:Al distribution in zeolite framework

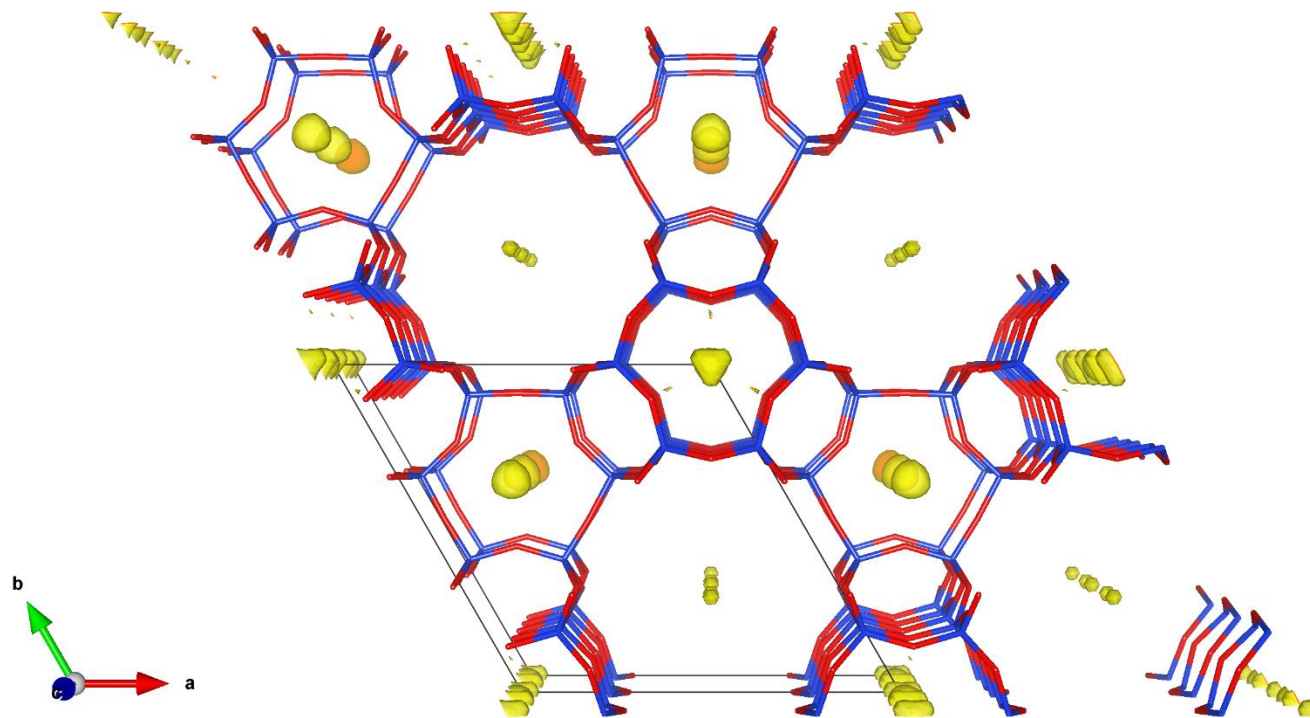
Protons and other light elements are poor scatterers and cannot be detected directly by X-ray diffraction methods

Brønsted acid sites or hydroxyl groups are balanced by framework charge associated to aluminum. Hence determination of Al positions allows on situating extra-framework entities



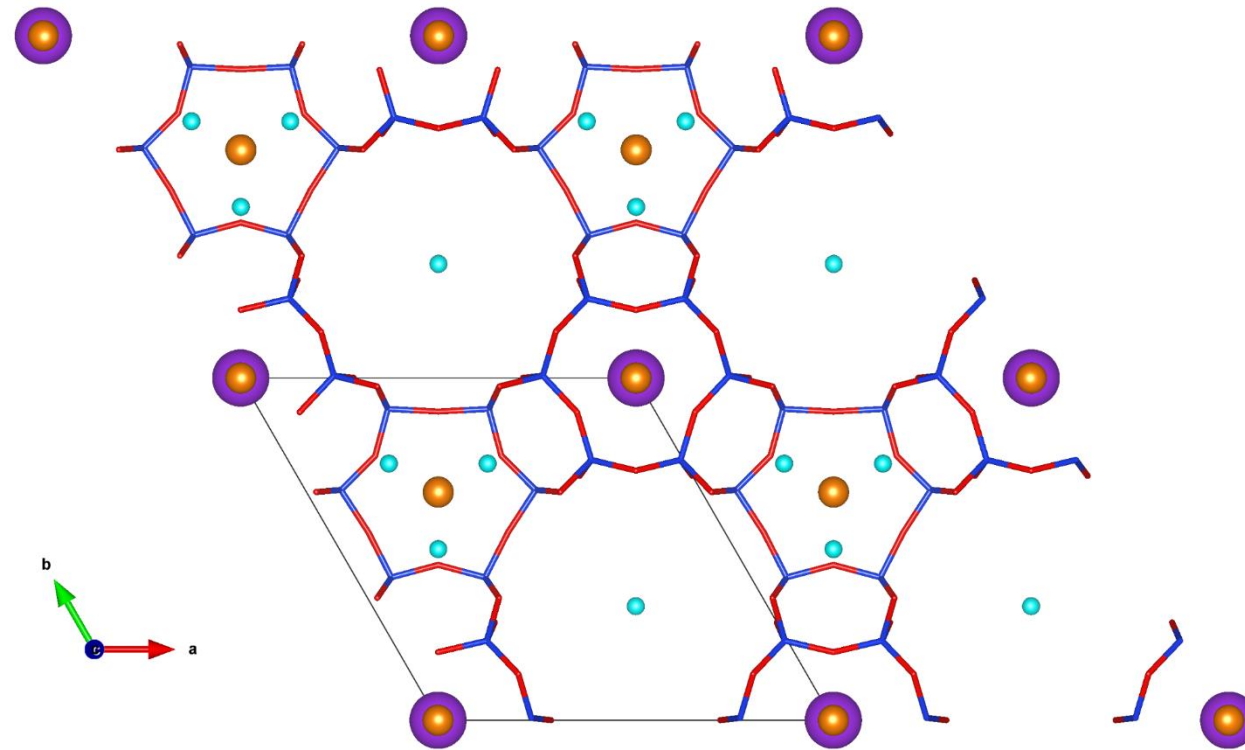
Difference density maps

fourier_map_formula=Fobs-Fcalc(model);



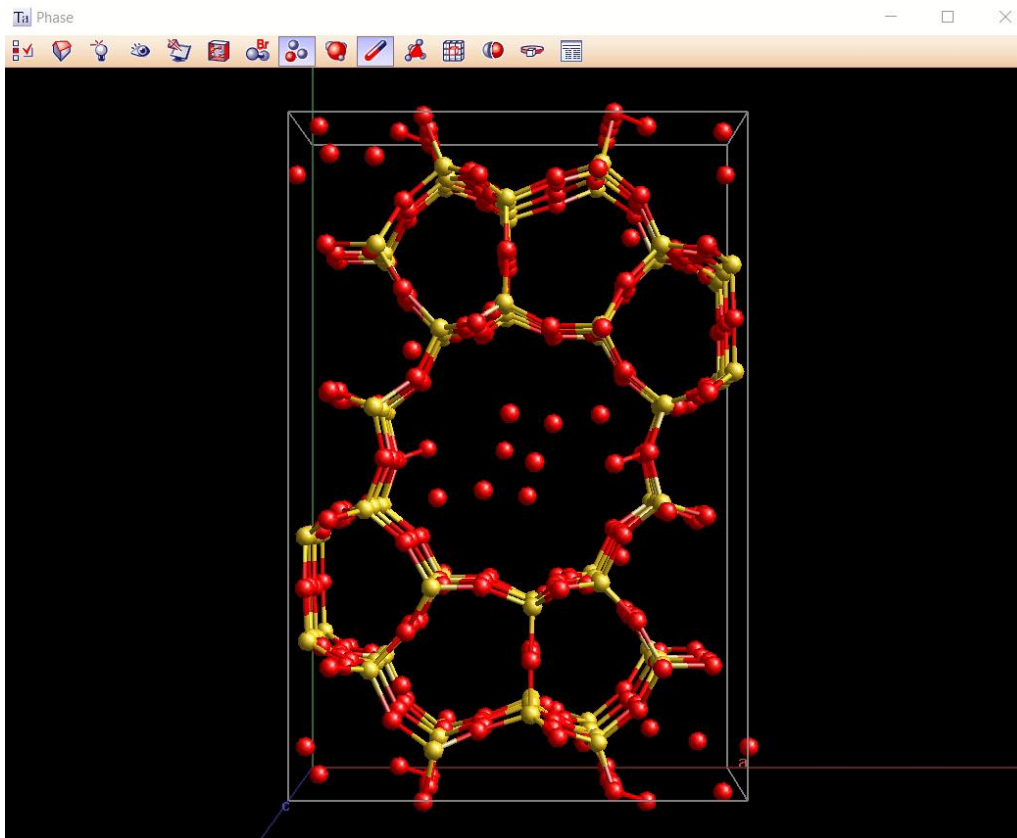
To investigate the positioning of the cations in Cu-OFF zeolite, the structure model containing only the framework atoms was subtracted from observed PXRD data.

The refinement of extraframework cations



The structure of Cu-OFF with input positions of the extra-framework cations adopted from DDM was refined using Rietveld analysis.

Structure Determination by Simulated Annealing



rigid

```
load z_matrix {  
    O1  
    H2 1 0.9687  
    H3 1 0.9687 2 104  
}
```

translate

tx @ 0 ty @ 0 tz @ 0

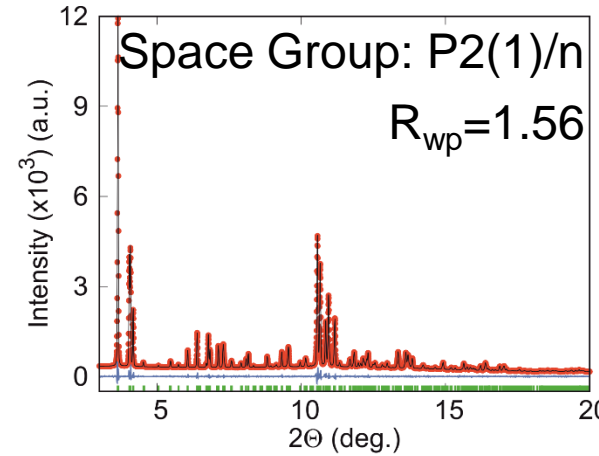
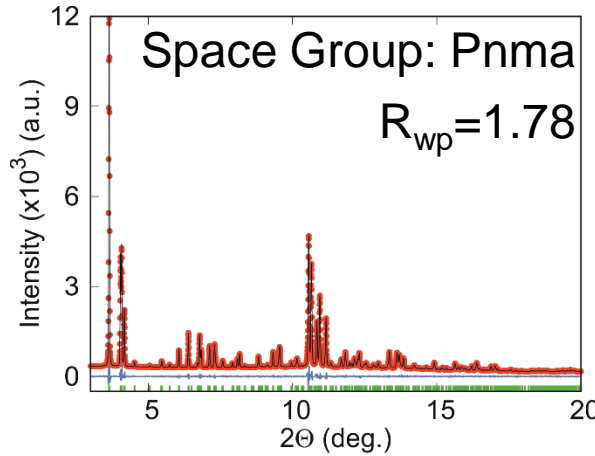
rotate

qa @ 0 qb @ 0 qc @ 0

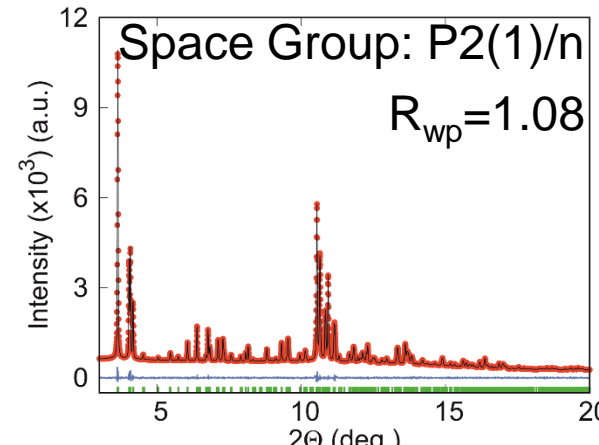
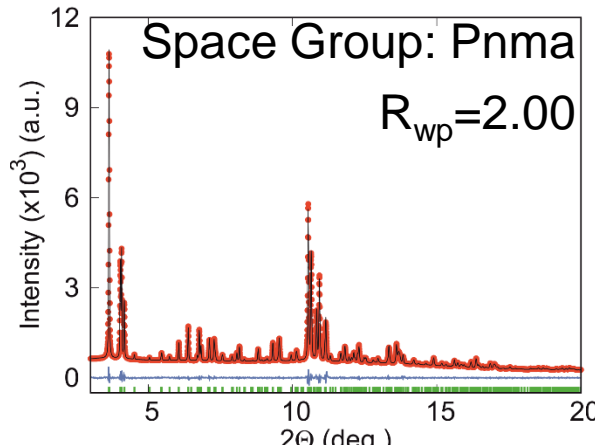
The simulated annealing algorithm approximates the global optimum of a given parameter in an environment of a large number of local optima.

Symmetry lowering with T-atoms alternations

ZSM-5 before desilication Si:Al=50



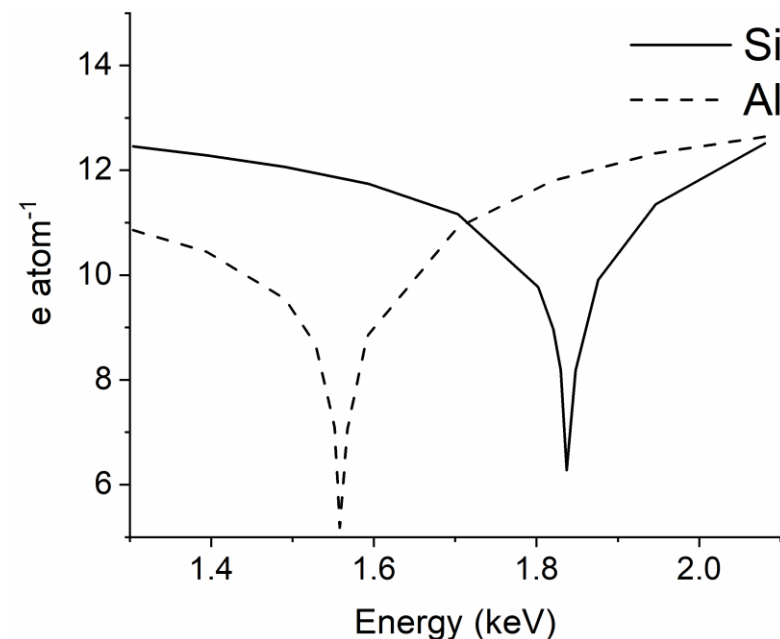
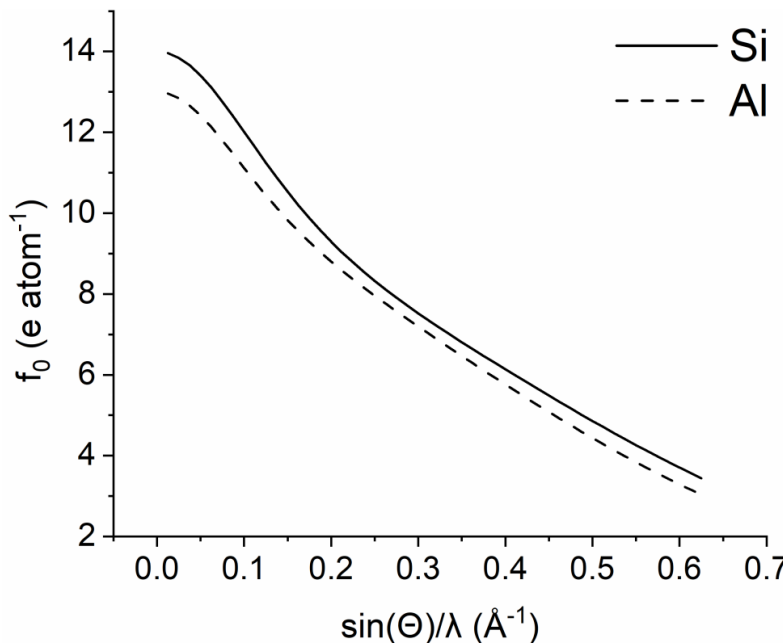
ZSM-5 after desilication Si:Al=25



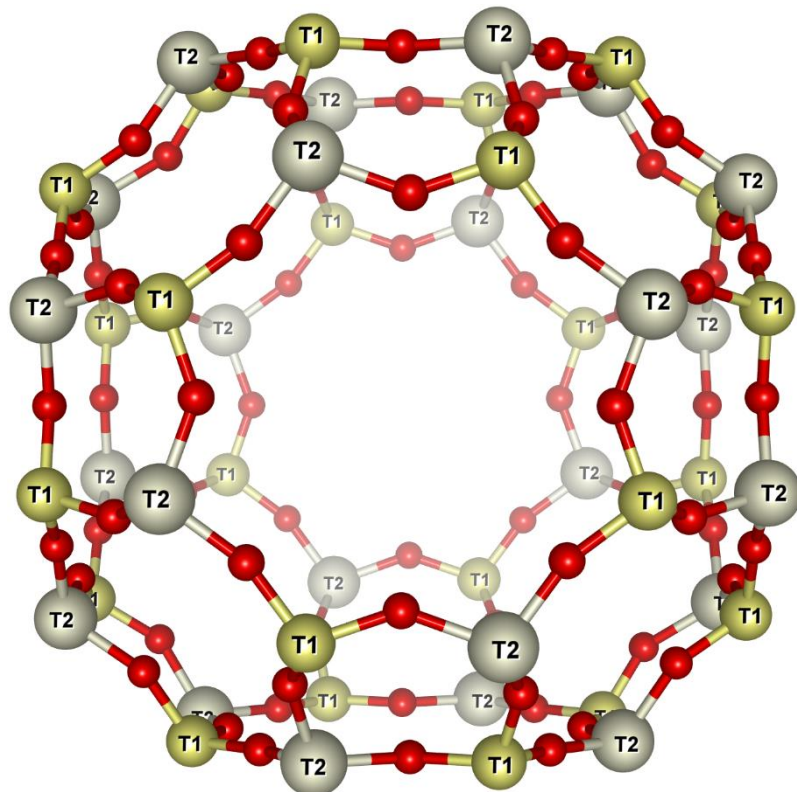
X-ray Anomalous Form Factor

Silicon and aluminum have similar atomic number ($Z=14$ and 13) and are difficult to be distinguished. However they display different absorption edges (1.84keV and 1.56keV).

Upon the vicinity of on-resonance X-ray absorption the scattering factor undergoes a change due to anomalous dispersion.



Refinement of anomalous data collected from LTA



site $T(1)$ $x 0.0$ $y 0.09344$ $z 0.18538$

occ $Si = ppSi$ beq 1

occ $Al = 1-ppSi$ beq 1

site $T(2)$ $x 0.0$ $y 0.18638$ $z 0.09067$

occ $Si = 1-ppAl$ beq 1

occ $Al = ppAl$ beq 1

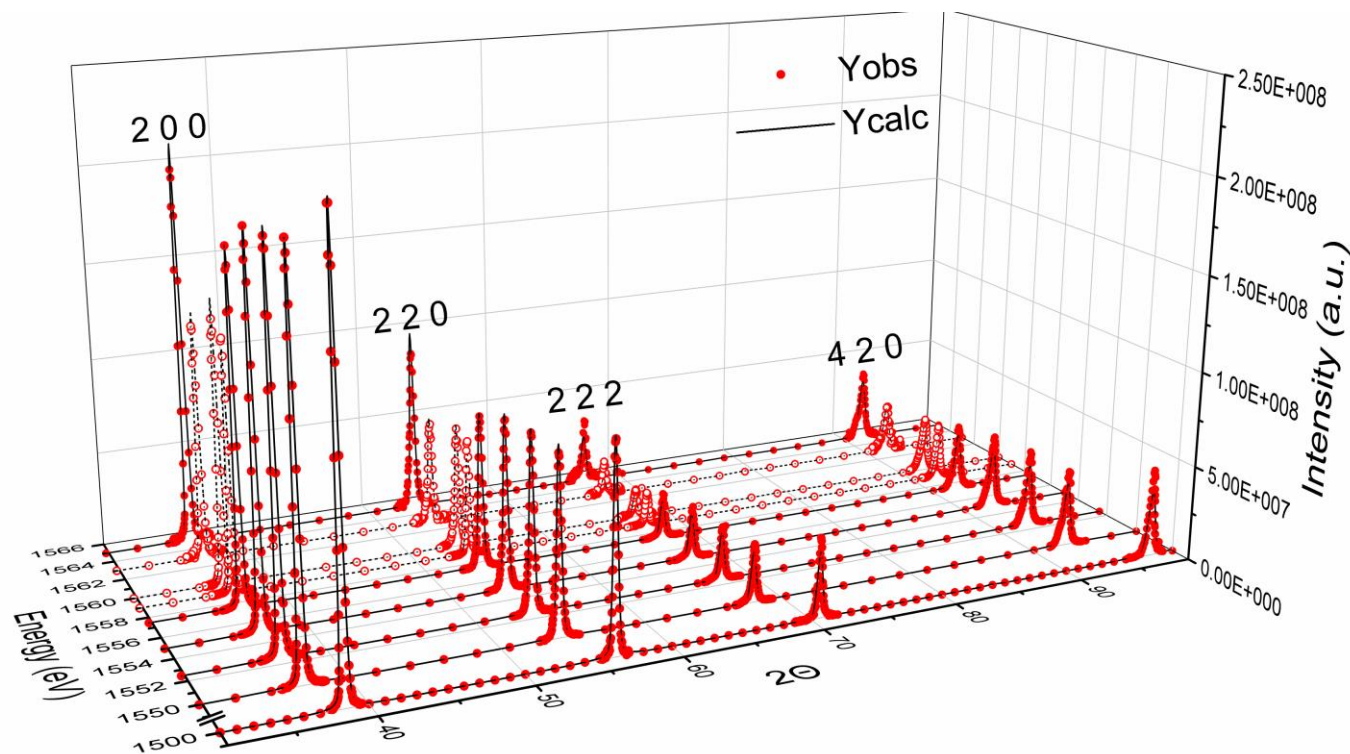
Prm @ Si 1

Prm @ Al 1

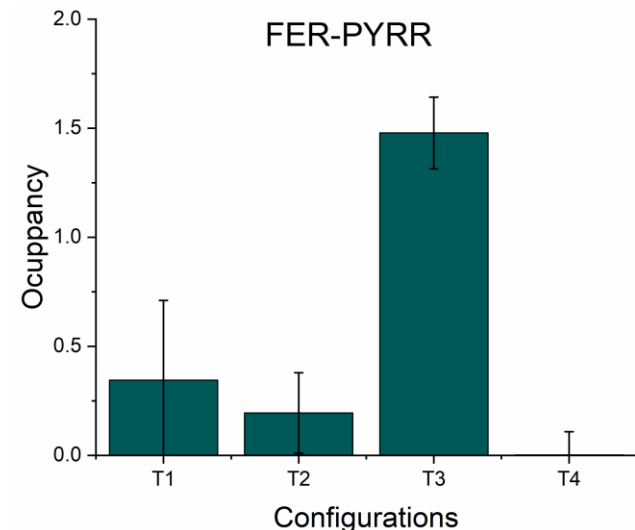
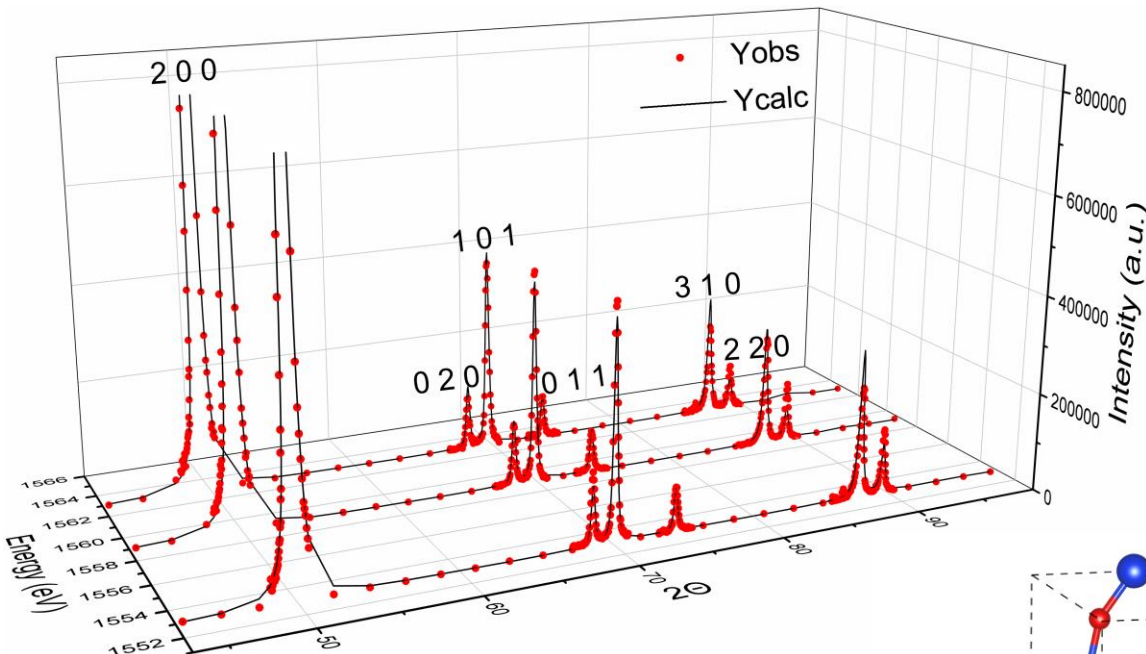
The Si:Al distribution in zeolite LTA is known as equals 1:1 and has to undergo Löwenstein's rule.

Refinement of anomalous data collected from LTA

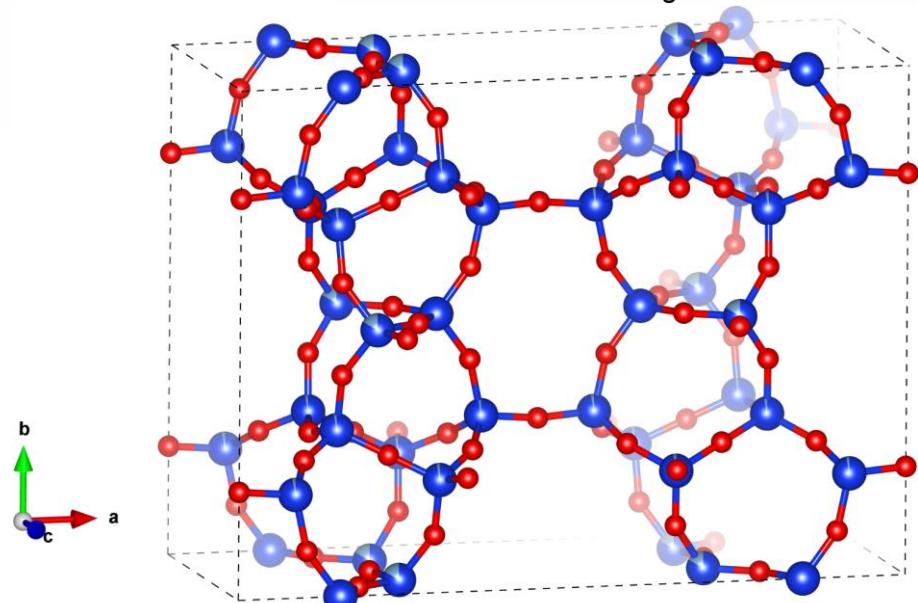
Anomalous X-ray diffraction data collected from zeolite LTA (Si:Al=1:1) displays the relative intensities of Braggs' reflections alternated across the aluminum absorption edge data as a function of X-ray radiation energy. Relative intensities are alternated across the K-edge



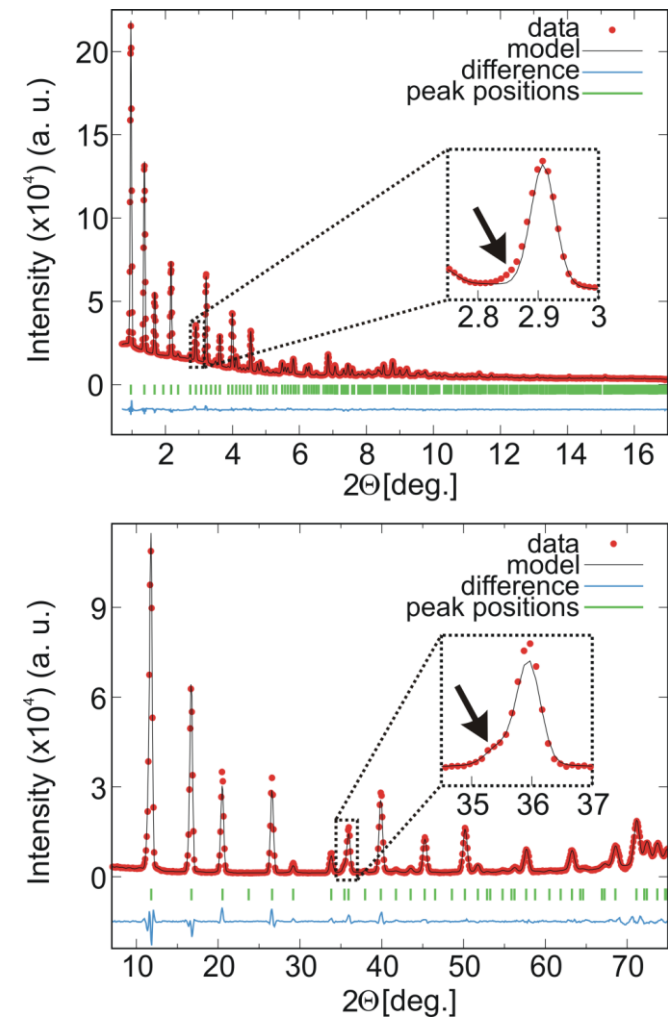
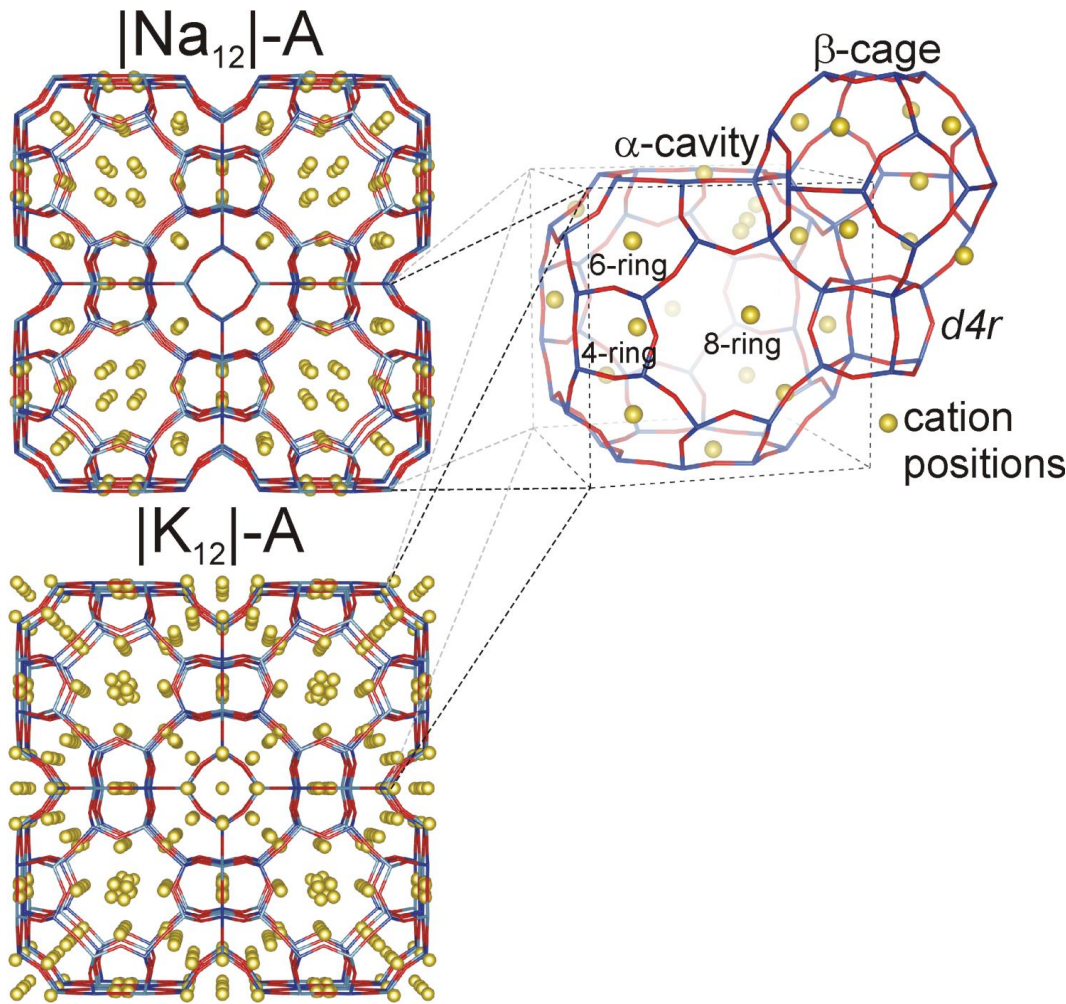
Refinement of FER-PYRR



Ferrierite is orthorhombic structure that displays 10-ring channels along z-axis. It is composed of 4 different T-atoms. Al concentrated at T(3) corroborates with X-ray emission spectroscopy study performed on the same samples (Bohinc 2007)

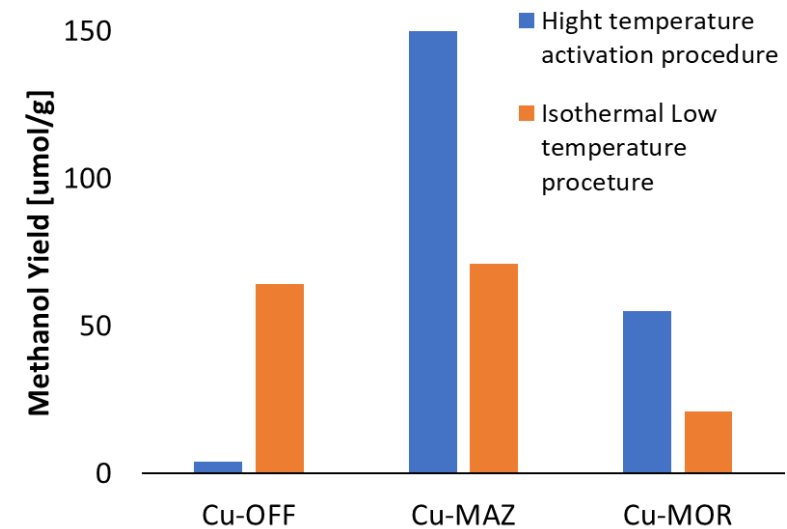
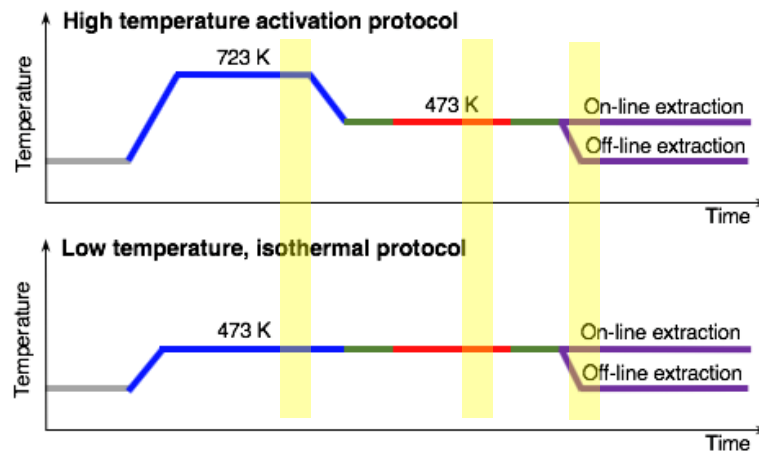


Structure of zeolite LTA



Anomalous diffraction across copper K-edge

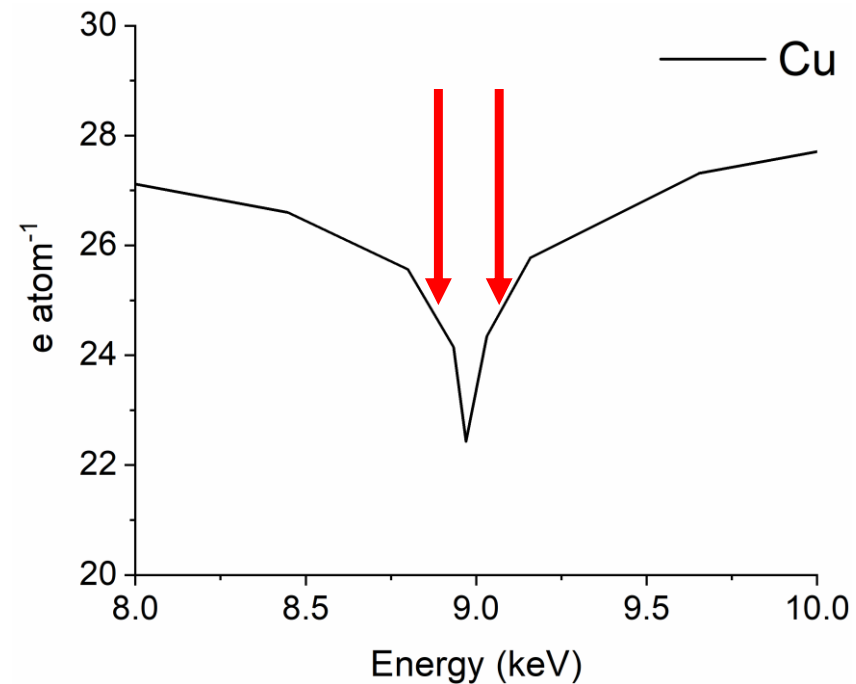
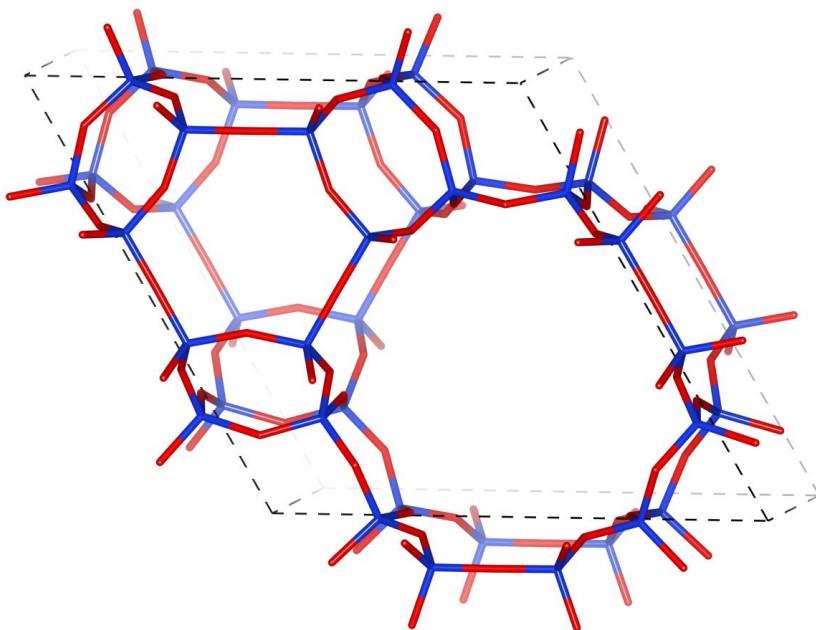
The aim of this project is to exploit anomalous scattering at the Cu K-edge to elucidate the structure of the copper species present during the partial oxidation of methane to methanol (MtM)



Copper offretite underwent isothermal and high-temperature procedures for methane-to-methanol conversion

Cu-offretite preforms better at lower temperature

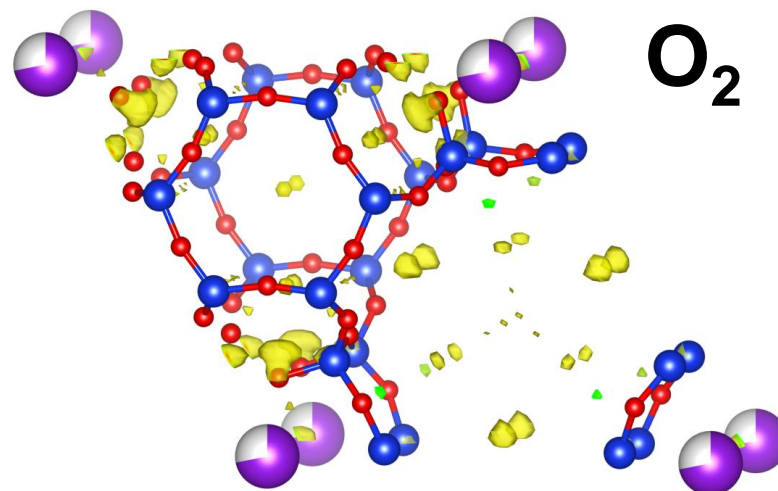
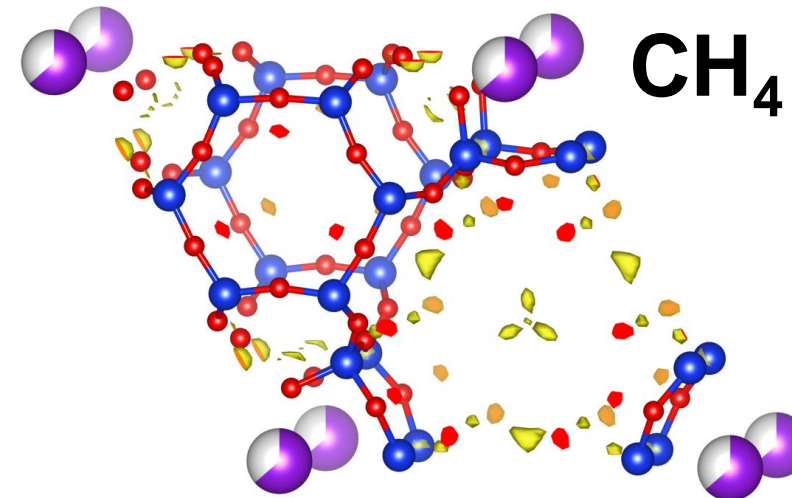
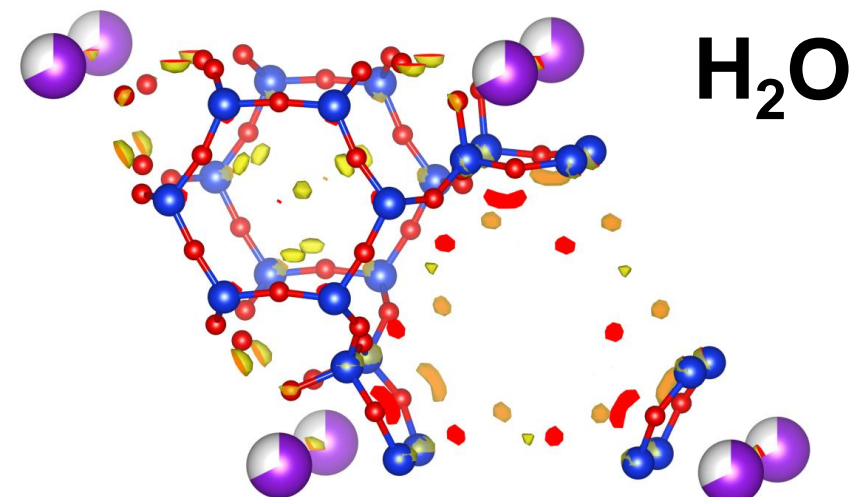
Anomalous diffraction across copper K-edge



Offretite is hexagonal structure with 12-ring channels along z-axis. It is composed of gmelinite and cancrinite cages

Each sample was measured at off-resonance (17.5 keV) and on-resonance conditions (8.97 keV and 8.98 keV)

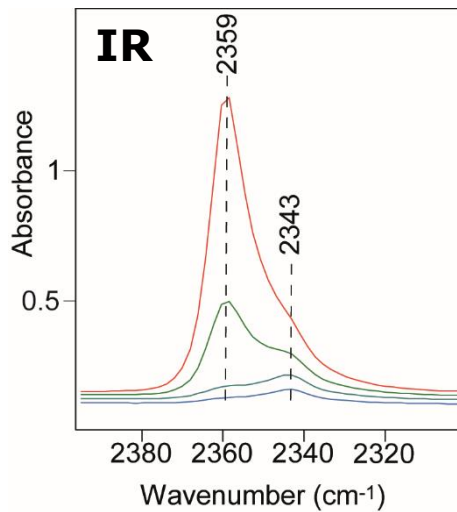
High resolution diffraction of offretite

 O_2  CH_4  H_2O

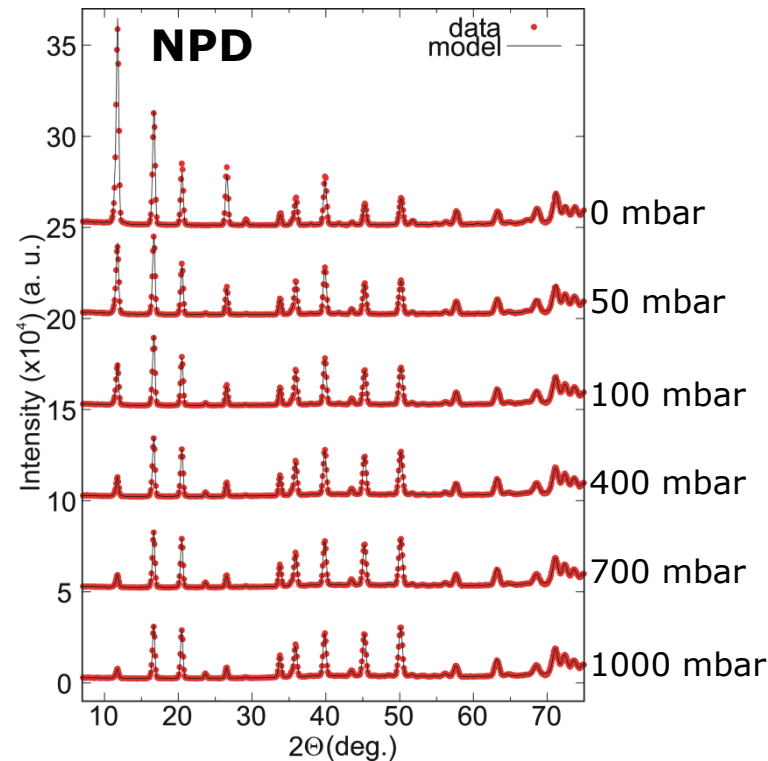
OFF structure reveals the electron densities near 8-ring window of gmelinite cage upon MtM protocol. Similar observation was done on Cu-Omega

Anomalous diffraction is needed for ambiguous assignment of these densities to copper, oxygen or carbon

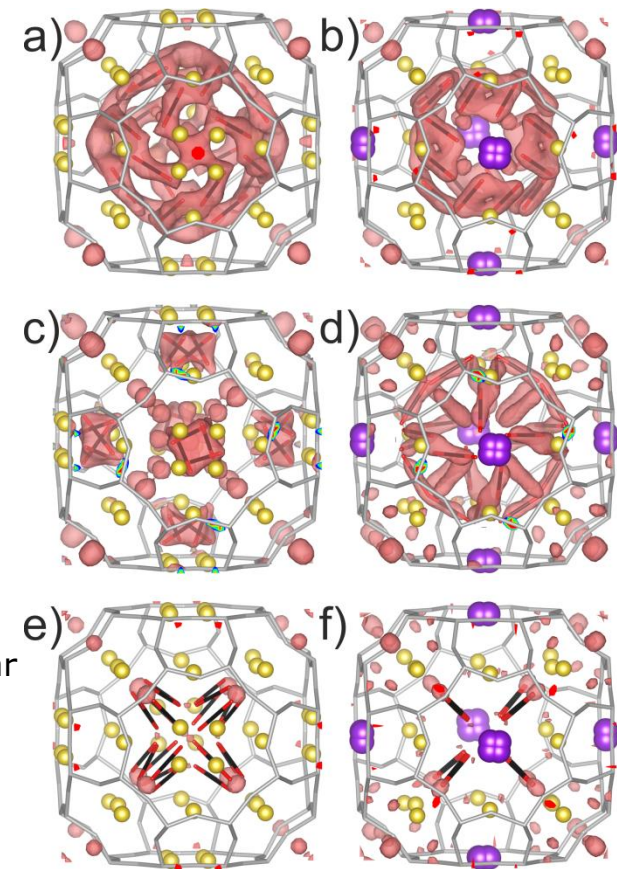
The chemical nature of physisorbed CO_2



IR bands showed differentiation of physisorbed CO_2 at $|\text{Na}_{12}|-\text{A}$

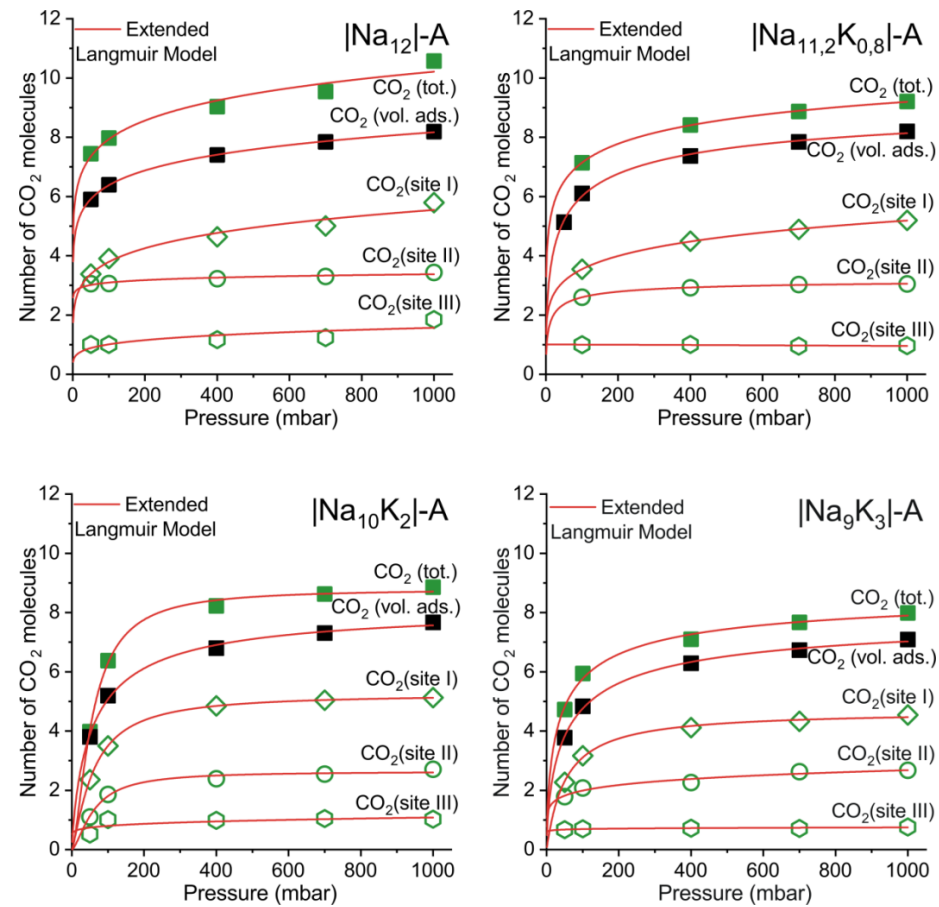
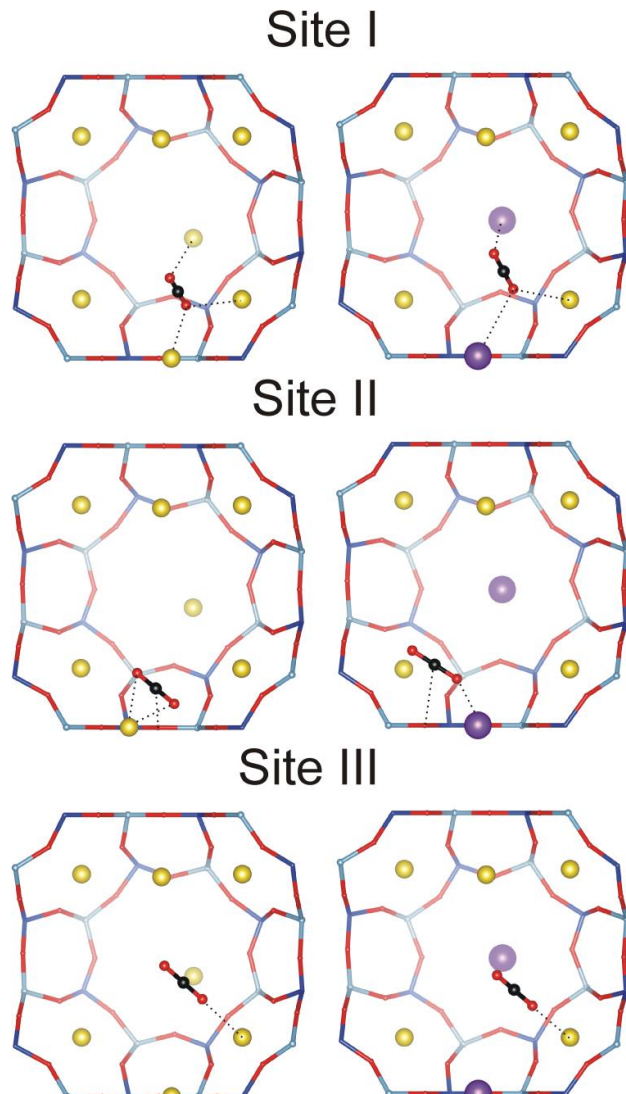


Rietveld analyses of the *in situ* neutron powder diffraction patterns of $|\text{Na}_9\text{K}_3|-\text{A}$



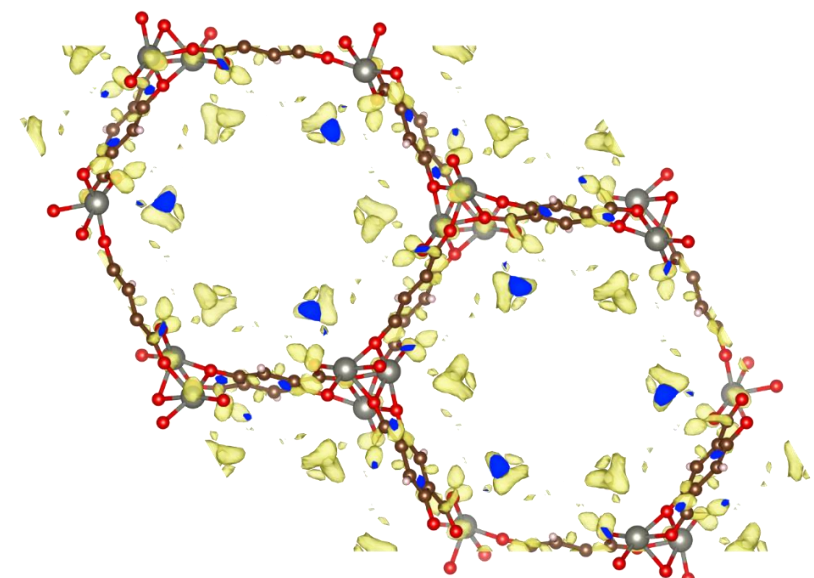
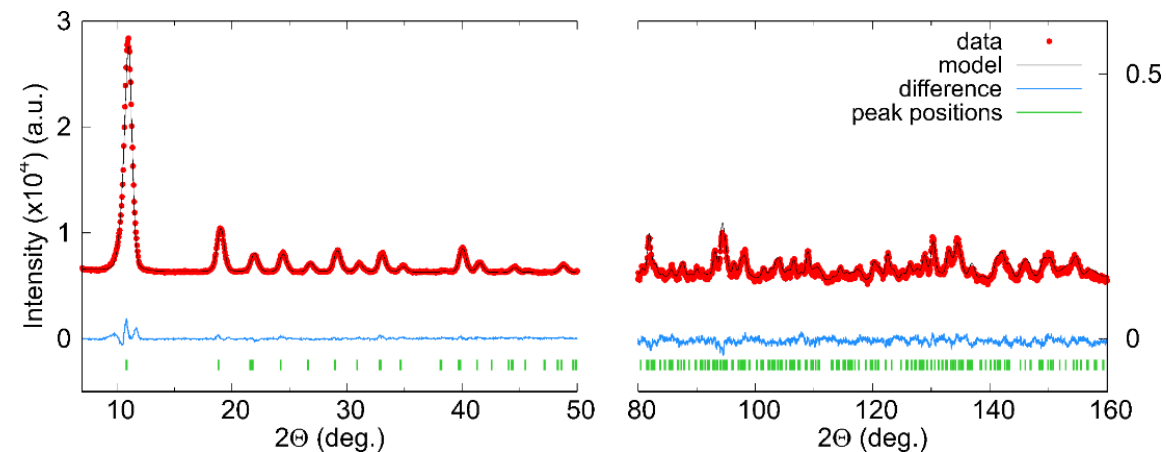
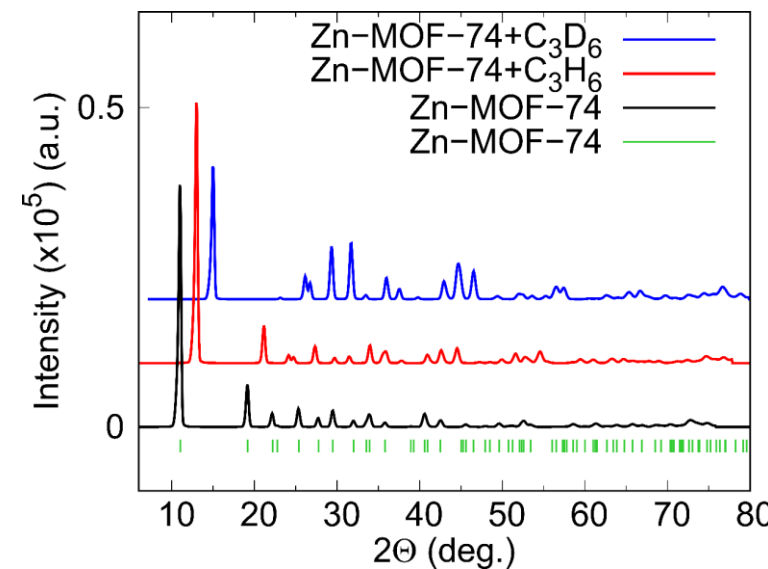
Difference Fourier maps of 3 sites of CO_2 for $|\text{Na}_{12}|-\text{A}$ (left) and $|\text{Na}_9\text{K}_3|-\text{A}$ (right)

Site-specific physisorption of CO₂



Atomic positions and site specific
isotherms of adsorbed CO₂

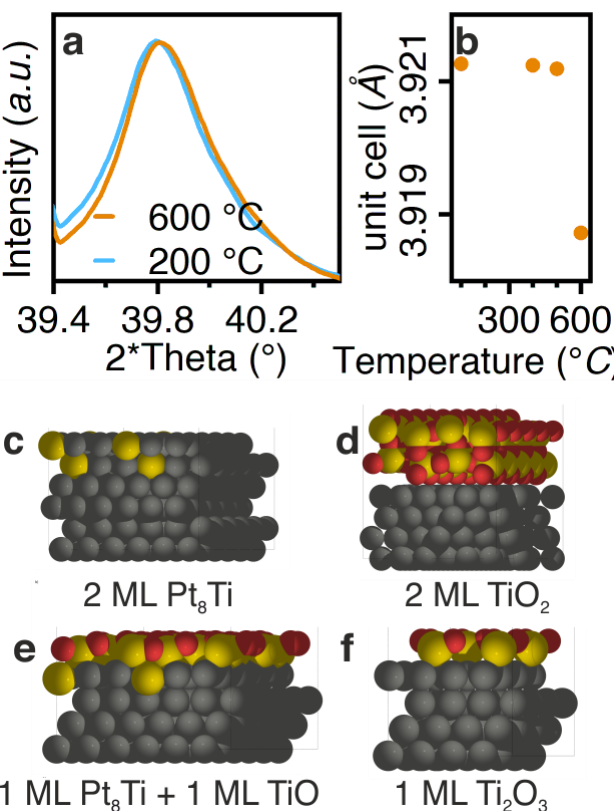
Adsorption of deuterated olefins



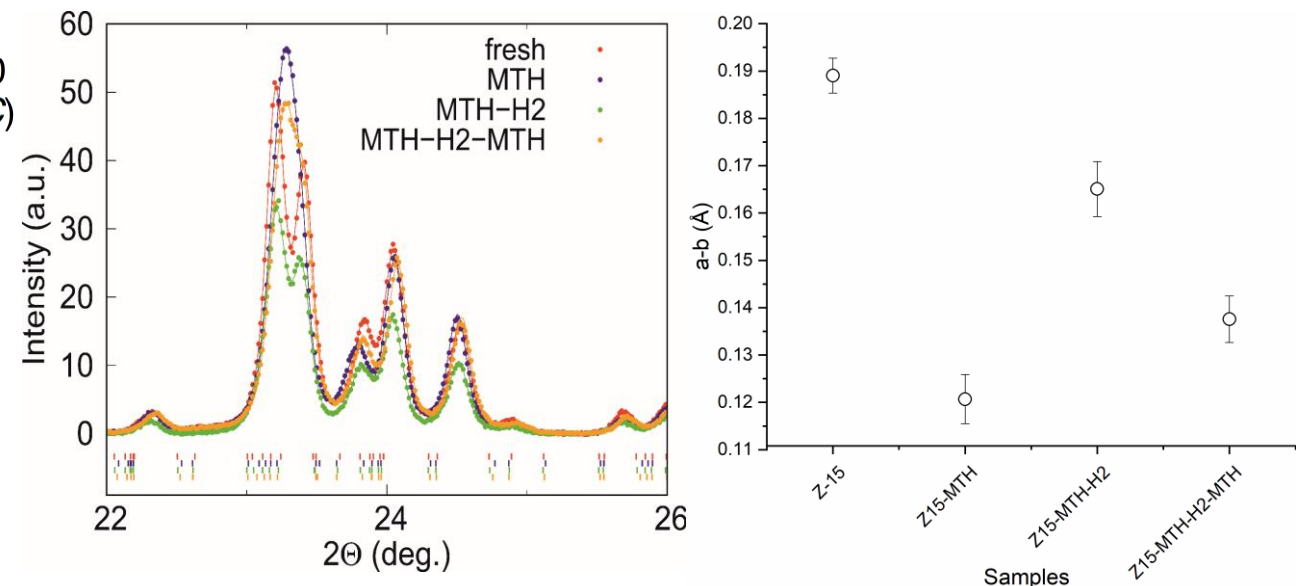
Rietveld refinement profile for dehydrated Zn-MOF-74 and loaded with C_6H_{12} and D_6H_{12} . The density peaks (right) correspond to C_6H_{12} positions.

Peak positions analysis

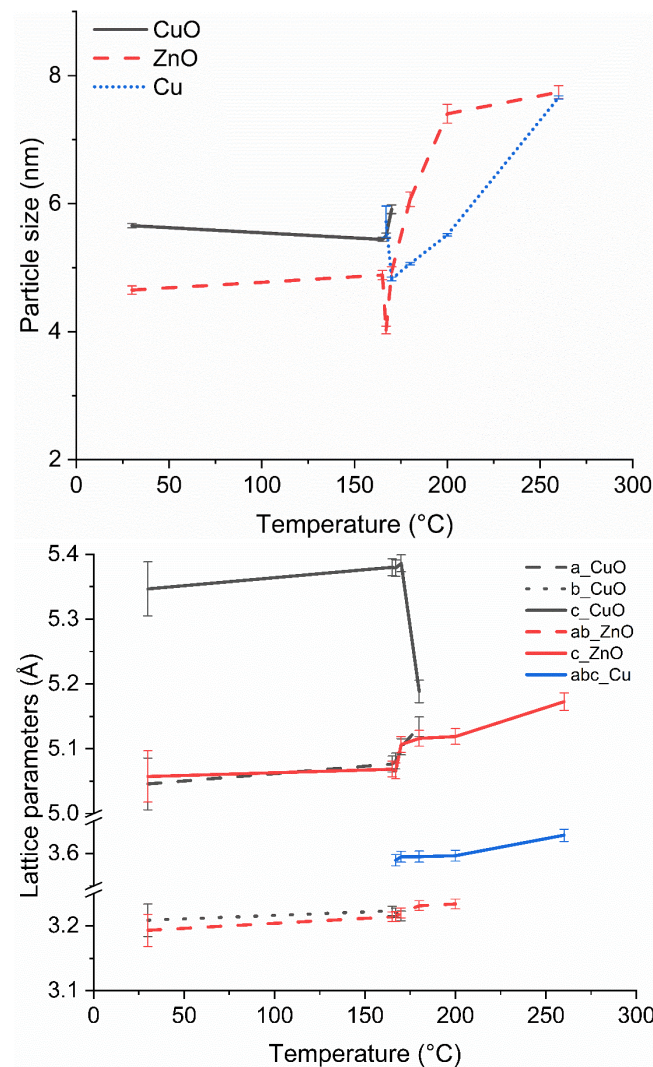
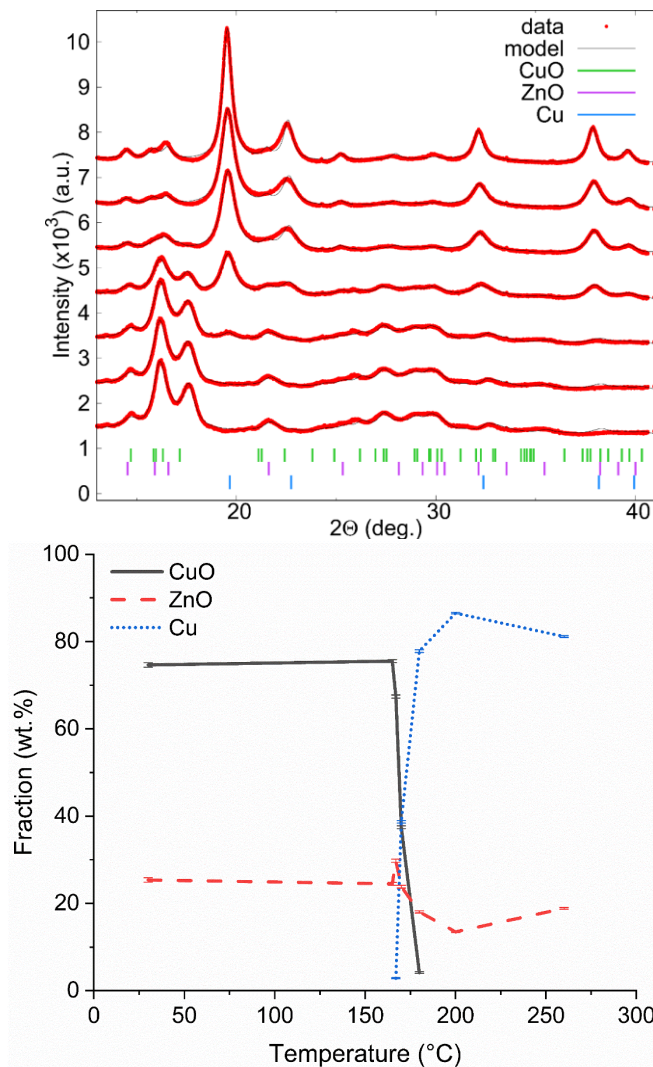
Formation of the strong metal support interaction (SMSI). Pt-Ti alloying.



The conversion of methanol to hydrocarbons (MTH) by ZSM-5 zeolite displayed by a-b lattice parameters change.

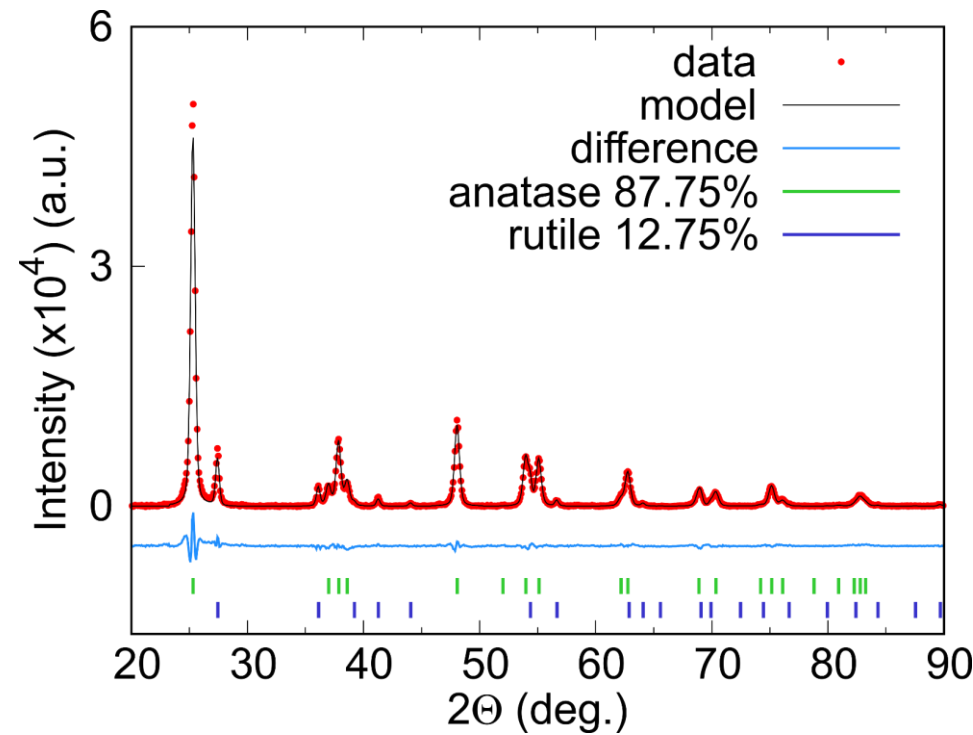


Phase analysis



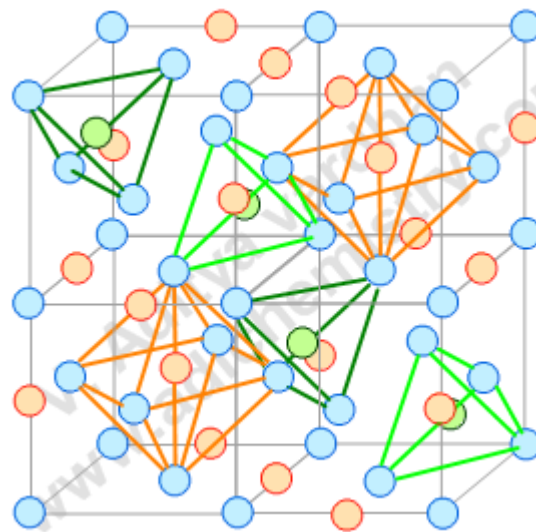
CZA catalyst reduction

Phase analysis

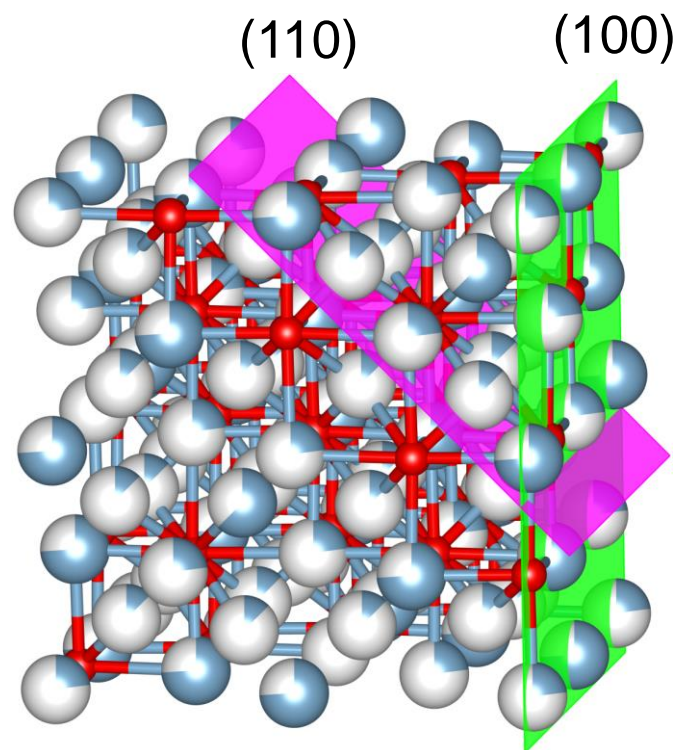


Proportions between anatase and rutile in P25 catalyst

Spinel structure of $\gamma\text{-Al}_2\text{O}_3$



Al cations are distributed over the octahedral ($16d$) and tetrahedral ($8a$) site



{100} set of planes is specific for octahedral aluminum

References

1. <http://pd.chem.ucl.ac.uk/pd/welcome.htm>
2. <http://prism.mit.edu/xray/education/downloads.html>
3. <http://www.crystal.mat.ethz.ch/people/staff/mlynne/>

Thank you for your attention!